1999-04-02

Structural and Signaling Proteins at the Synapse: Dystroglycan & Insulin Receptor Tyrosine Kinase Substrate p58/53: a Dissertation

Mary-Alice Abbott
University of Massachusetts Medical School

A Dissertation Presented

by

MARY-ALICE ABBOTT

Submitted to the Faculty of the
University of Massachusetts Graduate School of Biomedical Sciences
Worcester, Massachusetts
in partial fulfillment of the degree of:

DOCTOR OF PHILOSOPHY

APRIL 2, 1999

BIOMEDICAL SCIENCES

STRUCTURAL AND SIGNALING PROTEINS AT THE SYNAPSE:
DYSTROGLYCAN & INSULIN RECEPTOR TYROSINE KINASE SUBSTRATE p58/53

A Dissertation Presented

By

MARY-ALICE ABBOTT

Approved as to style and content by:

Neil Aronin, Chair of the Committee

Roger Davis, Member of the Committee

Steve Doxsey, Member of the Committee

Craig Ferris, Member of the Committee

Lou Kunkel, Member of the Committee

Justin Fallon, Dissertation Mentor

Thomas Miller, Dean of the
Graduate School of Biomedical Sciences

Department or Program Biomedical Sciences Program

Month, Day, and Year April 2,1999

ACKNOWLEDGMENTS

Many thanks to Justin Fallon, a fine teacher and role model, and to my excellent co-workers/friends: David Wells, Kate Deyst, Beth McKechnie, Laura Megeath, and Mike Rafii. I am grateful to Lou Kunkel and his talented lab, especially Susan Lacy and Helene Sadoulet-Puccio, for generously welcoming me and my science project to Boston for an extended summer. Also, I thank my thesis committee, for years of sincere guidance. I owe a special debt to my families: Abbott, for not asking when, and Ollari, for asking when; and especially to Chris Ollari, for perspective and quiet support.

ABSTRACT

The synapse is the primary locus of cell-cell communication in the nervous system. The elaboration of a functional synapse requires both a specialized structure and an efficient communication system. For my thesis work, I studied proteins implicated in each of these functions: the structural molecules dystroglycan and dystrophin, and the signaling elements Insulin Receptor Substrate p58/53 and insulin receptor.

The α/β-dystroglycan complex, believed to be the heart of cell-matrix adhesion in muscle and other tissues, provides a link between dystrophin, a cytoskeletal protein at the base of the muscle cell's Dystrophin Associated Protein Complex, and the extracellular matrix. In addition, dystrophin is found at central synapses, tightly associated with the postsynaptic density. The absence of dystrophin and the secondary loss of its associated proteins causes the genetic disease Duchenne Muscular Dystrophy. DMD affects both muscle and brain, causing a severe muscular dystrophy and lower IQs than control groups.

In the first portion of my thesis work, I sought to determine the role of dystroglycan, dystrophin's peripheral partner, at central synapses. I probed Northern blots of brain regions to delineate the distribution of brain β-dystroglycan mRNA and to uncover any β-dystroglycan-related transcripts in brain. Then, using subcellular brain fractions, and cultured hippocampal neurons, I determined that whereas α-dystroglycan is associated with central synapses, β-dystroglycan is not. This discovery is surprising, and differs from the finding that dystrophin and α- and β-dystroglycan colocalize at the presynaptic membrane of retinal photoreceptors.

In the course of the above mentioned work, using the anti-β-dystroglycan antiserum Ab98, I discovered a pair of proteins that were tightly associated with the postsynaptic density. These polypeptides of 58 kDa and 53 kDa (p58/53) were highly enriched in postsynaptic density (PSD) fractions from rat cerebral cortex, hippocampus, and cerebellum. In pursuit of a potential synapse-specific dystroglycan relative, I purified p58 and p53 by a combination of hydrophobic interaction

chromatography and two-dimensional gel electrophoresis. Mass spectroscopy and peptide microsequencing revealed that p58/53 is identical to the insulin receptor tyrosine kinase substrate p58/53 (IRSp53). Whereas IRSp58/53 has no significant homology to β-dystroglycan other than the one span of peptides that confers its antibody cross-reactivity, its localization to the PSD newly implicates insulin signaling at synapses.

Analysis of IRSp58/53 mass profiles, peptides, and mRNA indicated that IRSp58 and IRSp53 are the product of the same coding sequence. Immunolocalization showed that IRSp58/53 is expressed in the synapse-rich molecular layer of the cerebellum. Immunostaining of cultured hippocampal neurons showed that both IRSp58/53 and insulin receptor are highly concentrated at synapses. Like IRSp58/53, insulin receptors are a component of the PSD fraction. Together, these data suggest that the synapse is a specialized site for insulin signaling in the brain.

TABLE OF CONTENTS

Supplemental Pages:

• Abbott MA, Wells D, and Fallon J (1999) The Insulin Receptor Tyrosine Kinase Substrate p58/53 and the Insulin Receptor are Components of CNS Synapses. J Neurosci (In Press).

LIST OF TABLES

LIST OF FIGURES

Chapter I:

Chapter II:

CHAPTER I
DYSTROGLYCAN'S NONTRADITIONAL ASSOCIATIONS IN THE BRAIN

1. Introduction

Muscle and brain are two of the many tissues that contain the protein dystroglycan. In muscle, the α/β-dystroglycan complex works in at least two capacities. Along the muscle membrane, dystroglycan is a component of the dystrophin associated protein complex (DAPC). Within the sarcolemma, β-dystroglycan associates with dystrophin, a cytoskeletal protein that is aberrant in some forms of muscular dystrophy. The absence of dystrophin and the associated DAPC causes the muscle pathology, and perhaps the CNS abnormalities, characteristic of many muscular dystrophies. Dystroglycan is also a component of a modified DAPC that is specifically expressed at the neuromuscular junction (NMJ). Whereas α-dystroglycan interacts with the extracellular matrix protein laminin all along the surface of the muscle cell, it exhibits a particularly high binding affinity for agrin, a matrix molecule secreted by motor neurons exclusively at the site of the NMJ.

At both synaptic and nonsynaptic sites, dystroglycan links elements of the muscle cytoskeleton to components of the extracellular matrix. It is believed that dystroglycan participates in the maintenance of healthy muscle cells and has a role in normal brain development and function. The exact actions of dystroglycan in muscle continue to be elusive, and dystroglycan's role in the brain appears to be even more complex. The investigation of dystroglycan's role in the brain, and specifically at synapses, is therefore compelling. In this portion of my thesis work, I learned that what is true for dystroglycan in muscle is not necessarily true for dystroglycan in the brain. In brain, dystrophin is not ubiquitously associated with β-dystroglycan, and α- and β-dystroglycan are not invariably co-distributed. My findings indicate that the rules governing dystroglycan in muscle do not appear to be in effect in some brain regions, and forecast an unconventional role for dystroglycan at central synapses.

2. Background

Dystroglycan was first identified as a muscle protein that associates with dystrophin. Soon after, dystroglycan emerged as a NMJ protein with high binding affinity for laminin and agrin. Today, these associations are well established, but the ways in which dystroglycan contributes to the pathophysiology of muscular dystrophy, or to the development and maintenance of the NMJ, remain largely unknown. Expression of dystroglycan is not limited to muscle: many tissues contain this protein, including brain. Below is a summary of what is known about dystroglycan in muscle, in some non-muscle tissues, and in the CNS.

2.1 Dystroglycan in the Periphery

Dystroglycan is encoded by one gene, which is located on mouse chromosome 9 and human chromosome 3. The coding sequence includes two exons, 285 bp and 2400 bp, separated by a large intron. The 5.8 kb dystroglycan transcript encodes a 97 kDa precursor protein that is cleaved to produce α- and β-dystroglycan (Ibraghimov et al., 1992; Ibraghimov-Beskrovnaya et al., 1993; Gorecki et al., 1994).

α-Dystroglycan is a peripheral membrane protein that associates with the extracellular matrix. The primary sequence of α-dystroglycan predicts a 72 kDa protein, but tissue-specific post-translational carbohydrate additions give α-dystroglycan an apparent molecular weight that ranges from 120 kDa in brain to 156 kDa in muscle and to 190 kDa in *Torpedo* electric organ (Ibraghimov et al., 1992; Bowe et al., 1994). α-dystroglycan is tethered to the membrane by its noncovalent association with β-dystroglycan. β-dystroglycan is a 43 kDa transmembrane protein that acquires carbohydrate additions on its extracellular portion as well. Additionally, an intrachain disulfide bond forms within the extracellular domain of β-dystroglycan, between Cys669 and Cys713 (Deyst et al., 1995) (Figure 1).

2.1.1 Dystroglycan is a Dystrophin Associated Protein.

Dystroglycan is a prominent member of the dystrophin associated protein complex (DAPC), a group of proteins that remain tightly associated with dystrophin in muscle extracts purified on wheat germ agglutinin columns (Ervasti et al., 1990). To date, the DAPC includes laminin, α/β-dystroglycan, the sarcoglycan complex, the syntrophins, and the dystrobrevins (Figure 2).

Inside the muscle cell, the N-terminus of dystrophin associates with the actin cytoskeleton. The C-terminal tail of dystrophin contains a cysteine-rich region that binds to β-dystroglycan's proline-rich C-terminus (Jung et al., 1995). Outside the cell, α-dystroglycan binds the extracellular matrix molecule laminin-2. In this capacity, the α/β-dystroglycan unit links extracellular matrix to the cytoskeleton. This connection is thought to stabilize the myomembrane during the stress of muscle fiber contraction (Petrof, 1998).

In 1986, Dr. Lou Kunkel and colleagues discovered that defects in the gene for the 427 kDa protein dystrophin are responsible for the most well-studied of the muscular dystrophies, Duchenne and Becker (Monaco et al., 1986) (Table 1). Duchenne Muscular Dystrophy (DMD) is a severe X-linked genetic disorder that affects 1 in 3,500 boys. The disease is characterized by a progressive muscle degeneration that causes an affected boy to lose the ability to walk, potentially lose lung and cardiac function, and suffer an early death (Worton, 1995). In skeletal muscle from DMD patients, dystrophin is absent and levels of DAPC proteins are significantly decreased (Ohlendieck and Campbell, 1991). It is hypothesized that when some or all of the DAPC is missing, the myomembrane is more likely to tear and be damaged, but the exact pathophysiology of muscular dystrophy remains unknown.

Following the identification of the dystrophin gene as the primary defect in DMD, all members of the DAPC came under consideration as candidate genes for muscular dystrophies. It is now clear that genes encoding at least five of the DAPC proteins are responsible for muscular dystrophies. A defect in alpha, beta, gamma, or delta sarcoglycan can cause types of Limb Girdle Muscular Dystrophy (Table 1). The function of

the sarcoglycan complex in muscle remains unknown, however. Laminin-2 is a heterotrimer that is composed of one alpha-2 chain, which can bind α-dystroglycan, as well as a beta-1 and gamma-1 chain. Laminin-2 is highly expressed in striated muscle and peripheral nerve and is also found in the brain. Laminins participate in cell adhesion and migration, as well as in axon guidance and neurite outgrowth. Defects in the alpha-2 chain of laminin-2 are responsible for a type of muscular dystrophy as well (Bonnemann et al., 1996). Although expression of dystroglycan and the other components of the DAPC is reduced in most of the muscular dystrophies, no further DAPC components have been implicated in muscular dystrophies to date. Indeed, no disease has been linked to defects in the dystroglycan gene. Notably, "knocking out" the dystroglycan gene in mice is embryonically lethal (Williamson et al., 1997).

2.1.2 Dystroglycan is associated with the Neuromuscular Junction.

Dystroglycan is also associated with a complex of proteins at the NMJ (Figure 2). This peripheral point of cell-cell contact encompasses a motor neuron terminal, which secretes the neurotransmitter acetylcholine, and at the apposing muscle cell membrane, a specialized postsynaptic apparatus. This specialization develops as components of the synaptic machinery, including acetylcholine receptors (AChRs), cluster together under the nerve terminal. At this exceptional site the concentration of AChRs in particular swells to several thousand times that along the cell's non-synaptic membrane. At the NMJ, β-dystroglycan binds utrophin, an autosomally-encoded relative of dystrophin (Campanelli et al., 1994). Expression of beta-2-syntrophin and the form of dystrobrevin that contains a phosphotyrosine tail (dystrobrevin+PYCT) is restricted to the NMJ (Balasubramanian et al., 1998). Further, α-dystroglycan abandons its association with laminin-2, and is instead the major agrin binding protein (Bowe et al., 1994).

Agrin is secreted into the extracellular matrix by peripheral motor neurons. As the neuron approaches its target muscle, agrin works to shape and maintain the NMJ. First, agrin induces the clustering of AChRs and other molecules that contribute to the postsynaptic

specialization (Bowe and Fallon, 1995). Whereas agrin has high affinity for dystroglycan, agrin specifically activates MuSK, a muscle specific tyrosine kinase (Glass et al., 1996). Agrin and MuSK are both essential in NMJ synaptogenesis: mice with homozygous mutations in either agrin or MuSK die at birth. There is poor postsynaptic differentiation in muscle from these animals, with few to no AChR clusters at the NMJ. Since the communication system between nerve and muscle fails to develop, these mice cannot take their first breath (DeChiara et al., 1996; Gautam et al., 1996).

The steps that follow the agrin-MuSK interaction and lead to the special molecular organization of the NMJ are slowly being dissected. The activation of MuSK by agrin initiates multiple signaling pathways. The retrograde signal that instructs the incoming neuron to terminate its progression and form a presynaptic terminal depends on agrin. Similarly, the preferential transcription of AChR mRNAs by the muscle cell's sub-synaptic nuclei requires agrin and MuSK. This pathway requires the binding of ARIA, a neuregulin released by the nerve terminal, to its receptor tyrosine kinase erbB, which is clustered at the postsynaptic apparatus (Wells and Fallon, 1996). As mentioned, agrin also induces the clustering of postsynaptic components, including AChRs and some members of the DAPC. This phenomenon requires rapsyn, an AChR-associated protein. Since α-dystroglycan does not directly transduct the agrin signal that initiates this clustering of the postsynaptic apparatus, the function of α-dystroglycan at the NMJ remains undefined (Wells and Fallon, 1996).

There is some evidence that portends a role for β-dystroglycan in such signaling pathways, however. The juxtamembrane region of β-dystroglycan binds rapsyn, the 43 kDa cytosolic protein that is required for agrin-induced AChR clustering (Cartaud et al., 1998). In addition, the proline-rich C-terminus of dystroglycan interacts with the SH3 domain of Grb2, a small adapter protein that links receptor tyrosine kinases to small GTP binding proteins (Yang et al., 1995). Although the details of the complex mechanisms that coordinate the development and

maintenance of the NMJ remain unknown, α- and β-dystroglycan undoubtedly participate.

2.1.3 Dystroglycan in non-muscle tissues

Dystroglycan expression is also high in non-muscle tissues, including heart, brain, placenta, lung, liver, and pancreas. A prominent role for dystroglycan in embryonic development as well as during tissue epithelium morphogenesis is emerging. When the dystroglycan null mouse was created, it was abruptly evident that the dystroglycan gene product has important functions in development. Dystroglycan is required for the elaboration of Reichart's extra-embryonic basement membrane. Disruption of this structure causes gross abnormalities in the affected embryo's development that are incompatible with life (Williamson et al., 1997).

Dystroglycan also has a major role in the maternal mouse uterus during the periimplantation stage of pregnancy. The amount of dystroglycan mRNA in the decidual layer of the uterus 8.5 days after conception is 100 times higher than in a non pregnant uterus or in a mature placenta 12.5 days after conception. This dystroglycan expression is specifically localized to the decuidual cells that surround the implantation site. It is thought that dystroglycan mediates adhesion between decidual cells or between maternal decidual and placental trophoblast cells at this early stage in pregnancy (Yotsumoto et al., 1996). The associations that dystroglycan forms during the development of the embryo's Reichart's membrane and temporally in maternal decidual cells remain to be elucidated.

In several non-muscle tissues, dystroglycan is expressed on the basal side of epithelial cells and may help to affix these cells to basement membranes. In the kidney for example, dystroglycan is implicated in the morphogenesis of renal epithelium (Durbeej et al., 1995). Although epithelial cells express no dystrophin, the short dystrophin isoform DP71 (Figure 3) is expressed by all studied embryonic epithelial cells (Cullen et al., 1998; Stevenson et al., 1998). Interestingly, another short dystrophin isoform, DP140, is transiently expressed in a subset of kidney epithelial cells (Durbeej et al., 1997).

It appears that dystroglycan acts as to link one of these short forms of dystrophin to the extracellular matrix. The extracellular matrix protein that binds dystroglycan may be a non-muscle type of laminin: the E3 fragment of laminin-1 has been found to be involved in epithelial morphogenesis (Durbeej et al., 1998). Another extracellular matrix molecule that is expressed in kidney is agrin. In fact, α-dystroglycan from kidney binds agrin with a higher affinity than laminin-1, and agrin can coimmunoprecipitate α- and β-dystroglycan (Gesemann et al., 1998).

Indeed, in epithelia of various cell types, dystroglycan appears to provides a link between the cytoskeleton and the extracellular matrix. This may be dystroglycan's role early in development, in Reichart's membrane, and in the maternal uterus as well. The specificity of dystroglycan's cytoskeletal and extracellular matrix associations in these developmentally regulated contexts requires more thorough investigation.

2.2 Dystroglycan in the CNS

Dystrophin, dystroglycan, and other selected DAPC members are expressed in the CNS. Interestingly, a substantial fraction of the muscular dystrophy phenotypes manifest a CNS component. This suggests a role for dystroglycan and other DAPC members in brain. Agrin is also expressed throughout the brain, although its role there is as yet unknown. It is therefore instructive to review what is known about dystroglycan in the CNS in the context of disease manifestations and dystroglycan's binding partners.

2.2.1 The CNS component of dystrophinopathies

Duchenne Muscular Dystrophy, Classical Congenital Muscular Dystrophy, Walker-Warberg syndrome, and Fukuyama Congenital Muscular Dystrophy are muscular dystrophies with CNS involvement (Table 1). In addition, two animal mutants that have been used extensively as models of DMD exhibit CNS involvement. DMD patients, and to a lesser extent BMD

patients, suffer a mild, non progressive mental retardation (Emery, 1993). In general, the verbal IQ of a DMD patient is more affected than his performance or full scale IQ (Bushby et al., 1995). It is well established that the mental retardation is a primary deficit, and is not secondary to the child's musculoskeletal deficit. In addition, abnormal electroretinograms (ERGs), which indicate defective synaptic transmission in the retina outer plexiform layer (OPL), are seen in patients with DMD (Cibis et al., 1993; Pillers et al., 1995). The pathophysiology that leads to these CNS abnormalities in DMD is unknown.

Two animal mutants are available for studying the effects of these disease genotypes in the CNS. One, the *mdx* mouse, has a defect in the dystrophin gene. These mice express a dystrophin protein that is defective in its N-terminus. Correspondingly, the expression of DAPC proteins in muscle of *mdx* mice is diminished (Ohlendieck and Campbell, 1991). These mice suffer only a mild muscular dystrophy, however. During the first month of life, they experience muscle degeneration and extreme weakness, but after this critical period they no longer exhibit significant muscle impairment (Muntoni et al., 1993). A few behavioral studies reveal that *mdx* mice exhibit impaired passive avoidance learning, and are deficient in the consolidation processes required for long term memory in behavioral tasks (Muntoni et al., 1991; Vaillend et al., 1995). Unlike in DMD, ERGs from *mdx* mice reveal no abnormalities (Cibis et al., 1993). This raises the possibility that retinal function as measured by ERG does not require a functional dystrophin N-terminus or a complexed DAPC. The integrity of the dystrophin C-terminus in *mdx* mice may allow for retention of much of dystrophin's function, however.

The most common mutations in the dystrophin gene (65% in DMD and 85% in BMD) involve the N-terminus and rod domains of dystrophin (Figure 3). In general, mutations in which the reading frame is disrupted cause DMD, whereas mutations in which the reading frame is maintained cause the less severe BMD. Thus, most of the DMD mutations create premature stop codons, which presumably result in the expression of truncated proteins that lack the dystrophin C-terminus (Monaco et al., 1988).

The giant dystrophin gene has at least seven different promoters (Figure 3). Products of the dystrophin gene include tissue specific full-length dystrophins as well as truncated dystrophin isoforms. There are at least three promoters producing full-length dystrophin proteins: Muscle, Brain, and Purkinje. These three promoters each encode a different first exon which is spliced in frame with the common dystrophin second exon. The "Brain" promoter lies 5' to the muscle first exon, and expresses dystrophin in the cerebral cortex, the cerebellar Purkinje cell-specific dystrophin promoter's first exon is downstream of the first muscle exon. The overall product of these promoters is virtually identical, since the divergent first exons add only 3-12 unique amino acids (Gorecki et al., 1992). DP240 is a retina-specific transcript that uses a promoter located midway along the dystrophin gene (D'Souza et al., 1995). DP140 is a brain and kidney specific isoform with a start methionine in exon 51 (Lidov et al., 1995). A major brain product of the dystrophin gene is the shortest isoform, DP71. This transcript encodes seven new amino acids plus the very last 609 amino acids of dystrophin (Blake et al., 1992; Lederfein et al., 1993).

Since the genetic defect in *mdx* is a point mutation in exon 23 of the dystrophin gene, only the expression of full-length dystrophins is disrupted and short dystrophin isoforms are expressed normally. In *mdx* muscle, exogenous DP71 can reconstitute the missing DAPC (Cox et al., 1994; Greenberg et al., 1994). It is likely therefore that in brains of *mdx* mice, many of dystrophin's C-terminal associations can be achieved by unaffected endogenous short dystrophin isoforms. The genetic defect in the *mdx 3CV* mouse is different from that found in the classical *mdx*. In *3CV*, a mutation in intron 64 causes aberrant splicing and the gene products are terminated early, presumably lacking the dystrophin C-terminus. In *3CV* no forms of dystrophin are expected to be expressed. This mutant is somewhat "leaky" however, and minor amounts of dystrophin are expressed. Although no neuropathology is detectable on histologic sections of *3CV* brain and spinal cord (Cox et al., 1993), ERGs performed on *3CV* mice reveal abnormalities similar to those observed in DMD patients (Pillers et al., 1995). In *3CV*, it is expected that all

dystrophin C-terminal associations are disrupted. Since the genetic defect in *3CV* is similar to those found in DMD, one anticipates that *3CV* mice will display a CNS phenotype more similar to that seen in DMD patients than that reported in *mdx* mice. The *3CV* mouse is therefore a valuable tool in furthering the understanding the role of dystrophins in the CNS.

2.2.2 The CNS component of other muscular dystrophies

Fukuyama-type Congenital Muscular Dystrophy is one of Japan's most common autosomal recessive genetic disorders, affecting 1 per 10,000 births. The FCMD phenotype comprises a muscular dystrophy, mental retardation, and brain malformation due to a defect in neuronal migration that causes disruption of the orderly six layer neuronal lamination of the cortex. The disease gene for FCMD has recently been identified. In 87% of individuals with FCMD, the 3'UTR of a gene within chromosomal region 9q31 is disrupted by a 3 kb retrotransposal insertion of tandemly repeated sequences. This insertion is likely to cause a decrease in the mRNA's transcription or stability and thereby produce a loss of function phenotype. Two distinct point mutations in this gene can also cause FCMD (Kobayashi et al., 1998).

The predicted product of the FCMD disease gene is fukutin, a 461 amino acid secreted protein, with one site for N-linked glycosylation. Normally, fukutin mRNA is expressed predominantly in striated muscle, brain, and pancreas (Kobayashi et al., 1998). The role of fukutin in muscle and brain remains unknown. In FCMD muscle, whereas dystrophin is expressed at a normal level, the expression of laminin alpha-2 chain and members of the DAPC, especially β-dystroglycan, are greatly reduced (Hayashi et al., 1993; Matsumura et al., 1993). Electron microscopy of FCMD tissue reveals abnormalities in the basal lamina of muscle and brain (Ishii et al., 1997).

There are at least two other muscular dystrophies that commonly involve the CNS. Many patients with one form of congenital muscular dystrophy exhibit abnormalities of white matter, a slowing of motor nerve conduction velocities, and delayed somatosensory evoked

potentials. The genetic mutation that causes this type of muscular dystrophy occurs in the alpha-2 chain of laminin-2. As mentioned, laminin-2 is a dystrophin associated protein due to the binding of the alpha-2 chain to α-dystroglycan. Individuals with Walker-Warberg syndrome may display severe CNS aberrations such as a cobblestone-appearing cortex and cerebellar hypoplasia, and eye abnormalities including retinal dysplasia (Bonnemann et al., 1996). Muscle biopsies from two Walker-Warberg patients exhibit decreased immunostaining for laminin alpha-2 chain and β-dystroglycan (Kanoff et al., 1998). The genetic basis of Walker-Warberg syndrome has not been identified.

Since its level of expression is affected in the above mentioned disorders, dystroglycan is implicated in the CNS abnormalities associated with these disease. To determine the role of dystroglycan and its associated proteins the CNS however, the distribution of these proteins in the brain must first be detailed.

2.2.3 Expression of dystroglycan and associated proteins in the retina

The retina provides a useful window through which to begin an examination of dystroglycan in the CNS. Dystroglycan mRNA is expressed by photoreceptors and retinal ganglion cells. α- and β-dystroglycan are found in the outer plexiform layer (OPL) of the retina, along with short dystrophin isoforms (DP240, DP140 and DP71) (Ueda et al., 1998). In immunostained *mdx* retina, the expression of α- and β-dystroglycan and a dystrophin isoform in the photoreceptor synaptic membrane (OPL) is unaffected. Additionally, *mdx* ERGs are normal (Montanaro et al., 1995). In bovine retina, these proteins localize to the intracavital processes of the photoreceptor that form the lateral boundary of the synaptic cavity, distal from the synaptic vesicles but adjacent to the dendritic ending of the bipolar cell, indicating a presynaptic localization. In contrast, no immunostaining for β-dystroglycan or dystrophin is observed at the postsynaptic triad (Figure 4). Agrin, which has been detected in the chicken retina OPL (Kroger et al., 1996), may participate in a dystroglycan-associated complex as well. It is likely that dystroglycan and its traditionally associated proteins are involved in healthy

synaptic transmission between photoreceptor cells and bipolar cells in the retina. (Schmitz and Drenckhahn, 1997; Ueda et al., 1998).

Disruption of this complex may cause the ERG abnormalities seen in DMD patients. A C-terminal missense mutation in the dystrophin gene (cysteine 3340) has been identified in a DMD patient who exhibits mental retardation and abnormal ERG. This mutation, which is in the region of dystrophin that binds β-dystroglycan, causes decreased levels of dystrophin in all tissues, and a concomitant decrease in the level of β-dystroglycan staining in muscle. The phenotype of this patient suggests that a dystroglycan-dystrophin association is required for dystrophin to function properly in muscle, retina, and brain (Lenk et al., 1996). A causative role for this association could be shown by careful comparison of the behavioral and biochemical characteristics of a mice genetically engineered to express dystrophin defective only in its β-dystroglycan binding domain. An understanding of the exact role of the dystrophin and β-dystroglycan association in mental retardation and abnormal retinal function will require a deeper understanding of this relationship in the healthy CNS.

2.2.4 Expression of dystroglycan and associated proteins in the brain

There is a significant level of dystrophin expression in the healthy brain. In the hippocampus, pyramidal cells express dystrophin whereas granule cells of the dentate gyrus do not. Throughout the cerebral and cerebellar cortex, dystrophin immunoreactivity is localized almost exclusively in neurons (Lidov, 1996). Surprisingly, dystroglycan expression in brain does not match the pattern of dystrophin expression. In situ hybridization studies show that dystroglycan mRNA does colocalize with dystrophin mRNA in hippocampus, dentate gyrus, olfactory bulb and cerebellar Purkinje neurons, but no dystroglycan message is detectable in the cerebral cortex, a region in which significant amounts of dystrophin mRNA and protein are observed. In contrast, significant dystroglycan mRNA appears in neurons in the lateral septal nucleus of the thalamus, where no dystrophin mRNA is observed (Gorecki et al., 1994).

Based on what is known about dystroglycan at the NMJ, one would expect dystroglycan to link agrin to utrophin or PYCT+dystrobrevin at the central synapse. While neurons do express utrophin, glial cultures express significantly more (Khurana et al., 1992), and utrophin is absent from central synapses. It appears that utrophin and dystroglycan interact not at synapses but at the blood-brain interface. Utrophin, β-dystroglycan, and laminin immunoreactivities are found along brain-penetrating blood vessels and the pial surface (Lidov, 1996). In particular, both β-dystroglycan and utrophin localize to the perivascular endfeet of glial cells, and α-dystroglycan associates with the basement membrane of brain blood vessels (Khurana et al., 1992; Tian et al., 1996). Agrin is found associated with brain microvasculature as well. In the cerebellum at least, dystroglycan appears to link laminin-2 and utrophin, forming a complex that participates in the normal maintenance of the blood-brain barrier (Figure 5) (Tian et al., 1996).

The cell-cell contact of the central synapse incorporates dystrophin and not utrophin. Dystrophin immunostaining appears in a punctate pattern around the cell bodies and along the dendrites of cerebral cortical cells and cerebellar Purkinje cells (Lidov, 1996). Unlike in the photoreceptors of the OPL, dystrophin is associated with the postsynaptic specializations of cortical neurons (Lidov et al., 1993) and is concentrated in mouse and human brain postsynaptic density fractions (Kim et al., 1992). α-dystroglycan immunoreactivity appears in a similar pattern on the surface of Purkinje cell bodies, dendrites, and dendritic spines (Smalheiser and Kim, 1995; Tian et al., 1996). Surprisingly, β-dystroglycan immunoreactivity is not detected in these localizations (Lidov, 1996). In no other region is α-dystroglycan without β-dystroglycan (Figure 6).

In the periphery, agrin is made by both muscle cells and motor neurons. Neurons produce the agrin$_{(4,8)}$, agrin$_{(4,11)}$, and agrin$_{(4,19)}$ splice forms, which are secreted into the extracellular matrix at the NMJ. In cultured chick myotubes, neuronal agrin possess much more clustering AChR activity than muscle-produced agrin$_{(0,0)}$ and binds α-dystroglycan with higher affinity (O'Toole et al., 1996). In the brain,

large amounts of agrin are made by neurons and glia and are secreted into extracellular matrix. Neuronal-type agrin appears to bind to cultured hippocampal neurons at synaptic sites. In contrast, other agrin isoforms do not demonstrate synapse-specific binding sites (David Wells, Brown University). Unfortunately, the identity of these binding sites has not yet been determined.

Thus, in some areas, brain dystroglycan continues to be involved in linking the extracellular matrix to the cytoskeleton. At the blood-brain barrier for example, α- and β-dystroglycan colocalize with utrophin and laminin. In contrast, there appear to be brain regions in which β-dystroglycan does not colocalize with its usual partners. The presence of dystrophin and α-dystroglycan, and the absence of detectable β-dystroglycan, in synapse-rich regions is quite remarkable, and difficult to accept. Intrigued, I undertook a deeper examination of dystroglycan's brain distribution, hoping to reconcile dystroglycan's nontraditional arrangement at central synapses.

3. Methods

Northern blot hybridization

The ^{32}P-labeled dystroglycan oligonucleotide probes (probe1 and probe3) were synthesized by PCR using the dystroglycan clone DNI22 (provided by Yiu-mo Chan, Kunkel Lab) as template and the following primer pairs.

probe1: F1=GAACTGGACGACTCCAAGCCCCC R1=GGCTGGTAGGGAGGCGCATTGGG

probe3: F3=AGCCCCCACCGCCCTTCACAGTA R3=GGACATAGGGAGGAGGTGACCG

The human Multiple Tissue Northern Blots (MTN; Clontech; Palo Alto, CA) were prehybridized in ExpressHyb for 30 minutes at 68°C. The probe (probe1 or probe3) was denatured at 95°C, diluted in ExpressHyb, and incubated with the blot for 1.5 hours at 68°C. After hybridization, the blot was washed extensively; the most stringent wash performed was 0.1X SSC, 0.1% SDS, at 55°C for 40 minutes. Probe hybridization was analyzed by autoradiography.

Brain cDNA Library Screen and DNA sequencing

A random primed, rat hippocampus cDNA library constructed in the vector λgt11 (Clontech) was plated and screened as per manufacturer's protocol. Screening by hybridization was performed first for probe1. Positively hybridizing phage were plaque purified, and rescreened by hybridization with probe3. PCR with λgt11 primers was then used to determine the insert length of phage that hybridized positively with probe3. Each of the unique phage inserts was then sequenced at the Children's Hospital/HHMI sequencing facility (Boston, MA). Sequences were analyzed using the software Sequencher.

Brain Subcellular Fractions

Postsynaptic density (PSD) fractions were prepared using a modification of the procedures of Carlin and Dosemeci (Carlin et al., 1980; Dosemeci and Reese, 1993). Frozen rodent brains were obtained as follows: *mdx* mice and age/sex matched controls were obtained from the Jackson Laboratory, frozen *3CV* mice brain and muscle tissue was a

generous gift from Jeff Chamberlain, University of Michigan (Cox et al., 1993), and frozen adult rat brains were obtained from Pel-Freeze. Brain tissue was homogenized with a motor operated, tight-fitting, Teflon-glass homogenizer in homogenization solution (0.32M sucrose, 1 mM $MgCl_2$, 1 mg/ml leupeptin). The homogenized tissue was centrifuged 1400 x *g* for 10 minutes. The supernatant (S1) was saved and the pellet was resuspended, rehomogenized, centrifuged at 710 x *g* for 10 minutes, and the supernatant (S2) was collected and pooled with above (S1). This pooled material was spun 710 x *g* for 10 minutes and this supernatant is referred to as the "homogenate fraction" (H). The homogenate was centrifuged 13800 x *g* for 10 minutes, and the resulting pellet was resuspended in 0.32M sucrose, and layered onto a discontinuous sucrose gradient (1.2/1.0/0.85 M sucrose). Following centrifugation at 82,500 x *g* for 2 hours, the synaptosome-containing fraction was collected from the 1.2/1.0 M sucrose interface. This material was resuspended in 1 mM HEPES, pH 7.4, and is referred to as the "synaptosomal fraction" (SX). This was diluted with 1 volume of 1% Triton-X 100, 0.32 M sucrose and stirred on ice for 15 minutes. This solution was centrifuged 36,000 x *g* for 30 minutes. The Triton-insoluble pellet was resuspended in 0.32M sucrose with a Dounce homogenizer. This sample was layered onto a discontinuous sucrose gradient (2.1/1.5/1.0M). The gradients were centrifuged at 200,000 x *g* for 30 minutes. The fraction enriched with postsynaptic densities was collected from the 2.1/1.5M interface and diluted with 1 mM HEPES, pH 7.4. This fraction was then diluted with one volume of 1% Triton-X 100, 150 mM KCl, and layered onto a 2.1 M sucrose cushion and spun 200,000 x *g* for 30 minutes. The material at the interface was collected, resuspended in 20 mM HEPES, pH 7.4, and further purified on a final 2.1M sucrose cushion. The resulting "PSD fraction" (PSDs) was resuspended in 20% glycerol and stored at -80°C. The absence of presynaptic contaminants and presence of PSD proteins in the PSD fraction was confirmed by western blotting with antibodies to NMDAR1, αCaMKII, and synaptophysin (Wu et al., 1998).

Antibodies and Western Blotting

Ab98 antiserum was raised by immunizing a rabbit with the peptide KAPLPPPEYPSQ (a sequence in the cytosolic domain of β-dystroglycan that was used for the production of antibody PA3a (Yoshida et al., 1993) and affinity purified (Quality Controlled Biochemicals, Hopkinton, MA). The anti-peptide antiserum 12031C to β-dystroglycan was a generous gift of L. Kunkel. The anti-β-dystroglycan and anti-dystrophin monoclonal antibodies NCL-43DAG and DYS2, respectively, were obtained from Novocastra. DYS2 recognizes full-length dystrophin, as well as short forms of dystrophin. The anti-αCaMKII (#6G9) and anti-synaptophysin monoclonal antibodies were obtained from Boehringer Mannheim, the anti-NMDAR1 monoclonal antibody was obtained from Pharmingen, and the polyclonal anti-mouse CPEB antibody was obtained from Joel Richter, University of Massachusetts, Worcester (Wu et al., 1998).

Protein concentrations were determined with the BCA protein assay (Pierce, Rockford, IL), using bovine serum albumin (BSA) as a standard. Equal quantities of muscle lysate (provided by Helene Sadoulet-Puccio, Kunkel Lab), homogenate, synaptosomal, and PSD proteins were separated by SDS-PAGE, and transferred onto nitrocellulose. The primary antibodies used are described above. Species specific alkaline phosphatase-conjugated goat anti-rabbit or anti-mouse IgG (Boehringer Mannheim) was used as the secondary antibody, and the bound antibody was visualized using the BCIP/NBT substrate system (Promega, Madison, WI). For Western blotting with DYS2, horseradish peroxidase-conjugated anti-mouse IgG was used as the secondary and the immunoreactivity was visualized by ECL chemiluminescence with equivalent exposures (Amersham).

Ligand Overlay Assay

Nitrocellulose blots of homogenate, synaptosome, and PSD proteins were blocked for 4 hours at 4°C in Hanks Buffered Saline Solution, 5% nonfat dry milk, 1% bovine serum albumin, 10% horse serum, pH 7.4. Blots were incubated overnight at 4°C in the presence of 1 mM EGTA or 1 mM Ca^{++} and heparin (1 mg/ml) or antibody IIH6 (1:5, gift from Kevin Campbell (Ervasti and Campbell, 1991)) where indicated. Recombinant rat

agrin was collected from the conditioned medium from COS cells transfected with cDNA clones encoding rat agrin$_{(4,8)}$ or agrin$_{(0,0)}$. Blots were washed and incubated with a second layer containing 1 µg/ml iodinated (^{125}I) (IODOGEN, Pierce) anti-agrin monoclonal antibody 131 (Amersham) (^{125}I-MAb-131) for 30 minutes. Blots were then washed and dried, and agrin binding polypeptides were visualized by autoradiography.

Hippocampal neuron cultures and immunohistochemistry

Low density cultures were created as previously described (Goslin and Banker, 1991). Briefly, the hippocampus was removed from E18 rat embryos, trypsinized (0.25%), dissociated by trituration, and plated onto poly-L-lysine (1 mg/ml) coated glass coverslips in modified Eagle's medium (MEM, Gibco) with 10% horse serum for 4 hours. The coverslips were then transferred to dishes containing a monolayer of glial cells in growth medium consisting of MEM, ovalbumin (100 µg/ml) pyruvate (1.1 µg/ml), glucose (0.6%) and N2 supplement. The culture medium was changed weekly. After 19-21 days, the cells were fixed with 4% paraformaldehyde at 37°C for 20 minutes, covered with saponin (0.05%) for 5 minutes and then incubated in blocking solution (MEM, 10% horse serum, 1% goat serum, 1% BSA). The primary antibodies, mouse anti-synaptophysin (Boehringer), NCL-43DAG (Novocastra), were applied overnight at 4°C and species specific secondary antibodies, directly conjugated to either FITC (Caltag) or Cy3 (Jackson Laboratory), were applied for 1 hour at room temperature. The coverslips were mounted onto glass slides with Citifluor (Ted Pella).

Neuron and glia cell lysates

Neuron and glia cultures were plated at high density (300,000 cells/10 cm culture dish), and grown as described above. After 1 week in culture, cells from 3-4 dishes were rinsed in 16 mM HEPES, pH 7.4, lysed for 20 minutes at 4°C in 20 mM HEPES, pH 7.4, 1% Triton X-100, 150 mM NaCl, 0.5 µg/ml leupeptin, 1 mM PMSF, and collected by scraping. Collected material was homogenized (10 strokes) in a small Dounce

homogenizer. Cell homogenate was spun at 36,000 x *g* for 45 minutes and supernatant (trichloroacetic acid precipitate) and pellet were analyzed by western blotting.

4. Results

In muscle, dystroglycan is both a member of the DAPC and a NMJ protein with high affinity for agrin and laminin. At the presynaptic membrane of photoreceptors in retina, dystroglycan and dystrophin colocalize. Since dystrophin is also found concentrated at central synapses, I hypothesized that brain dystroglycan or a dystroglycan-like protein colocalizes with dystrophin at these synapses. I therefore initiated a careful examination of dystroglycan's expression in the brain and at synapses. I first assayed the expression of the dystroglycan transcript(s) in various brain regions and pursued a potential dystroglycan splice variant. Next, I established the distribution of α- and β-dystroglycan in normal brain biochemical fractions enriched for synaptic proteins, and assessed the effects of dystrophic genotypes on dystroglycan's synaptic fractionation profile. Lastly, I determined the pattern of dystroglycan expression in cultured glial and hippocampal neuronal cells.

4.1 Distribution of dystroglycan mRNAs in regions of brain

I began my investigation of brain dystroglycan by determining the distribution of dystroglycan transcripts among various regions of the brain. I screened a human brain region Northern blot with two DNA fragments, probe1 and probe3, that corresponded to the proximal and distal C-terminal regions of dystroglycan, respectively (Figure 7). Both probes hybridized to an approximately 6 kb mRNA that was highly expressed in all brain regions. Hybridization with probe1, but not with probe3, revealed other transcripts. A larger transcript (over 10 kb), which was expressed in cerebral cortex as well as occipital and frontal lobe, represented a potential splice variant of dystroglycan that lacked the sequence encoding the dystroglycan C-terminus.

This observation suggested that in brain there is at least one transcript in addition to dystroglycan that contains sequence similar or

identical to probe1 but not probe3. To pursue such brain-specific, potentially dystroglycan-related transcripts, I used both probes to screen a rat brain (hippocampal) library. By pursuing only plaques that were positive for probe1 and negative for probe3, I avoided many standard dystroglycan cDNAs that were positive for both dystroglycan probes.

The proximal probe1 hybridized to approximately 50 plaques. I plaque purified these, and found that the distal probe3 did not hybridize to approximately 20 of the 49 probe1-positive phage. I determined that 15 of these phage contained uniquely-sized cDNA inserts and each was sequenced. I compared all of the cDNA insert sequences to the published mouse dystroglycan cDNA (DAG1). With the exception of one exceptionally large insert (4.5 kb), which contained genomic sequence in addition to dystroglycan coding sequence, there was complete sequence identity to the published dystroglycan cDNA. Since many of the sequences ended abruptly just upstream of the region corresponding to the distal probe3, it appeared that in the course of the library's construction, this region of the dystroglycan cDNAs was disproportionately targeted for cleavage. None of the cDNA fragments that I isolated contained sequence that diverged from the dystroglycan sequence (Figure 8).

The Northern analysis verified the extensive dystroglycan expression in all regions of human brain. The extensive library screen however furnished no evidence of alternative splicing in dystroglycan's C-terminal region.

4.2 Distribution of dystroglycan and an immunologically related protein

Since dystroglycan's associations in muscle and retina suggested that brain dystroglycan is present at central synapses, I then focused my investigation on the potential synaptic distribution of brain dystroglycan.

4.2.1 Synaptic Subcellular Fractions

Like the NMJ, central synapses have elaborate postsynaptic apparatuses. At central synapses, just below the postsynaptic membrane, is a dense parcel of proteins, the postsynaptic density (PSD). The position and make-up of this neuronal specialization suggests that it is important in the development, function, and plasticity of the synapse (see Chapter II).

Biochemical preparations that are enriched for this synaptic machinery have proven valuable for investigating the synaptic structure. Many molecules that have a role in synaptic function are concentrated in preparations that successively enrich for synaptic membranes (synaptosomes) and postsynaptic densities (PSDs) (Figure 9). To determine if brain dystroglycan associates with synaptic components, I biochemically prepared brain homogenate, synaptosome, and PSD-enriched fractions and probed western blots of these subcellular fraction proteins for α- and β-dystroglycan.

4.2.2 Dystroglycan in Synaptic Subcellular Fractions

To first follow the subcellular fractionation profile of α-dystroglycan, I employed a well-described method for α-dystroglycan detection, the ligand blot overlay (Deyst et al., 1995). I incubated a blot of subcellular fraction proteins with in vitro produced rat agrin, and then detected the agrin, specifically bound to α-dystroglycan, with a radiolabeled anti-agrin monoclonal antibody.

I found that α-dystroglycan was present in brain homogenate and was concentrated in the synaptosome fraction. In addition, a small population of α-dystroglycan was detectable in the PSD fraction. The agrin-binding properties of rat brain α-dystroglycan appeared to mirror those of *Torpedo* electric organ α-dystroglycan (Bowe et al., 1994; O'Toole et al., 1996): the binding of the isoform agrin$_{(0,0)}$ exceeded the binding of agrin$_{(4,8)}$ (Figure 10A). α-dystroglycan's agrin-binding capacity required the presence of Ca^{++}, was increased in the presence of heparin, and was inhibited by the anti-α-dystroglycan antibody IIH6 (not shown).

Then, using standard western blotting techniques, I probed similar blots of subcellular fractions with antibodies to β-dystroglycan. Like its associate α-dystroglycan, β-dystroglycan was present in brain homogenate and was concentrated in the synaptosomal fraction. This pattern was observed in subcellular fractions isolated from rat cortex, hippocampus, and cerebellum. In contrast, β-dystroglycan was not detected in the PSD fraction (Figure 10B,C).

One β-dystroglycan antiserum, Ab98, recognized not only β-dystroglycan, but also a pair of polypeptides of 58 kDa and 53 kDa that were selectively enriched in PSD fractions from all brain regions. These PSD-enriched polypeptides were designated p58/53. Antibodies NCL-43DAG and 12031C revealed a similar distribution of β-dystroglycan in these fractions, but these reagents bound neither p58 nor p53 (not shown). The presence of dystrophin and α-dystroglycan in the PSD fraction, and the absence of detectable β-dystroglycan in the PSD fraction, made these β-dystroglycan-like proteins intriguing.

4.2.3 Dystroglycan in synaptic subcellular fractions from brains of *mdx* and *3CV* mutant mice

Whereas full-length dystrophin is concentrated in the PSD fraction, I found that β-dystroglycan was concentrated in the synaptosome fraction. Interestingly, I determined that the brain-specific short dystrophin isoform DP71 fractionated in a pattern like that of β-dystroglycan (Figure 11). In DMD, *mdx*, and *3CV* affected muscle, the expression of the DAPC is diminished, presumably in response to the absence of dystrophin. To assess the response of brain dystroglycan to the absence of full-length dystrophin and to the absence of all short dystrophin isoforms, I performed the experiments described above using subcellular fractions prepared from *mdx* and *3CV* mice.

It has been shown that levels of β-dystroglycan are unaffected in *mdx* brain (Ibraghimov et al., 1992). To confirm this, I demonstrated that levels of α- and β-dystroglycan were normal in synaptosomes prepared from *mdx* mice. Others have shown this as well (Greenberg et al., 1996). Before examining the effect of the *3CV* genotype on the

expression of brain dystroglycan, I established that the synaptic markers αCaMKII and NMDAR1 were unaffected in *3CV* fractions, and verified that DP71 was absent from *3CV* mice subcellular fractions (not shown).

Then, using ligand overlay experiments, I found that the level of α-dystroglycan was slightly lower in *3CV* brain as compared to *mdx* or unaffected mice. By probing western blots with the β-dystroglycan antibody NCL-43DAG, I determined that levels of β-dystroglycan in the brains of *3CV* mice were substantially decreased (Figure 12). Greenberg et al. have obtained similar results (Greenberg et al., 1996). In contrast, levels of p58/53 were unaffected in *mdx* or *3CV* mice, suggesting that p58/53 does not interact with any form of dystrophin (not shown).

The results from the *mdx* subcellular fraction studies suggest that no population of α- or β-dystroglycan functionally interacts with full length dystrophin in mouse brain. In contrast, the parallel distribution and decrease of DP71 and α/β-dystroglycan in the fractions from *3CV* mouse brain suggests that, unlike in muscle, a population of α-dystroglycan and a majority of β-dystroglycan are associated with DP71 and/or other short forms of dystrophin.

4.3 Dystroglycan in cultured neurons and glia

The concentration of the α- and β-dystroglycan in the synaptosomal fraction suggests that they cofractionate with synaptic membranes and may be associated with synapses in vivo. Indeed, immunofluorescent staining of cultured hippocampal neurons with an antibody directed against brain α-dystroglycan (cranin) revealed a striking pattern of staining that colocalizes with synapses (not shown; David Wells, Brown University).

The distribution of β-dystroglycan did not parallel that of a-dystroglycan, however. Immunofluorescent staining with a b-dystroglycan-specific monoclonal antibody revealed β-dystroglycan immunoreactivity

throughout glia and hippocampal neurons in a pattern that was not synapse-specific (Figure 13A). To corroborate this finding, I used Western blotting to demonstrate large quantities of β-dystroglycan in cell lysates from cultured glia (not shown) and hippocampal neurons (Figure 13B).

4.4 p58/53 is not a β-dystroglycan-related protein

In contrast to β-dystroglycan, p58/53 was not detected in glial or hippocampal neuron lysates. However, p58/53 was found associated with the neuronal detergent insoluble pellet (Figure 13C), while β-dystroglycan was not (not shown). Interestingly, p58/53 was found specifically concentrated at synapses in the hippocampal neuron cultures.

Resolved to determine if p58/53 was a β-dystroglycan relative, I sought the identity of this polypeptide pair. I purified a sufficient amount of p58/53 for MALDI-TOF analysis and peptide microsequencing. Database searches with these data revealed that p58/53 is a known protein, Insulin Receptor Tyrosine Kinase Substrate p58/53, and its cDNA has been cloned (IRSp53) (see Chapter II). Sequence analysis exposed a region of similarly between IRSp58/53 and β-dystroglycan that accounts for their immunologic relatedness. In addition, both proteins possess proline-rich regions that probably represent WW binding domains. This is the extent of the similarity between IRSp58/53 and β-dystroglycan, however.

5. Discussion

The dystroglycan transcript, which is expressed throughout the brain, encodes a single propeptide from which both α- and β-dystroglycan derive. Although α- and β-dystroglycan are linked at the level of translation, it appears that once cleaved into distinct proteins, their association is customary but not compulsory. As a unit, α/β-dystroglycan link matrix molecules to dystrophin-like cytoskeletal proteins. As a complex or individually, the dystroglycans may have additional associations.

The function of dystroglycan in muscle has been inferred by both its protein-protein associations, and the cellular consequences of its decreased expression in disease environments. For the most part, dystroglycan's protein associations are similar in brain and in muscle: β-dystroglycan binds utrophin, dystrophin, and short dystrophin isoforms, while its associate, α-dystroglycan, binds types of laminin or agrin. Thus, one of dystroglycan's main biologic functions in muscle and in some areas of the brain is to anchor cells to the basement membrane. In many muscular dystrophies, the secondary loss of dystroglycan contributes to the breakdown of the muscle cell. Thus, dystroglycan is believed to participate in maintaining the integrity of the muscle cell membrane. The CNS consequence of these disease states is more complex, however. To understand the role of dystroglycan in diseased brains, the associations and function of dystroglycan in the healthy brain must first be understood.

At some brain sites, including the blood-brain barrier, dystroglycan maintains typical associations and performs its usual function, linking the cellular cytoskeleton to the extracellular matrix. In retina, at the photoreceptor's presynaptic membrane, α/β-dystroglycan and a form of dystrophin colocalize, and appear to form a complex. At central synapses however, traditional dystroglycan associations may be abandoned. Here, dystrophin is concentrated at the postsynaptic apparatus, and α-dystroglycan colocalizes to synapses as well, in the absence of detectable β-dystroglycan. These results indicate that at

brain synapses, neither α-dystroglycan nor full-length dystrophin is associated with β-dystroglycan. This atypical situation suggests that α- and β-dystroglycan may have functions distinct from their traditional cell-matrix union work and that there may be dystroglycan associations that have yet to be uncovered.

A variety of experimental strategies can be used to obtain further information about dystroglycan's role in the brain. To directly assay the physiologic role of dystroglycan in brain, the new technology of tissue specific knockout animals is obviously attractive. Using the Cre recombinase *loxP* system, with tissue specific, inducible promoters, transgenic mice can be created that overexpress or underexpress a chosen gene in a selected tissue during a given time. Careful examination of the cells, tissue, and behavior of an animal whose brain lacks dystroglycan is the most direct way to assess the effects of dystroglycan on CNS development as well as during adulthood. Though this method is enticing, it is not yet well tested, is labor-intensive, and may yield nonviable pups or animals without an identifiable mutant phenotype. Alternatively or additionally, more traditional biochemical, immunochemical, and molecular methods can be used to establish further insight into the role of dystroglycan in the brain.

5.1 A dystroglycan-utrophin complex at the blood-brain barrier

At the blood-brain barrier, α- and β-dystroglycan appear to function in cell-matrix adhesion, linking glial utrophin to laminin in the epithelial extracellular matrix. It appears that a "utrophin associated protein complex" helps to enforce the blood-brain barrier. One would thus predict a leaky blood-brain boundary in individuals with the congenital muscular dystrophy caused by mutations in the gene for the alpha-2 chain of laminin. This hypothesis could be directly tested by analyzing the integrity of the blood-brain interface in the *dy* mouse, which carries a mutation in the gene for the alpha-2 chain of laminin.

Since there are many types of laminin, it is likely that other laminins can partially compensate for the loss of the alpha-2 chain. Thus, in individuals or mice that lack alpha-2 laminin, the matrix defects may be subtle. The phenotype exhibited by patients with abnormal expression of alpha-2 chain indicates that the role of this laminin in brain is complex.

5.2 Dystroglycan and DP71: A brain "DAPC"?

The above-mentioned results from experiments using tissue from *mdx* and *3CV* mice indicate that a population of α- and β-dystroglycan are associated with one or more of the short forms of dystrophin. Mice lacking full-length dystrophin (*mdx*) exhibit normal levels of brain dystroglycan, whereas mice with diminished expression of all forms of dystrophin (*3CV*) exhibit a decreased expression of dystroglycan. The retention of dystroglycan in *mdx* mice may be partially explained by a compensation for full-length dystrophin by short dystrophin isoforms. Alternatively, it may be that β-dystroglycan does not associate with any of the full-length dystrophin in brain, and the major dystroglycan-associated cytoskeletal components are utrophin and short dystrophins such as DP71.

Indeed, new results indicate that the *3CV* mouse is a more appropriate model than classical *mdx* for studying the CNS effects of DMD. This is not surprising in light of the observation that, unlike DMD patients and *3CV* mice, *mdx* mice have normal ERGs. New data shows that microsomes isolated from DMD affected brains exhibit greatly reduced levels of β-dystroglycan (Finn et al., 1998). This result parallels the finding that *3CV* synaptosomes have decreased levels of β-dystroglycan and α-dystroglycan. These results implicate dystroglycan's relationship with short dystrophins in the cognitive impairment seen in DMD. One would thus expect *3CV* mice to suffer from mild "cognitive" deficits. However, no cerebral abnormalities have been identified to date.

In order to pursue the existence of this putative dystroglycan-DP71 complex in brain, the brain regions and cell types in which the

presumed dystroglycan-DP71 complex exists must be established. In situ hybridization studies show that DP71 mRNA is specifically expressed in the granule cells of the dentate gyrus in the hippocampus, as well as in olfactory bulb, cerebral cortex, and the CA-3 region of the hippocampus (Gorecki and Barnard, 1995). Thus, DP71 and dystroglycan transcripts are found together in at least the dentate gyrus and olfactory bulb. Do the patterns of protein expression overlap as well? Although standard immunofluorescence studies would be well suited to this task, distinguishing amongst the dystrophin isoforms is, at present, difficult. One way to simplify this investigation would be to utilize tissue from *mdx* mice. Dystroglycan levels are unaffected in these mutants and, since full-length dystrophin is not expressed, antibodies directed against the C-terminus of dystrophin will identify only short forms. SDS-PAGE can be used to subsequently determine the relative isoform expression in the region or cell types studied.

Another piece of evidence supporting the existence of a dystroglycan-DP71 complex exists. When solubilized brain samples are run on sucrose gradients, the majority of the DP71 and β-dystroglycan cofractionate, whereas in liver samples, only a fraction of the DP71 cofractionates with β-dystroglycan (Greenberg et al., 1996). Despite the likelihood of a physical interaction between β-dystroglycan and DP71, coimmunoprecipitation attempts have failed (Greenberg et al., 1996). Upon identification of cell types that express both dystroglycan and DP71, that cultures of these or similar cells can be examined. Successful coimmunoprecipitation might be accomplished from sources enriched for these two molecules, such as synaptosomes or an appropriate cell lysate. It is possible that β-dystroglycan associates with other short forms of dystrophin such as DP140, instead of or in addition to DP71. As mentioned, the antibodies that recognize the C-terminus of dystrophin cannot distinguish amongst the short isoforms. Thus, isolation of a native dystroglycan-dystrophin isoform complex would verify which of the isoforms interacts with dystroglycan, since the molecular weight of the dystrophin form can be determined by SDS-PAGE. Methods for the isolation of such a complex are discussed below.

What is the role of a dystroglycan-DP71 complex in the brain? Although the absence of short dystrophins in causes abnormal retinal findings, in *3CV* no additional CNS dysfunctions have been identified. When this brain complex is disrupted in *3CV*, what is the consequence? These mice must be carefully examined and compared to *mdx* and normal mice in behavioral and learning paradigms. In addition, the subcellular expression of dystroglycan and DP71 (DP140) in normal and affected cells must be examined. Primary neuronal and glial cultures from dystrophin mutant mice (*mdx* and *3CV*) or from their heterozygous litter mates (which express both dystrophin positive and negative cells) can be generated. Using this system, the glial as well as synaptic and nonsynaptic expression of α- and β-dystroglycan, full-length dystrophin, and short dystrophin isoforms can be compared in normal and affected cells.

Does this putative dystroglycan-DP71 complex represent the core of a brain DAPC? Although one expects the DAPC to be recapitulated centrally, such a complex has not yet been isolated from brain. Standardly, the DAPC is isolated from muscle extracts using affinity chromatography (WGA) methods. Presumably, these techniques can be optimized to isolate dystroglycan-DP71 complexes from brain fractions such as synaptosomes, or from cell cultures of neurons or glial cells. Similarly, immunoaffinity chromatography might yield a non denatured dystroglycan-dystrophin isoform complex. Successful biochemical isolation of a dystroglycan-DP71 complex from brain would indicate whether or not a brain DAPC that resembles the muscle DAPC exists. Indeed, the identification of any brain proteins that associate with dystroglycan and DP71 would shed light on this current question.

It may be that the complex formed by dystroglycan-DP71 and associated proteins cannot withstand biochemical isolation. If this is the case, then associated proteins must be identified individually. Overlay methods are commonly used to successfully identify binding proteins for a protein of interest. It is often difficult to uncover interacting brain proteins because of the complexity of this protein source. On a standard protein blot of brain homogenate, many bands will appear to bind a protein such as dystrophin. To successfully identify

brain proteins that specifically interact with dystroglycans or dystrophins, the complexity of the protein source must be lessened. One way to achieve this end employs standard biochemical techniques. Synaptosomes represent a brain protein source that is likely to be concentrated for proteins which interact with synaptic dystrophin forms. The powerful separation technique of two dimensional (2D) gel electrophoresis can then be used to increase the electrophoretic resolution of the synaptosome fraction (see chapter II). One might successfully identify brain DAPC members by probing a blot of synaptosomes, separated by 2D gel electrophoresis, for protein spots which bind dystroglycan and/or forms of dystrophin. Since 2D separated proteins have a characteristic shape and isoelectric mobility, binding proteins exposed in this way would be readily identified.

Alternatively, valuable information about dystroglycan's protein-protein interactions might be obtained through the use of molecular methods. The yeast two hybrid assay has been used extensively by many labs to screen muscle cDNA libraries for interactions among DAPC proteins. In this case, one would screen a brain cDNA library for protein fragments that interact with regions of dystroglycan and/or DP71. A cDNA that interacts with one of these "baits" may represent a novel protein, or may encode a brain protein that had not yet been appreciated as a dystroglycan or DP71 binding partner. Identification of dystrophin-DP71 associated proteins would provide valuable information about the nature of this alliance.

5.3 Dystroglycan at central synapses

It is increasingly evident that in many regions of the CNS, α/β-dystroglycan interacts with short forms of dystrophin, including DP240, DP140, and DP71. In retina, this complex has been implicated in healthy retinal synaptic transmission. In brain homogenate and synaptosomes, there are substantial amounts of both dystroglycan and DP71, and a similar complex is now thought to exist in vivo in some regions of the

brain. In the DMD and *3CV* (but not *mdx*) genotypes, the level of brain dystroglycan expression is affected, indicating that dystroglycan and forms of dystrophin are likely to interact. Additionally, the CNS component of many muscular dystrophies suggests a role for dystroglycan in cognition. Dystroglycan appears to have many roles in the CNS. Of these however, its role in neurons is the most mysterious.

Large amounts of β-dystroglycan are produced by rat hippocampal neurons in culture. Does neuronal dystroglycan have a role at synapses? Indeed, dystroglycan appears to be engaged in atypical associations at central synapses. Here, the localization, makeup, and perhaps function of dystroglycan and its associated proteins is altered. The results presented above show that at synapses, β-dystroglycan is not detected, while α-dystroglycan and full-length dystrophin are colocalized. One surprising conclusion may be that synaptic α-dystroglycan does not associate with β-dystroglycan, and β-dystroglycan does not associate with full-length dystrophin. This would suggest that, individually, α- and β-dystroglycan may find alternate associations and have distinct functions. The observation that α- and β-dystroglycan do not coexist at synapses must be validated with further investigation, since this is the first instance in which α- and β-dystroglycan are not found together. Is the synapse site extraordinary, or are there other sites in which α- and β-dystroglycan do not coexist? Often, evidence for the presence of one dystroglycan species has been considered sufficient proof that the other is present as well. Now, at all sites, both α- and β-dystroglycan must be accounted for before it is concluded that the two coexist.

What is the role of DAPs at synapses? In the healthy brain, dystrophin is localized to the postsynaptic apparatus, and α-dystroglycan colocalizes with dystrophin at synapses in vivo. First, the role of dystrophin at synapses can be examined. In *mdx* mice, disruption of full-length dystrophin expression may affect memory. At *mdx* synapses, is dystrophin replaced by an alternate such as DP71 or utrophin? What are the physical or functional consequences from the absence of dystrophin's N-terminus in *mdx*? If compensation does occur, mice that express no dystrophins (*3CV*) or neither dystrophin nor utrophin

(*mdx*/utrophin null) must be examined for functional synapses. To achieve this, neurons from mutant mice can be grown in culture, and the development of spines and the function of the synapses can be assayed.

Both α- and β-dystroglycan are associated with the synaptosomal subcellular fraction. At least two explanations for this finding must be considered. High levels of β-dystroglycan have been demonstrated in the pia mater layer of the brain (see above). If membranous pial material co-fractionates with synaptic membranes in the synaptosomal fraction, this subset of brain α-dystroglycan may be that associated with pial β-dystroglycan. This question could be answered by comparing the standard synaptosome preparation to one that includes a simple filtering step to trap the pial material.

Alternatively, β-dystroglycan may be associate with a subset of α-dystroglycan at a synaptic location. Interestingly, only α-dystroglycan is concentrated at synapses in culture. This synaptic population of α-dystroglycan may correspond to the small subpopulation of α-dystroglycan that associates with the PSD fraction. What is the role of the synaptic α-dystroglycan? There is not yet enough data to form a convincing conclusion. Currently there is no evidence for an agrin activated, brain specific kinase analogous to MuSK. However, blot immobilized brain α-dystroglycan has the capacity to bind in vitro expressed $agrin_{(0,0)}$ and $agrin_{(4,8)}$. Interestingly, the pattern of α-dystroglycan immunostaining on cultured hippocampal neurons overlaps the pattern of $agrin_{(4,8)}$ binding sites, but not that of $agrin_{(0,0)}$ binding sites. Demonstration of a physical or functional association between neuronal agrin and α-dystroglycan has yet to be firmly established, however.

In some way, α-dystroglycan is associated with the synaptic membrane. Whether this association is pre- or postsynaptic could be resolved with immuno-electron microscopy, as it was for dystrophin. More importantly perhaps, is the question of whether or not synaptic α-dystroglycan and dystrophin are functionally linked. Although there is no apparent change in the level of α-dystroglycan expression in brains from mice that lack dystrophin (*mdx*), it may be that only a very small

population of α-dystroglycan associates with dystrophin. Thus, synapses from these mutants must be assayed for the presence of α-dystroglycan.

If α-dystroglycan remains associated with the synapse in the absence of dystrophin, there is little reason to suspect that the two are physically linked. Otherwise, a fascinating question arises: what links α-dystroglycan and dystrophin, if not β-dystroglycan? The successful isolation of a synaptic dystrophin complex or the identification of new α-dystroglycan or dystrophin interacting proteins might resolve this question. The C-terminus of dystrophin contains a WW domain, a protein-protein interaction module. This region is distinct from dystrophin's dystroglycan binding site. Dystrophin has a site available for interaction with the proline-rich (WW binding) region of a potential binding protein. To date, no proteins have been identified that interact with dystrophin's WW domain. This region of dystrophin therefore represents a potentially fruitful bait for the yeast two hybrid assay.

Although α-dystroglycan and dystrophin are each associated with synapses, a relationship between the two has not been established. If there is a physical association, the mechanism by which this occurs remains unknown; the traditional physical link, β-dystroglycan, is missing at synapses. Could there be a β-dystroglycan-like protein at synapses? Seemingly not. The Northern analysis and a cDNA library screen presented above provided no evidence for brain-specific splice forms of dystroglycan. Two proteins that are immunologically related to β-dystroglycan have been identified in the PSD fraction. Mummery et al. describe a 164 kDa protein in PSD fractions that is recognized by a β-dystroglycan antibody (Mummery et al., 1996). No further similarities between the 164 kDa PSD polypeptide and dystroglycan have been shown since, however. I have identified the PSD polypeptide pair, p58/53, that is bound by our β-dystroglycan antiserum and determined that it is decidedly not a dystroglycan-like protein.

5.4 Novel dystroglycan associations

There may be dystroglycan binding partners that have yet to be realized at synapses, as well as at nonsynaptic sites. One potential dystroglycan associated protein may be fukutin, the product of the FCMD disease gene. In muscle, a functional association between dystroglycan and fukutin is probable. Muscle levels of β-dystroglycan and laminin alpha-2 chain are reduced when fukutin is absent, and the basal lamina surrounding the muscle is abnormal. Fukutin is expressed in brain too, where the basal lamina of FCMD brain is similarly disrupted (Hayashi et al., 1993; Matsumura et al., 1993).

If indeed an association between dystroglycan and this novel protein is established in vitro and in vivo, a new role for dystroglycan in muscle and brain may emerge. Antibodies specific for fukutin have not yet been successfully generated. Once this tool is available, the pattern of overlap between fukutin and dystroglycan expression can be determined and perhaps a fukutin protein complex can be isolated. Then, an examination of the effect of fukutin deficiency on dystroglycan expression in brain may indicate a relationship between dystroglycan and fukutin. The identification of any fukutin-associated proteins will further our knowledge about how fukutin deficiency causes the CNS abnormalities seen in FCMD. The potential association between fukutin and dystroglycan is intriguing. If dystroglycan-fukutin associations are detected, the understanding of one of dystroglycan's roles in the brain will advance significantly.

5.5 Conclusion

The functions of dystroglycan in the brain and at synapses remain largely undiscovered. It seems likely that in the brain, alternative associations occur among proteins known to interact with dystroglycan. As information regarding the cellular and subcellular brain expression profiles of proteins such as DAPC members and agrin are obtained, the

functions of these proteins in the brain can be considered. Further studies of disease phenotypes such as FCMD should provide insights concerning the function of affected gene products and their partners. Brain specific dystroglycan knockouts are likely to provide functional information as well. The presence of CNS pathologies in a variety of muscular dystrophies, and the potential nontraditional associations of dystroglycan in the brain and at synapses, suggest that an understanding of dystroglycan's role in the brain will provide deep insights into brain development and function.

6. Tables and Figures

6.1 Figure Legends

Figure 1. Dystroglycan

The dystroglycan coding sequence includes two exons separated by one large intron. The dystroglycan mRNA is 5.8 kb. The regions of the transcript that correspond to the two DNA probes (probe1 and probe3) used for the Northern blotting and cDNA library screen (discussed in Results) are indicated. The dystroglycan transcript encodes a 97 kDa precursor protein that undergoes posttranslational modifications including cleavage and carbohydrate additions. α-dystroglycan contains a short signal peptide and a mucin-like region in its midsection. Other sites of potential glycosylation and glycosaminoglycan (GAG) additions are indicated. β-dystroglycan's transmembrane region is noted. Within its intracellular C-terminus are binding sites for rapsyn and dystrophin. regions. The C-terminal regions that correspond to the peptides against which the polyclonal antiserum Ab98 and the monoclonal antibody NCL-43DAG are directed are indicated.

Figure 2. The Dystrophin Associated Protein Complex (DAPC)

The details of the DAPC, as well as the differences between the extrajunctional (A) and the NMJ (B) complex, continue to be elucidated. The following represents the current understanding of these complexes. Along the muscle membrane, dystrophin, an actin binding cytoskeletal molecule, associates with the DAPC members, while at the neuromuscular junction, a similar complex associates with the dystrophin related protein utrophin. α-dystroglycan (also known as the 156 kDa Dystrophin Associated Glycoprotein, 156DAG) and β-dystroglycan (43DAG) are expressed in many tissues and form the dystroglycan complex (DG). The members of the sarcoglycan complex (SG) are expressed in skeletal and cardiac muscle and include alpha SG (also known as adhalin and 50DAG), beta SG (A3b, 43DAG, the only SG expressed in brain), gamma SG (35DAG),

and delta SG. Recently, the cardiac-specific epsilon SG was identified. There are at least three 59 kDa syntrophins, with different patterns of expression. Alpha syntrophin is expressed only in muscle, beta1 syntrophin is ubiquitously expressed, and beta2 syntrophin is restricted to the NMJ. Two major dystrobrevins (also known as A0 or torpedo 87 kDa), alpha and beta, head a family of dystrobrevin isoforms with varying tissue expressions. Dystrobrevin containing a phosphotyrosine tail (PYCT) is specifically localized to the NMJ. Neuronal nitric oxide synthase (nNOS) is a DAPC member as well. In fast twitch myofibers, a1 and/or b1 syntrophin bind nNOS. Slow twitch myofibers lack nNOS. Other dystrophin associated molecules include caveolin and the transmembrane sarcospan.

Figure 3. Dystrophin and Isoforms
The dystrophin gene (white rectangle) comprises 2.4 million bases of the X-chromosome and has 79 exons (note that there are three different promoter-specific first exons, B1, M1, and P1, each encoding a full-length dystrophin). A total of seven promoters (arrows) have been identified. Thus, the dystrophin gene encodes dystrophins of 427 kDa, 260 kDa, 140 kDa, 116 kDa, and 71 kDa. Protein domains include the N-terminal actin binding domain, present only in full-length forms and the rod domain, present in all but DP71.

Figure 4. Dystroglycan in Retina: Outer Plexiform Layer
β-dystroglycan interacts with one of the short dystrophin isoforms in the presynaptic membrane of photoreceptor cells. α- and β-dystroglycan and a short dystrophin are found along the intracavital processes of the photoreceptor that form the lateral boundary of the synaptic cavity but not at the postsynaptic triad.

Figure 5. Dystroglycan at the Blood-Brain Barrier
This schematic depicts likely dystroglycan associations at the blood brain barrier. A dystroglycan complex is found at brain-penetrating blood vessels and the pial surface. β-dystroglycan and utrophin localize

to the perivascular endfeet of glial cells, and α-dystroglycan associates with the basement membrane of brain blood vessels.

Figure 6. Dystroglycan at Central Synapses
Unlike at the photoreceptor OPL, dystrophin is associated with the postsynaptic (and not presynaptic) specializations of cortical neurons and is concentrated in mouse and human brain postsynaptic density fractions. α-dystroglycan immunoreactivity appears on the surface of Purkinje cell bodies, dendrites, and dendritic spines. β-dystroglycan immunoreactivity is not detected in these localizations, however.

Figure 7. Northern Blot analysis of dystroglycan mRNAs
Northern blots of human tissues and brain regions were probed with probe1 and probe3, which correspond to the proximal and distal C-terminal regions of dystroglycan, respectively (see Figure 1). Both probes hybridized to an approximately 6 kb mRNA that was highly expressed in all tissues and brain regions. Hybridization with probe1, but not with probe3, reveals a larger transcript (over 10 kb), in cerebral cortex as well as occipital and frontal lobe.

Figure 8. Rat brain cDNA library screen "contig"
From a rat brain cDNA library, 15 phage that contained uniquely-sized cDNA inserts to which probe1 but not probe3 hybridized were isolated and sequenced. Using the Sequencher software, each of the phage insert sequences was compared to the mouse dystroglycan cDNA (DAG1). Each sequence obtained was found to be identical to a region of the DAG1 cDNA. The location of each of insert-DAG1 homologies is depicted graphically in this "contig." Epitope1 = probe1, epitope3 = probe3.

Figure 9. Brain subcellular fraction proteins
A. Subcellular fractions (H, homogenate; SX, synaptosomes; PSD, postsynaptic densities) were separated by SDS-PAGE and protein stained (CB), revealing enrichment for many proteins in the PSD fraction.

B. Western blots (WB) of subcellular fractions were probed with antibodies against presynaptic components (synaptophysin) and components of the postsynaptic density, including the NMDAR1 subunit, the mRNA 3'UTR binding protein CPEB, and αCaMKII.

Figure 10. α/β-dystroglycan distribution in subcellular fractions
A. Ligand overlay with agrin isoforms on blots of subcellular fractions reveals that α-dystroglycan is present in brain homogenate (H), is concentrated in the synaptosome fraction (S), and is detectable in the PSD fraction (PSD). The binding of the agrin$_{(0,0)}$ isoform exceeds the binding of agrin$_{(4,8)}$.
B. Western blots of subcellular fractions were probed with β-dystroglycan antibody Ab98. β-dystroglycan is present in brain homogenate and is concentrated in the synaptosomal fraction in subcellular fractions isolated from rat cortex (as well as from brain stem, cerebellum, and hippocampus, not shown). Ab98 also recognizes a pair of polypeptides that are selectively enriched in the PSD fraction, p58/53.
C. Western blots of synaptosomal fractions prepared from brain stem (BS), cerebellum (CB), and hippocampus (HP) were probed with NCL-43DAG. Different amounts of β-dystroglycan are detected in each of the regional synaptosomal fractions examined (equal protein loading).

Figure 11. Comparison of dystrophin, DP71, and β-dystroglycan distribution in subcellular fractions. Equivalent western blots probed with DYS2 (**A**) or NCL-43DAG (**B**). Whereas full-length dystrophin is concentrated in the PSD fraction, β-dystroglycan and DP71 are concentrated in the synaptosome fraction. (M, muscle extract)

Figure 12. α- and β-dystroglycan expression in *mdx*, *3CV* and control mice brain fractions.
Ligand overlay with agrin$_{(0,0)}$ shows that the level of α-dystroglycan (αDG) in *3CV* synaptosomes is similar to control. Western blot with the

antibody NCL-43DAG shows diminished β-dystroglycan (βDG) expression in fractions isolated from *3CV* mouse brain.

Figure 13. β-dystroglycan in glia and hippocampal neurons and lysates
A. Inverse images of immunofluorescent staining with anti β-dystroglycan antibody NCL-43DAG reveals β-dystroglycan immunoreactivity throughout glia and hippocampal neurons. This pattern is not synapse-specific.
B. Western analysis of cell lysates from cultured hippocampal neurons shows large quantities of soluble β-dystroglycan.
C. Western analysis with Ab98 comparing the p58/53 in the detergent-insoluble pellet from hippocampal neuronal cell lysate to PSDs.

6.2 Tables and Figures

Table 1. The Muscular Dystrophies: A Family of Genetic Diseases

Muscular Dystrophy	Genetic Locus Gene Product	Peripheral Manifestations	Central Nervous System Manifestations
	• Affected gene often encodes a member of the DAPC	• Progressive breakdown of striated muscle • Variation in myofiber size • Muscle cell necrosis and regeneration • Proliferation of connective and adipose tissue	• Variable
X-linked Limb Girdle Muscular Dystrophies			
Duchenne Muscular Dystrophy (DMD) • Diagnosed in 30/100,000 births	• Xp21 • dystrophin • *mdx* mouse • *3CV* mouse	• Onset before age 5 • Progressive weakness of limb girdle muscles • Inability to walk after age 12 • Kyphoscoliosis • Respiratory failure in 2nd to 3rd decade • Cardiomyopathy	• Nonprogressive intellectual impairment • Average IQ approximately 1 standard deviation below the mean • IQs lower than those of children with comparable physical disorders • Verbal ability affected more than performance ability
Becker Muscular Dystrophy • Diagnosed in 3/100,000 births	• Xp21 • dystrophin	• Onset in early to late childhood • Slowly progressive weakness of limb girdle muscles • Ability to walk after age 15 • Respiratory failure after the 4th decade • Cardiomyopathy	• Mental retardation is seen less frequently than in DMD
Autosomal Dominant Limb Girdle Muscular Dystrophies		• Normal DAPC expression	• Normal
LGMD Type 1A	• 5q31	• Slow progression • Dysarthria from palatal weakness	• Normal
LGMD Type 1B	• 1q11-21	• Cardiomyopathy	• Normal

Autosomal Recessive Limb Girdle Muscular Dystrophies		• Onset in early childhood to adulthood • Slowly progressive weakness of shoulder and hip muscles • Symmetric involvement of the pelvic and periscapular muscles • Cardiomyopathy	• Intellectual function remains normal
LGMD Type 2A	• 15q15 • calpain 3 (protease)	• Onset at approximately age 10 • No cardiac involvement • Normal dystrophin and sarcoglycan complex	• Normal
LGMD Type 2B	• 2p13	• Onset at approximately age 15 • Normal dystrophin and sarcoglycan complex	• Normal
LGMD Type 2C • Formerly Severe Childhood MD	• 13q12 • gamma sarcoglycan	• A more severe LGMD, high CK levels early • Decreased expression of dystrophin and sarcoglycan complex	• Normal
LGMD Type 2D • Formerly Severe Childhood MD	• 17q12-21 • alpha sarcoglycan	• A more severe LGMD, high CK levels early • Decreased expression of dystrophin and sarcoglycan complex	• Normal
LGMD Type 2E • Formerly Severe Childhood MD	• 4q12 • beta sarcoglycan	• A more severe LGMD, high CK levels early • Decreased expression of dystrophin and sarcoglycan complex	• No detected abnormalities
LGMD Type 2F • Formerly Severe Childhood MD	• 5q33-34 • delta sarcoglycan • BIO14.6 hamster	• More severe LGMD, high CK levels early • Decreased expression of dystrophin and sarcoglycan complex	• Normal

Classical Congenital Muscular Dystrophies			
Laminin alpha-2 chain Positive		• Hypotonia and weakness apparent at birth • Ambulation is usually achieved	• Normal
Laminin alpha-2 chain Negative	• 6q22-23 • laminin alpha-2-chain • *dy* mouse	• More severe initial presentation, higher CK levels • Increased laminin alpha-1 immunostaining • Ambulation is not achieved • Slowing of motor nerve conduction velocities	• Abnormality of white matter (leukodystrophy) • Seizures

Congenital Muscular Dystrophies with CNS Abnormality (Autosomal recessive)			• Variable abnormalities
Fukuyama-type Congenital MD (FCMD)	• 9q31 • fukutin	• Neonatal hypotonia, weakness, elevated CK levels • Delayed psychomotor development • Loss of ability to stand by age 4 • Mean life span is 10 years • Decrease in expression of laminin alpha-2 and dystroglycan	• General tonic-clonic seizures • Mental retardation, developmental delay • Microencephaly and enlarged ventricles • Defective neuronal migration
Walker-Warberg Syndrome		• High degree of neonatal lethality • Histopathology of muscular dystrophy • Decreased beta-2 laminin and alpha sarcoglycan immunoreactivity in muscle	• Severe CNS abnormalities • Polymicrogyria • Cerebellar hypoplasia • Retinal dysplasia
Muscle-Eye-Brain Disease		• Ability to stand or walk is often achieved • Decreased alpha-2 laminin, normal beta-2 laminin in muscle	• Similar though less severe CNS abnormalities as in Walker-Warberg Syndrome

Distal Muscular Dystrophies		• Distal muscles first affected	• Normal
Miyoshi • may be LGMD 2B • Autosomal recessive	• 2p21		
Nonaka • Autosomal recessive			
Welander • Autosomal dominant			
Tibial (Udd) • Autosomal dominant			

Other Related Diseases			
Myotonic Dystrophy • Diagnosed in 13.5/100,000 births • Autosomal dominant	• 19q13.3 • myotonin-protein kinase • expanded CTG trinucelotide repeat	• Onset at any age • Slowly progressive weakness of the eyelids, face, neck, and distal limb muscles • Myotonia • Cardiac conduction defects • Cataracts • Frontal baldness and gonadal atrophy • 5% of cases: eleveted insulin levels, type II DM (insulin resistance)	• Mild mental retardation
Fascio-Scapulo-Humeral MD • Diagnosed in 5/100,000 births • Also known as Landouzy-Dejerine • Autosomal dominant	• 4q35 (plus other autosomal loci)	• Onset before age 20 • Slowly progressive weakness in face, shoulder, limb girdle, and foot dorsiflexion • Hypertension	• Increased incidence of nerve deafness
Oculo-pharyngeal Dystrophy • Autosomal dominant	• 14q11.2-q13 (plus other autosomal loci)	• Onset 5th to 6th decade • Slowly progressive weakness of extraocular, eyelid, face, and pharyngeal muscles • Cricopharyngeal achalasia • Ptosis and dysphagia	
Cerebro-ocular Dysplasia MD • Autosomal dominant			• Corneal abnormalities, cataracts, retinal dysplasia and hypoplasia of optic nerve • Hypomyelination of cerebral white matter
Bethlem Myopathy • Autosomal dominant	• 21q22.3 subunits A1 & A2 of type VI collagen • 2q37	• Early onset proximal myopathy • Slow progression • Multiple contractures	
Emery-Draifus Muscular Dystrophy • X-linked	• Xq28 (plus autosomal loci)		

(Isselbacher et al., 1994; Bonnemann et al., 1996; Dubowitz, 1997)

Figure 1. Dystroglycan

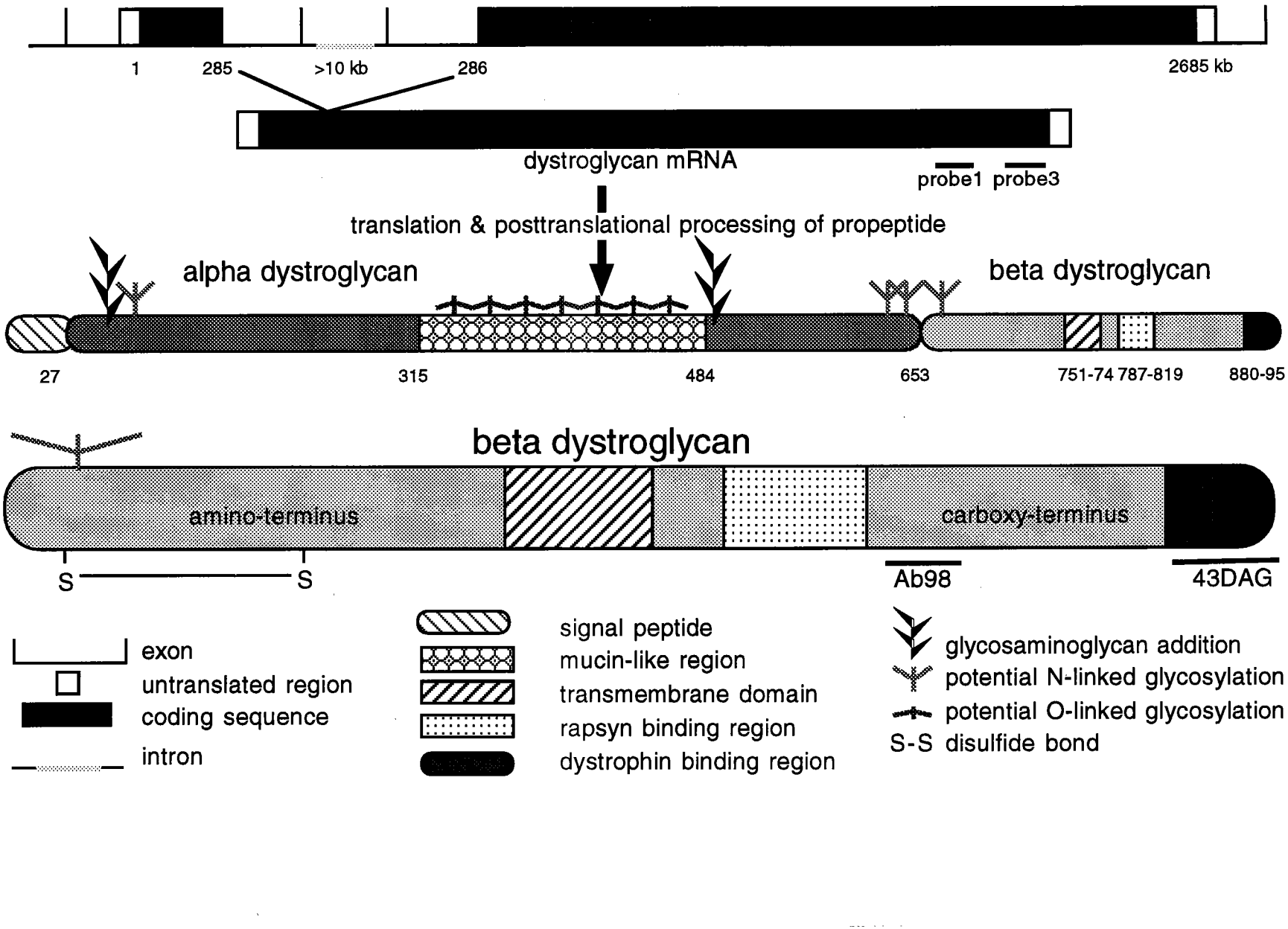

Figure 2. The DAPC

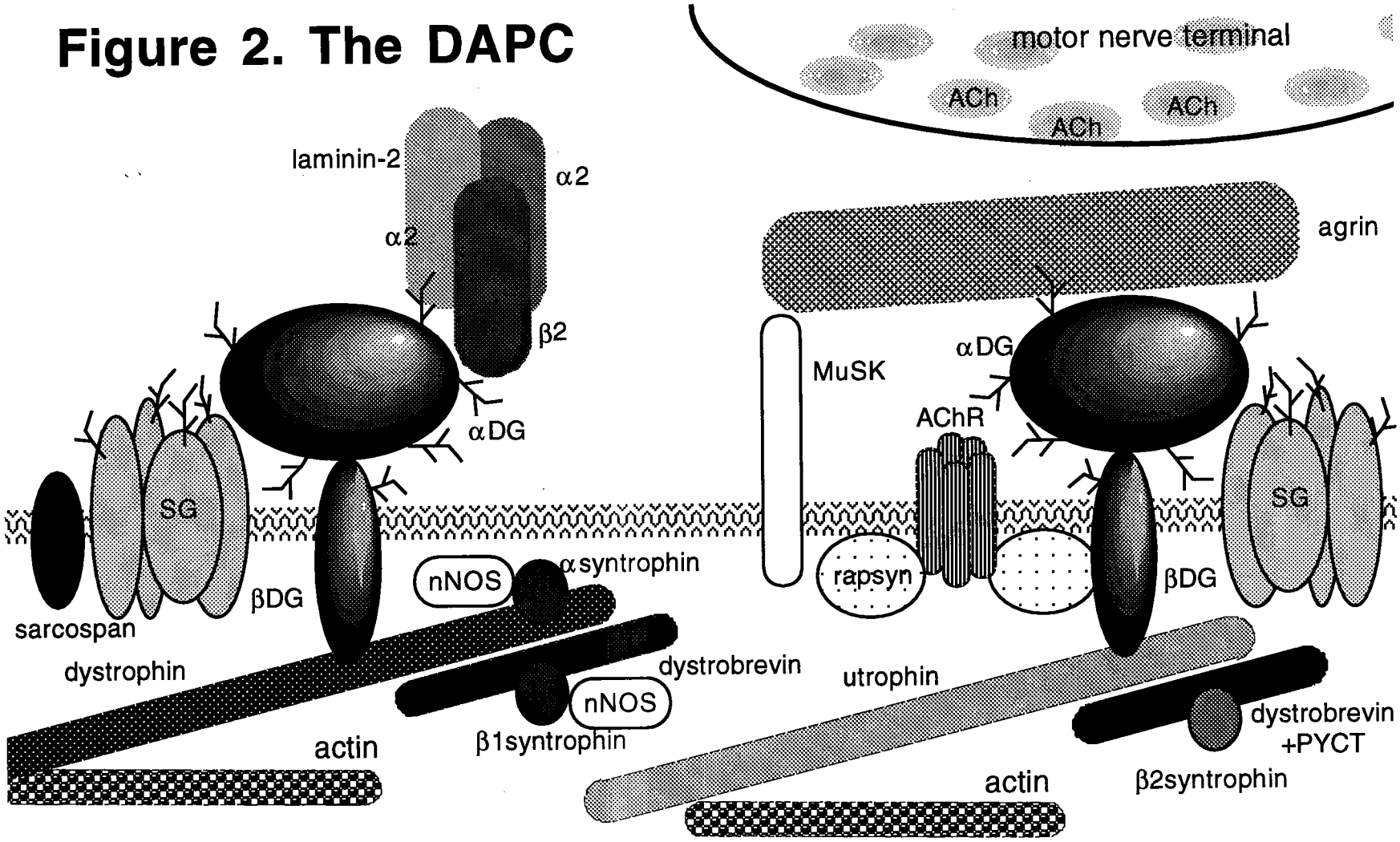

Extrajunctionally

At the NMJ

Figure 3. Dystrophin and Isoforms

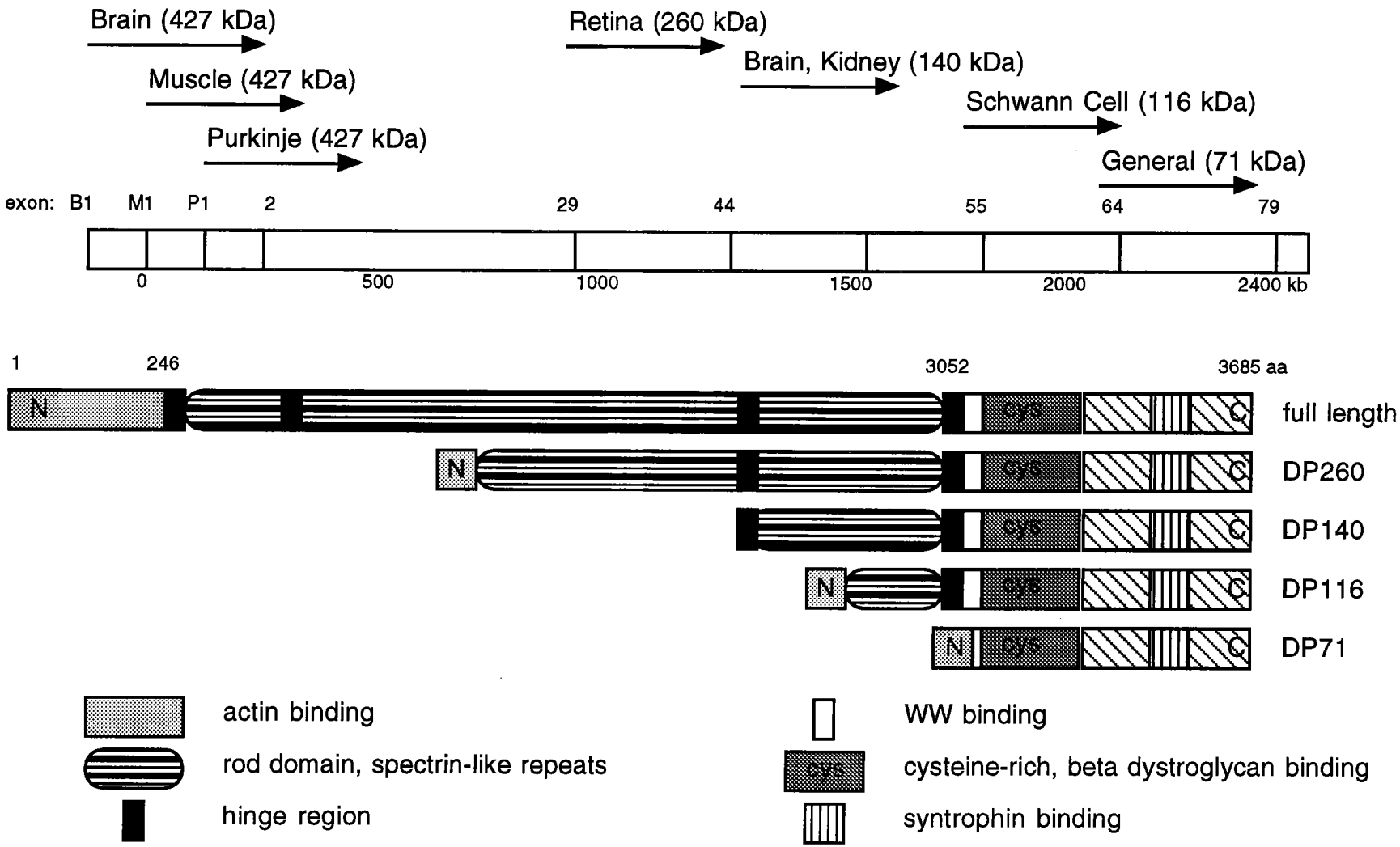

Figure 4. Dystroglycan in retina

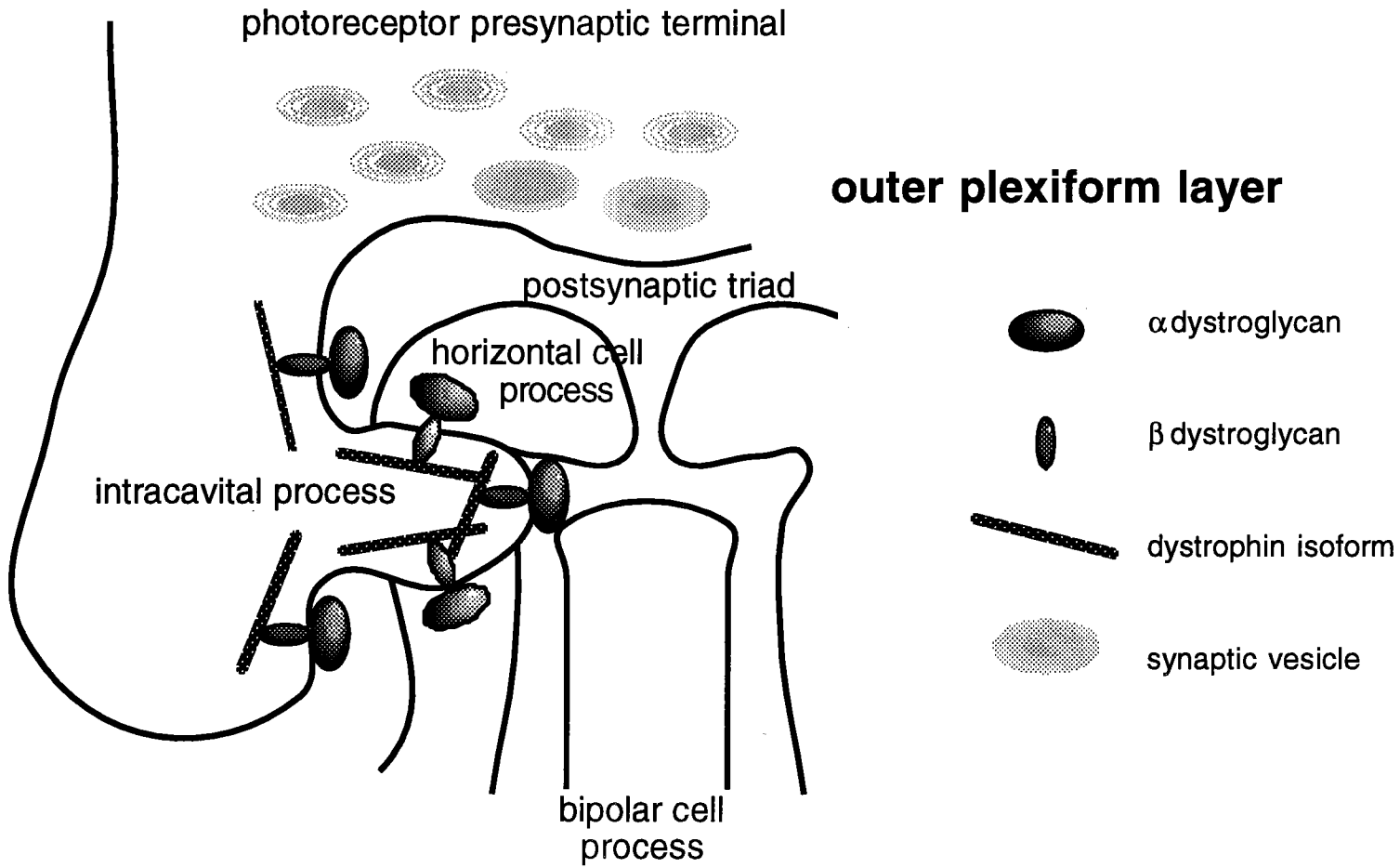

Figure 5. DG at the Blood-Brain Barrier

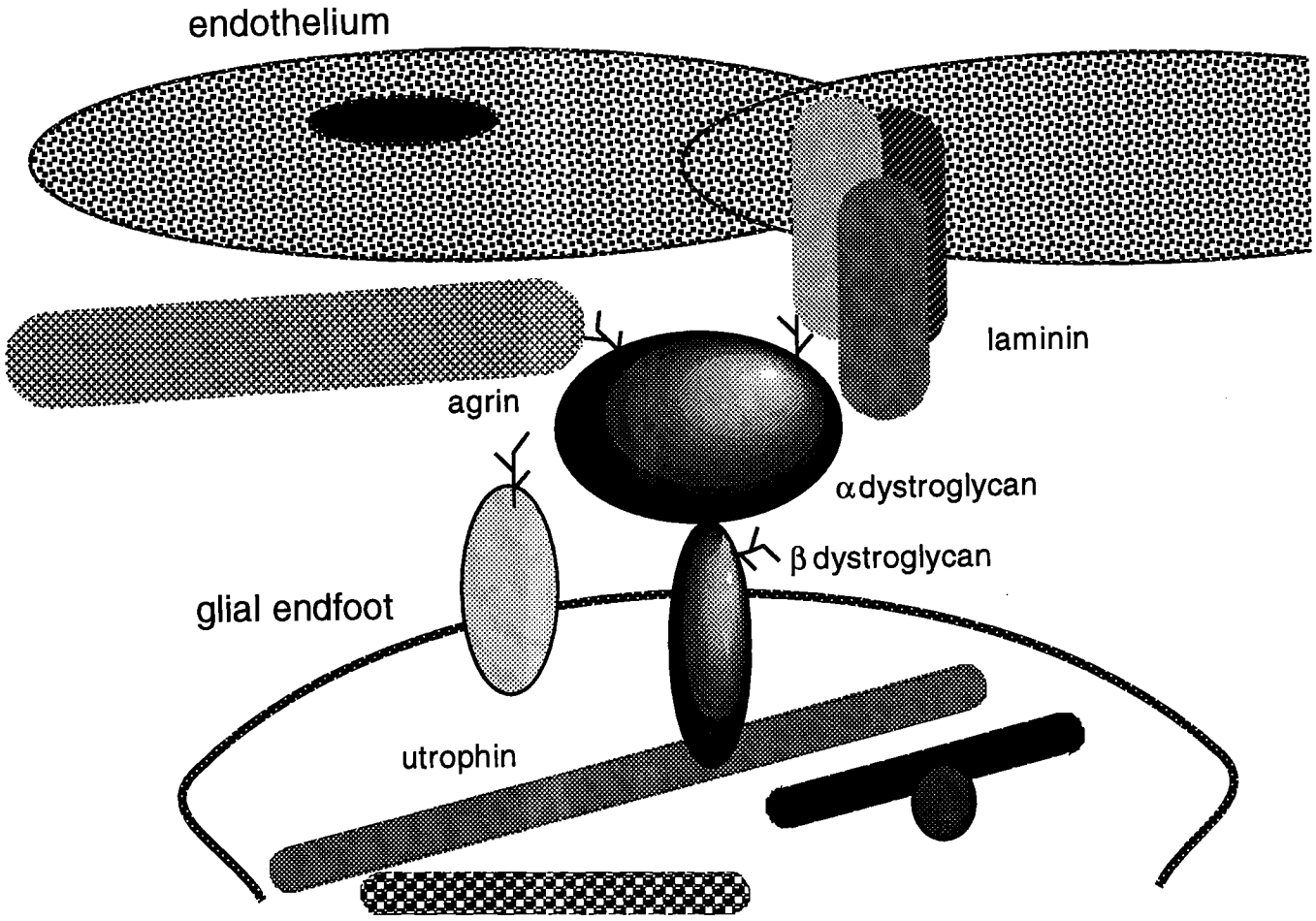

Figure 6. DG at Central Excitatory Synapses

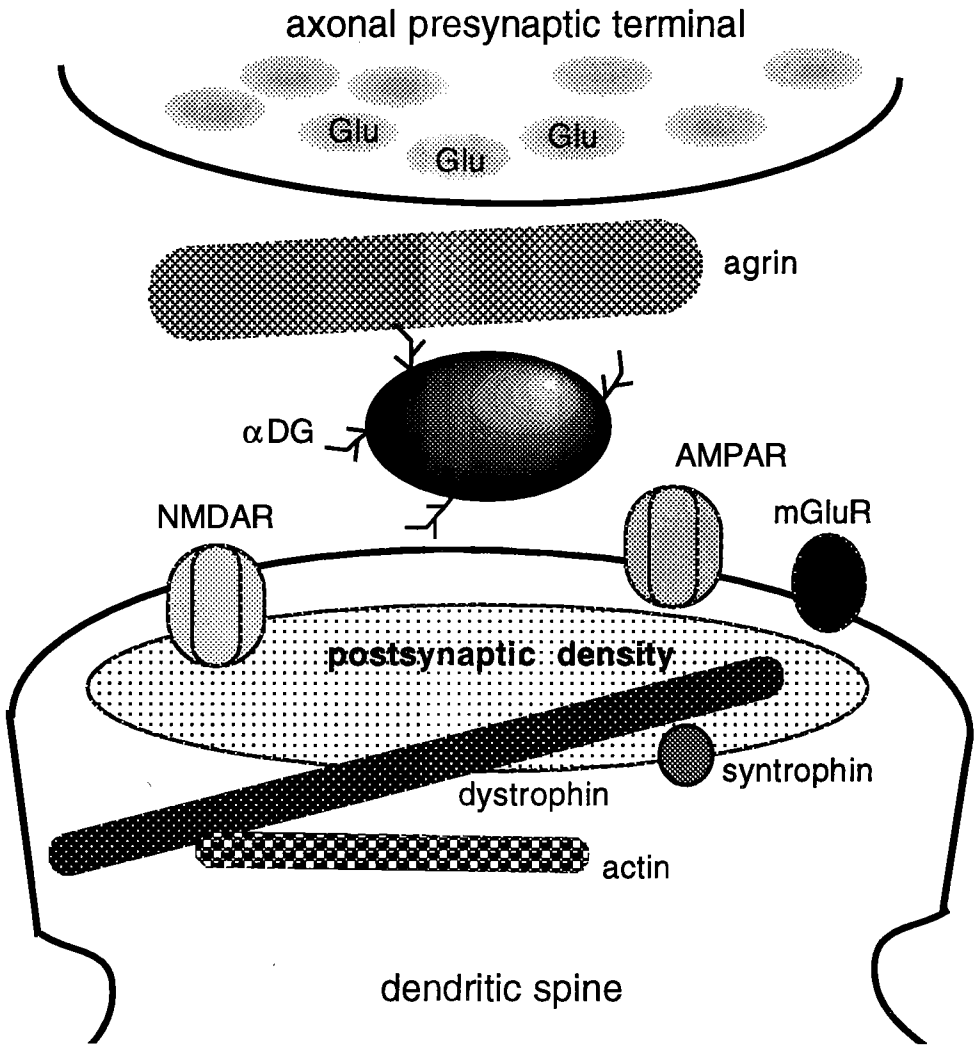

Figure 7.

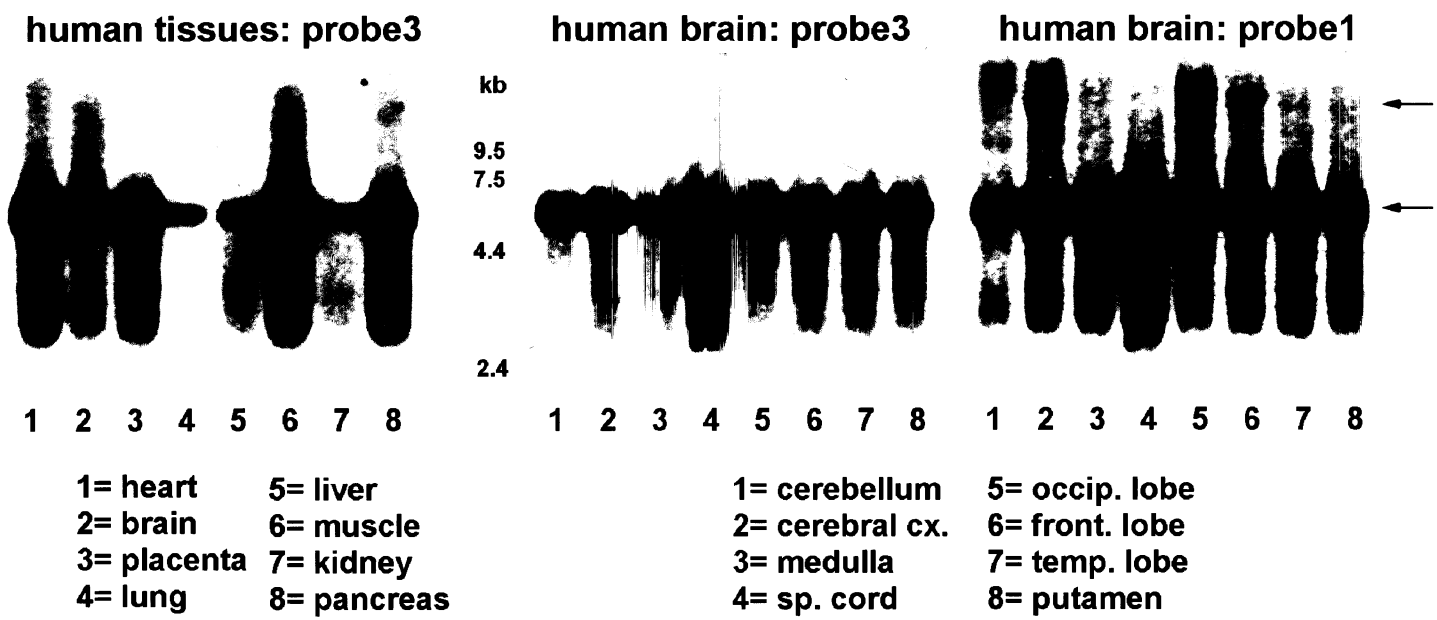
human tissues: probe3
human brain: probe3
human brain: probe1
kb
9.5
7.5
4.4
2.4
1 2 3 4 5 6 7 8
1 2 3 4 5 6 7 8
1 2 3 4 5 6 7 8
1= heart
2= brain
3= placenta
4= lung
5= liver
6= muscle
7= kidney
8= pancreas
1= cerebellum
2= cerebral cx.
3= medulla
4= sp. cord
5= occip. lobe
6= front. lobe
7= temp. lobe
8= putamen

Figure 8.

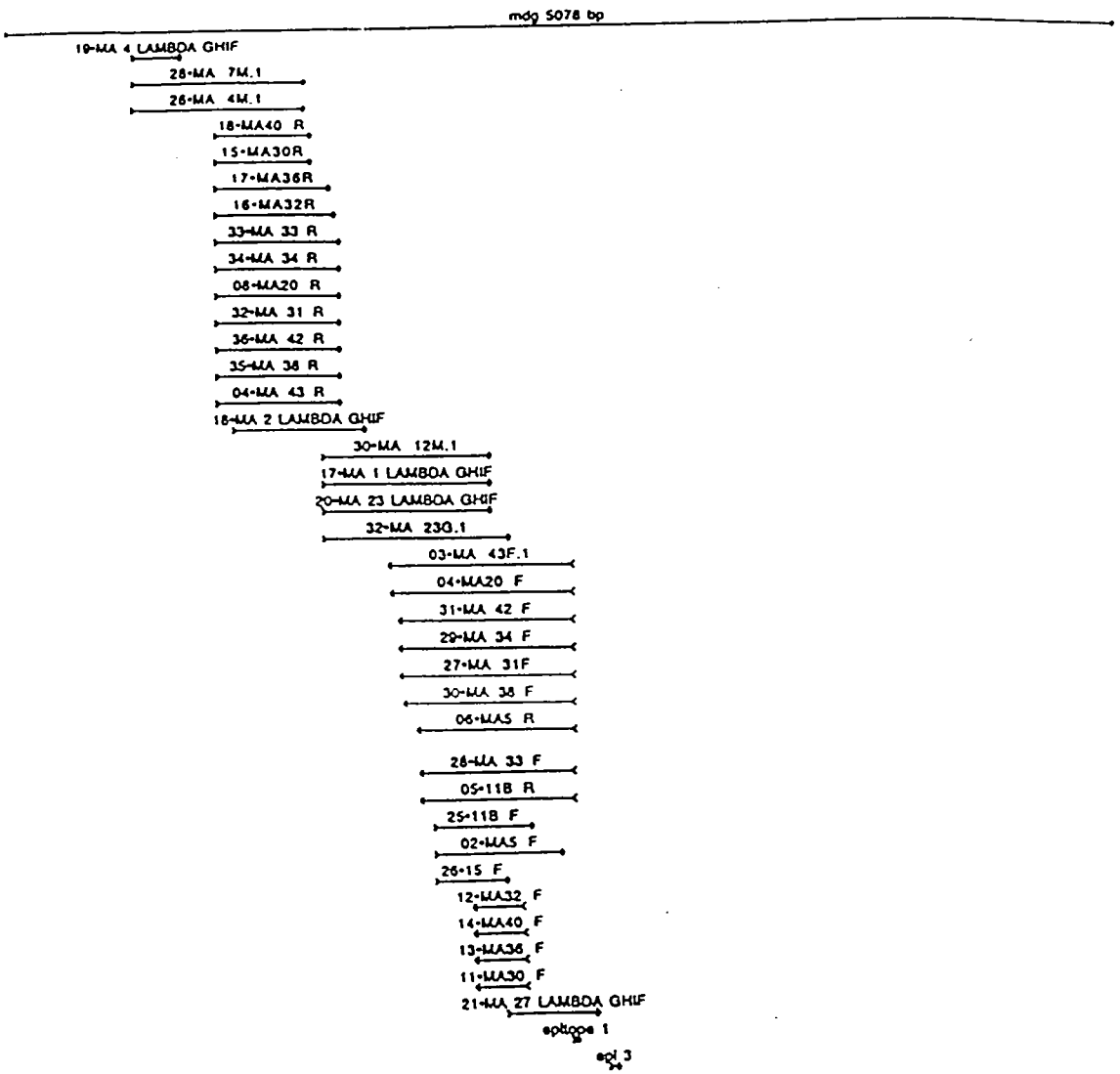
mdg 5078 bp
19-MA 4 LAMBDA GHIF
28-MA 7M.1
26-MA 4M.1
18-MA40 R
15-MA30R
17-MA36R
16-MA32R
33-MA 33 R
34-MA 34 R
08-MA20 R
32-MA 31 R
36-MA 42 R
35-MA 38 R
04-MA 43 R
18-MA 2 LAMBDA GHIF
30-MA 12M.1
17-MA 1 LAMBDA GHIF
20-MA 23 LAMBDA GHIF
32-MA 23G.1
03-MA 43F.1
04-MA20 F
31-MA 42 F
29-MA 34 F
27-MA 31F
30-MA 38 F
06-MA5 R
28-MA 33 F
05-11B R
25-11B F
02-MA5 F
26-15 F
12-MA32 F
14-MA40 F
13-MA36 F
11-MA30 F
21-MA 27 LAMBDA GHIF
epitope 1
epi 3

Figure 9.

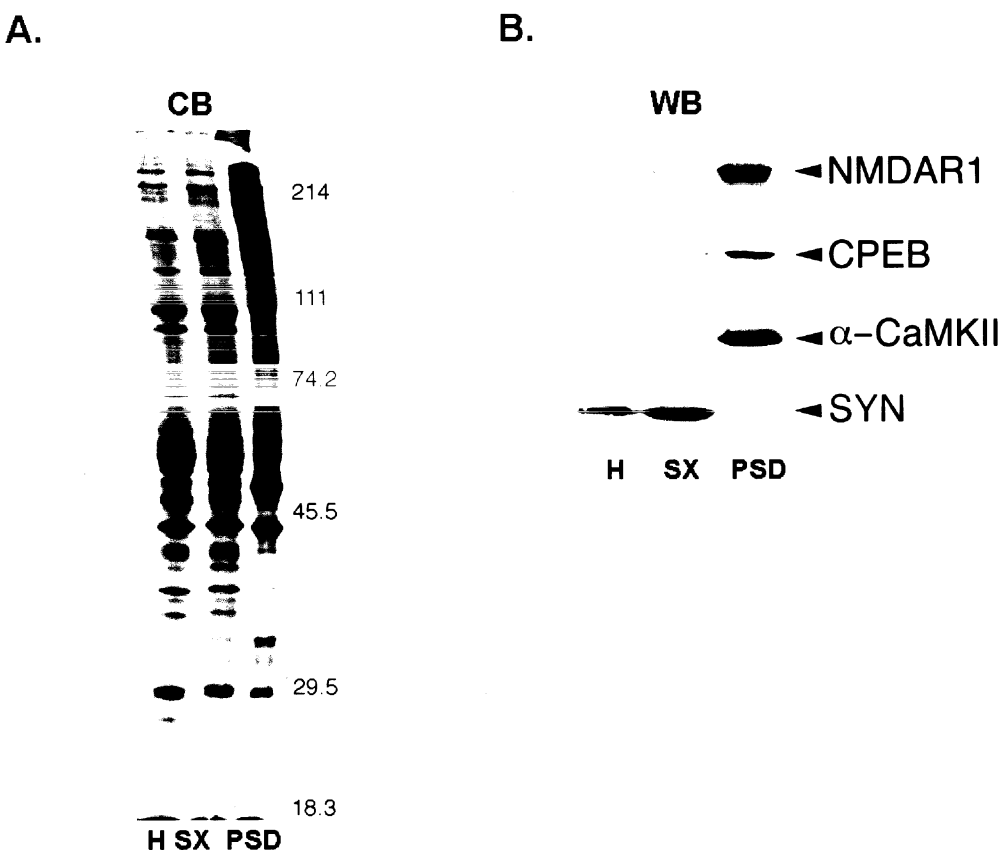
A.
CB
214
111
74.2
45.5
29.5
18.3
H SX PSD
B.
WB
NMDAR1
CPEB
α-CaMKII
SYN
H SX PSD

Figure 10.

A.

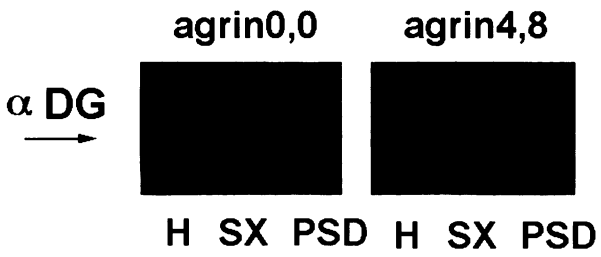

B.

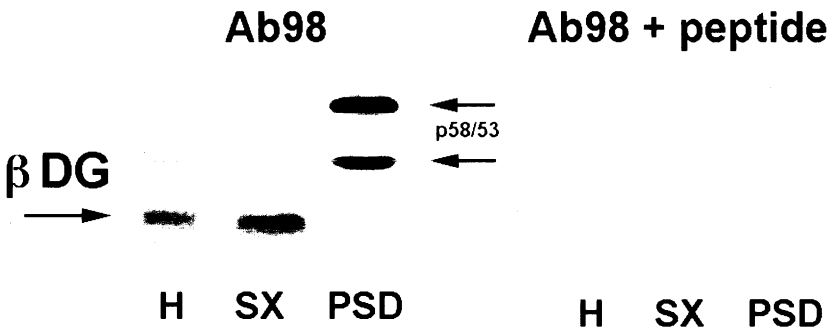

C.

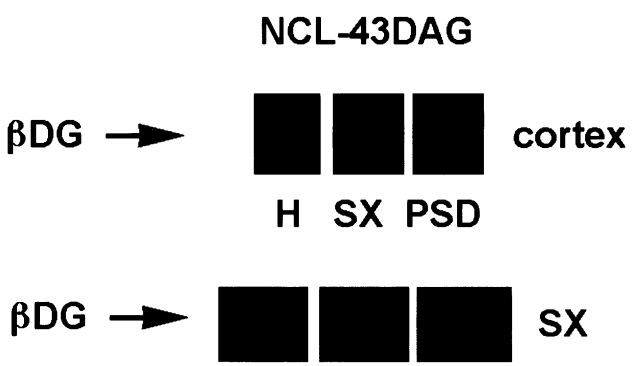

Figure 11.

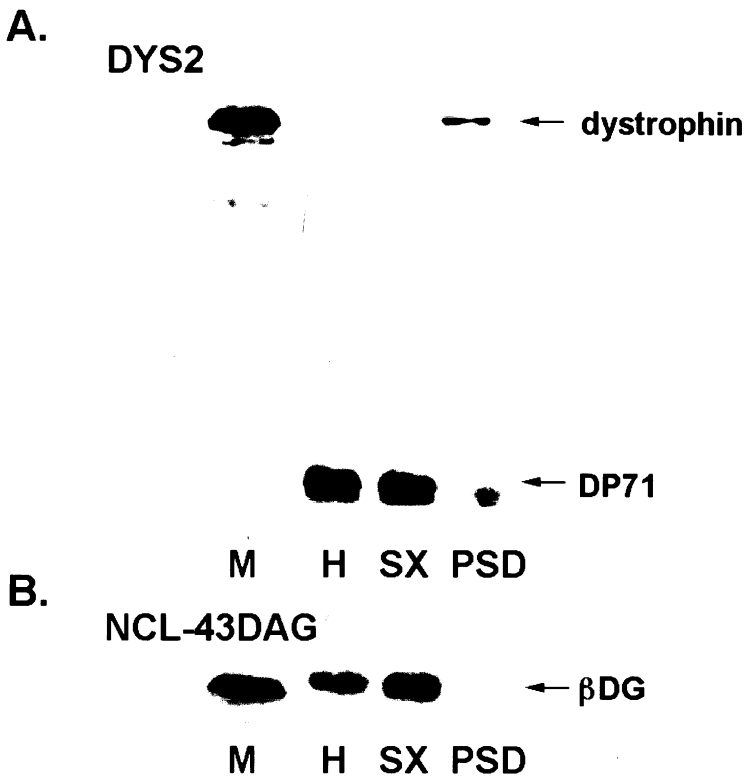

Figure 12.

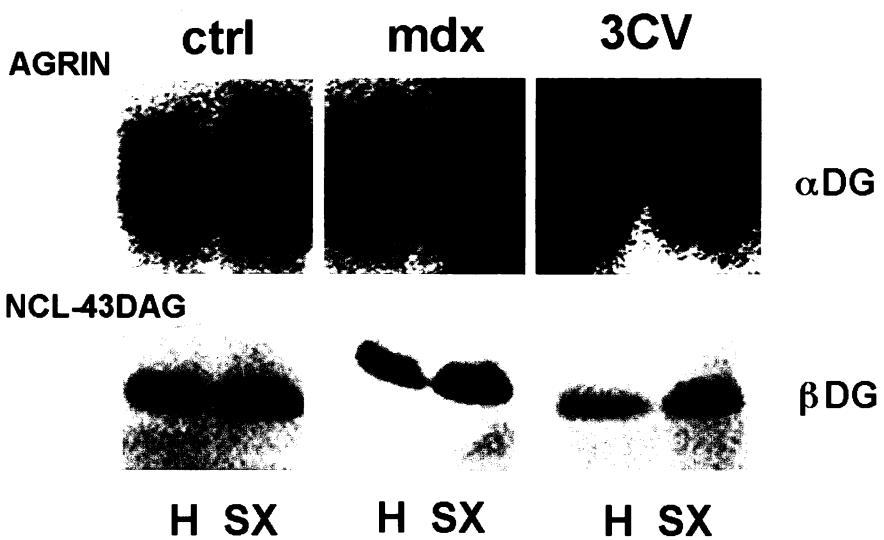

Figure 13.

A.

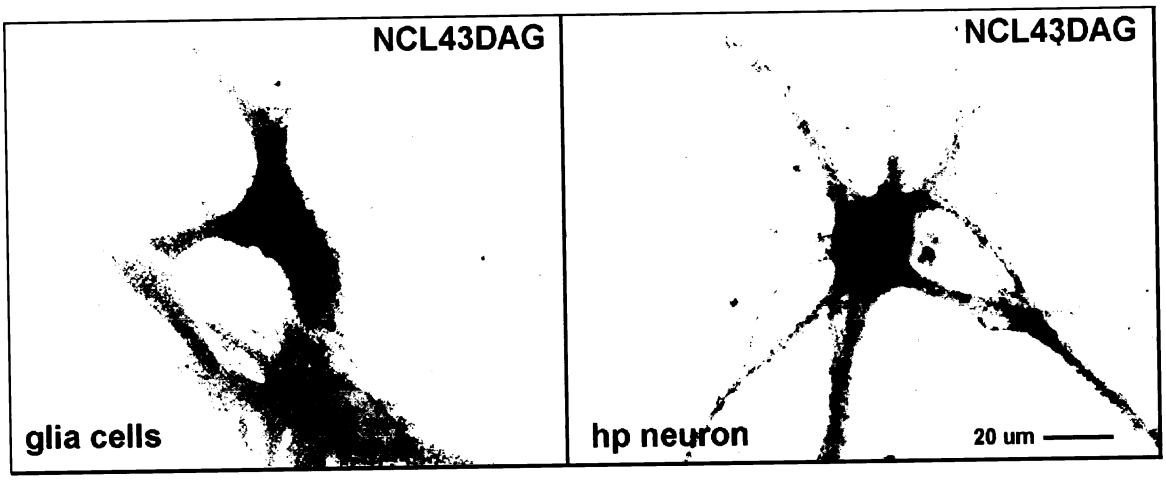

B.

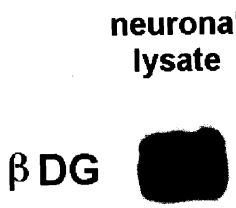

C.

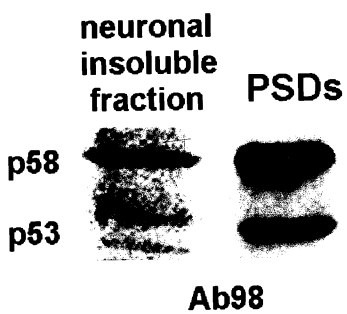

CHAPTER II

INSULIN RECEPTOR TYROSINE KINASE SUBSTRATE p58/53 AND INSULIN RECEPTOR ARE COMPONENTS OF THE SYNAPSE

1. Introduction

I have characterized the protein IRSp58/53, a known substrate of the insulin receptor tyrosine kinase, and determined that it is selectively concentrated in the rat brain postsynaptic density (PSD) fraction, is localized to the synapse-rich layers of the cerebellum, and is concentrated at synapses in cultured hippocampal neurons. The insulin receptor is also concentrated at synapses in cultured hippocampal neurons. In addition, I have found that a population of brain insulin receptors is localized to the postsynaptic density fraction. I expect that other components of a synaptic insulin receptor pathway will be found at the postsynaptic apparatus in vivo, and a regulatory role for insulin signaling at the central synapses will emerge.

2. Background

The importance of peripheral insulin as a regulator of the body's energy balance is undisputed. More contested however, is the consequence of insulin in the brain. Whereas the signaling pathways that execute the biological effects of insulin in the periphery are quickly being dissected, the mere presence of insulin signaling systems in the brain has not been appreciated until recently. A brief overview follows of insulin-dependent signaling pathways and their biologic consequences in peripheral tissues, the current understanding of these systems in the brain, as well as a review of the central synaptic signaling apparatus that lies below the postsynaptic membrane of glutamatergic synapses, the postsynaptic density (PSD).

2.1 Insulin Signaling in Peripheral Tissues

Insulin plays an essential role in the regulation of the body's glucose metabolism. An increase in the level of circulating glucose causes pancreatic beta cells to release the anabolic hormone insulin into the bloodstream. Insulin stimulates the uptake of glucose into muscle, liver, and adipose cells, and the synthesis of protein, glycogen, and triglycerides in these cells. At these target cells, insulin initiates a series of signaling events that result in multiple biologic outcomes. In target cells that express the GLUT4 glucose transporter, insulin dependent signaling processes lead to a translocation of GLUT4 from intracellular sites to the plasma membrane, enabling the cell to rapidly import circulating glucose. Insulin can have other types of cellular effects as well, such as affecting gene transcription. For example, chronically low insulin states, such as in insulin dependent diabetes or during sustained fasting, lead to a reduced expression of the gene that encodes GLUT4.

2.1.1 Insulin and Diabetes

Close to 5% of the United States' population suffer from diabetes. This chronic disease is characterized by hyperglycemia (high levels of circulating glucose), a condition that can adversely affect virtually every organ in the body. At the cellular level, diabetes is caused by target cells' insufficient response to insulin. Despite high levels of circulating glucose, the absence of effective insulin causes glucose uptake by target cells to dwindle. This shifts the body into a catabolic state wherein protein, glycogen, and fat are broken down. Chronic hyperglycemia and inappropriate catalysis have harmful effects on the body. Complications of diabetes can include nephropathy which can lead to kidney failure, retinopathy which can lead to blindness, neuropathy and extensive vascular disease which can lead to limb amputation.

Diabetes is caused by either an absolute deficiency of insulin secretion (type I or insulin-dependent diabetes mellitus (IDDM)) or resistance of peripheral target tissues to insulin (type II, or non-insulin-dependent diabetes mellitus (NIDDM)). IDDM develops following the destruction of the insulin-producing beta cells by auto-antibodies. The cause of the beta cell autoimmunity is unknown. Once more than 90% of an individual's beta cells have been destroyed, diabetes becomes clinically apparent. Patients with IDDM require exogenously supplied insulin to maintain their body's homeostasis.

It is NIDDM that accounts for ~90% of the diabetes cases in the United States. In these patients, despite sufficient insulin secretion, the effects of insulin on target tissues are blunted. Often, even elevated levels of insulin are unable to maintain the body's normal glucose levels, and a state of relative insulin deficiency results. Unlike IDDM patients, NIDDM patients do not depend on exogenous insulin. For many type II diabetics, their condition can be greatly or even completely overcome by weight loss and diet control. Some patients however cannot control their diabetes in this way, and they require treatment with oral hypoglycemic agents or even insulin injections (Lieberman, 1996). The cause of type II diabetes is not yet well

understood and is likely to involve many levels of insulin's signaling pathways.

2.1.2 The Insulin Receptor is a Receptor Tyrosine Kinase

For insulin to achieve its biological effects, it must bind to a functional insulin receptor on the surface of the target cell. The human insulin receptor (IR), cloned in 1985 (Ullrich et al., 1985), is one of a large family of growth factor receptors. Generally speaking, these receptors are group I membrane proteins. They span the cell membrane once, the N-terminal protein domain is on the extracellular side of the membrane, and the C-terminus is on the cytoplasmic side of the membrane. Some growth factor receptors are single polypeptides, like the epidermal growth factor (EGF) receptor. Others, including the insulin receptor, are disulfide bonded dimers (Figure 1). Some of these receptors have phosphatase activity, and all of them possess protein kinase activity.

Protein kinases transfer phosphate groups onto their target proteins. They exist either within the membrane, as receptor protein kinases, or within the cytoplasm as cytosolic protein kinases. There are two major types of kinases, categorized by the amino acids on which they phosphorylate their target proteins. The majority of the receptor kinases, including EGF and insulin receptors, phosphorylate substrates' tyrosines. More than 50 receptor tyrosine kinases (RTKs) are known. Although there are many cytosolic tyrosine kinases, and some dual specificity cytosolic kinases, serine/threonine kinases are the most common type of cytosolic kinases, and are responsible for the majority of cellular phosphorylation events. In addition, tyrosine and serine/threonine phosphatases are available to reverse the phosphorylation events procured by RTKs.

Enzymatic activity can activate two types of signaling pathways. For one, small second messengers can be activated by phospholipases, which cleave lipids from larger substrates, or kinases, which phosphorylate lipids. Phosphatidyl inositol 3' kinase (PI3-K) works by phosphorylating the lipid inositol. Alternatively, enzymatic activation can initiate a cascade of interacting proteins. Usually, these proteins

are kinases, each activating the next by phosphorylating it. The ultimate kinase in the relay typically acts on proteins that elicit global changes in the cell, such as transcription factors. These signaling pathways amplify the initial stimulus as it passes from one component to the next. If a component of the pathway has multiple downstream targets, the signal may branch into multiple pathways. In this way, an initial stimulus can elicit diverse biologic responses (Lewin, 1997).

The insulin receptor is very similar in size and structure to the insulin-like growth factor-I receptor (IGF-I) and the insulin-receptor related receptor. These receptors have some affinity for each other's ligands, but the insulin receptor exhibits a pharmacological preference for insulin. The insulin receptor is a dimer of units each composed of an α and a β subunit linked together by disulfide bonds. The extracellular α subunit contains the ligand binding domain and the β subunit, a group I membrane protein, comprises a short extracellular domain and the cytoplasmic tyrosine kinase activity (Fujita-Yamaguchi, 1984) (Figure 1).

When insulin binds to the extracellular domain of its receptor, it induces a conformational change that affects the overall organization of the receptor, which activates the kinase activity of the cytoplasmic domains. The receptor then autophosphorylates; the kinase activity of one subunit phosphorylates the other, and vice versa. Autophosphorylation has at least two consequences. For one, phosphorylation within the receptor's kinase region can increase its catalytic activity. Alternatively, receptor phosphorylation at other cytoplasmic tyrosine residues leads to transfer of the signal to downstream components as target proteins associate with these phosphorylated tyrosines of the receptor's cytoplasmic domains. The quintessent function of RTKs is tyrosine phosphorylation; a receptor with a mutated kinase domain is biologically inactive, despite its preserved ability to bind ligand (Lewin, 1997).

Activated receptors may interact with several types of signaling proteins. In one type of association, a target protein is activated by

binding the intracellular domain of the receptor, but is not phosphorylated. This tethered target protein then activates an enzyme, which amplifies and continues the pathway. Second, proteins that are substrates of the receptor's kinase activity can bind to and become phosphorylated by the receptor. If the substrate itself is a kinase, this phosphorylation event may activate it, and in turn the pathway will proceed by activating successive kinases. Finally, some receptor substrates, such as a cytoskeletal proteins, are end targets of the pathway. Phosphorylation of such proteins alters their physical state and leads to assembly of a new structure.

2.1.3 Insulin's actions are mediated by docking proteins

In many cases, the primary interaction between signaling proteins and an activated receptor kinase is mediated by SH2 domains. Either the autophosphorylated tyrosines bind src homology 2 (SH2) domains of signaling proteins, or the increased activity of the kinase mediates tyrosine phosphorylation of cytosolic substrates known as "docking proteins" that recruit SH2 proteins. The signaling pathway is continued through other protein-protein or protein-lipid interaction domains including phosphotyrosine binding (PTB) and pleckstrin homology (PH), src homology 3 (SH3), PDZ, and WW domains (see below). The first identified member of this family of proteins, which link RTKs to downstream signaling molecules, is the insulin receptor substrate, IRS-1 (White and Yenush, 1998) (Figure 2).

These functionally-related docking proteins, IRS-1, IRS-2, and IRS-3, and Gab-1 and $p62^{dok}$, share several protein motifs. At the N-terminus is a PH and/or PTB domain; at their C-terminus are proline-rich regions which mediate binding of SH3 or WW domains, multiple tyrosine-containing sequences which can bind SH2 domains, and serine/threonine-rich regions which may regulate function as well. Shc is a member of another group of docking proteins. It has an N- terminal PTB domain, a C-terminal SH2 domain, a proline-rich region, and a few phosphotyrosine sites through which it binds the SH2 domain of Grb2. SH2 domains mediate high affinity interactions, close to three orders of magnitude tighter

than the usual kinase substrate interaction. Typically, the site that binds an SH2 domain contains only a phosphotyrosine and a few amino acids C-terminal to it. Whereas Shc interacts with the insulin receptor by its PTB domain, its SH2 domain allows Shc to interact with another RTK, the activated EGF receptor.

Docking proteins are useful for coordinating flexible and diverse signaling systems. Receptors that specifically interact with IRS proteins can achieve an amplified signal: since the docking interaction is transient, many IRS proteins can be phosphorylated by one receptor. In addition, they escape the fate of internalization that is likely to await ligand-bound receptors, and can carry the signal to downstream signaling components. Lastly, many receptors have the specificities to engage different IRS proteins. By engaging multiple pathways, one receptor can initiate diverse signals. Similarly, different RTKs share specificities for the same IRS proteins. This allows for the integration of multiple signals (White and Yenush, 1998).

The biologic effect of insulin and insulin receptor substrates is dependent on a specific insulin receptor motif. A decade ago, the importance of the juxtamembrane NPXY motif of the insulin receptor was revealed: mutations here reduce the tyrosine phosphorylation of IRS-1 while diminishing insulin's biologic effects. It is now understood that the tyrosine phosphorylated NPXY motif can bind PTB domains. In fact, many IRS proteins achieve specific and transient docking through their PTB domain. This domain binds weakly but specifically to the phosphorylated NPXY motifs of the insulin receptor, the IGF-1 receptor, and the IL-4 receptor. The interaction of several residues N-terminal to the NPXY motif adds specificity to individual PTB:NPXY associations.

In addition to the PTB domain, this family of docking proteins utilizes another protein motif in its interactions with RTKs. The PH domain of IRS-1 is important for its interaction with the insulin receptor. The PH motif is similar to the PTB domain, yet its specific three dimensional structure cannot be predicted based by primary amino acid sequence alone. PH domains bind a diverse set of ligands, yet this

motif does not bind the insulin receptor directly, suggesting that other docking protein domains participate in this interaction. The presence of IRS-1's PH domain and not its PTB domain is sufficient for its activation by the activated insulin receptor. However, IRS-1 lacking its PH domain undergoes little tyrosine phosphorylation following insulin stimulation.

Activated IRS proteins generate downstream signals by engaging SH2 domains of other signaling proteins. IRS-1 interacts with PI3-K, as well as with others including Grb2, SHP2, Fyn, and a number of proteins that do not contain SH2 domains, including 14-3-3. IRS-1 and PI3-K are implicated in many biologic effects including insulin-stimulated translocation of GLUT4 and subsequent glucose transport (Figure 3). The heterodimer PI3-K is composed of an 85 kDa regulatory subunit and a 110 kDa catalytic subunit. The p85 subunit contains an SH2 domain that binds phosphotyrosine residues of IRS-1. This interaction causes activation of the associated catalytic subunit's kinase activity and phosphorylation the 3' position on inositol molecules. Since IRS-1 and IRS-2 contain about nine phosphotyrosine motifs with which to bind SH2 domains, and PI3-K activation is maximal when both of the p85 SH2 domains are bound, these IRS proteins are ideal for signal transmission via PI3-K.

IRS-1 also interacts with the phosphotyrosine phosphatase SHP2, which contains two SH2 domains. During insulin stimulation, SHP2 binds IRS-1 as well as the insulin receptor itself. It is likely that SHP2 regulates insulin signaling. SHP2 may diminish the insulin signal by reversing the tyrosine phosphorylation of IRS-1. SHP2 may be important for some downstream insulin signaling events: when Shpt's phosphatase activity is inactivated, insulin stimulated MAP Kinase and c-fos transcription is disrupted (White and Yenush, 1998).

Insulin stimulation is linked to intranuclear events by Grb2, a small, SH2 containing adapter molecule. Tyrosine phosphorylated docking proteins IRS-1 or Shc bind Grb2. Once associated, the Shc/Grb2 complex recruits SOS, a Ras guanylnucleotide exchange factor, to the membrane through one of Grb2's two SH3 domains. SOS can then interact with Ras, a small GTP-binding protein which is confined to the membrane, causing it

to exchange its GDP for GTP and regain its activated state. Activated Ras can then react with its target molecule. The signaling component that follows Ras in this signaling pathway is the cytosolic serine/threonine kinase Raf. It is known that ras and Raf interact at the membrane, but the events that cause the activation of Raf are unknown. Raf directly phosphorylates two serine residues on MEK, a dual specificity cytosolic kinase. The activation of MEK represents a point where pathways can converge. MEK Kinase, which is activated by G proteins, can activate MEK as well. Activation of MAP Kinase, a serine/threonine kinase with several targets, requires both tyrosine and threonine phosphorylation by MEK. From this step on, the cascade continues along various branches through serine threonine phosphorylation events. Ultimately, this pathway of kinases activate or inactivate nuclear transcription factors which can modulate transcription events.

It is clear that subcellular localization plays an important role in executing signaling pathways. Components require close proximity for interaction. IRS-3 (pp60), like IRS-1 and IRS-2, has a PH and a PTB domain and phosphotyrosine motifs that interact with the SH2 domains of PI3-kinase and Grb2, yet IRS-3 is much smaller than its relatives and has regions of sequence dissimilar from IRS-1/2. Interestingly, IRS-3 exhibits a different subcellular distribution than IRS-1/2. In rat adipocytes, IRS-1/2 are primarily associated with the low density microsome and cytosol fractions, yet IRS-3 remains associated with the plasma membrane fraction (Anai et al., 1998).

It is clear that insulin accomplishes its many biologic effects by employing an array of substrates, diverse in their domain structure, binding specificities, and their cellular and subcellular localizations, to initiate a variety of complex signaling pathways.

2.1.4 IRS and Diabetes

The relationship between insulin signaling components and NIDDM is not well understood. Persons who express one of the known IRS-1 polymorphisms are twice as likely to develop type II diabetes as control

individuals (Laakso et al., 1994), yet in mice, the absence of IRS-1 does not lead to type II diabetes. Mice lacking IRS-1 are only mildly insulin resistant, since insulin secretion increases to compensate for the resistance (Araki et al., 1994; Tamemoto et al., 1994). The functional relationship between the insulin receptor and its substrate IRS-1 may have a role in type II diabetes however.

Mice that are double heterozygous for null alleles in both the insulin receptor and IRS-1 genes are, at birth, slightly more insulin resistant that mice heterozygous for either the enzyme or substrate alone. During their first 4-6 months however, about half of these mice develop type II diabetes (Bruning et al., 1997). This is one piece of evidence for the importance of the enzyme-substrate relationship between the insulin receptor and insulin receptor substrates in glucose metabolism.

IRS-1 and IRS-2 are highly homologous, yet have different interactions with activated insulin receptors and distinct tyrosine phosphorylation motifs in their C-termini (Miele et al., 1999). These findings portend unique signaling patterns for these insulin receptor substrates. Indeed, recent work has shown that disruption of IRS-2 causes diabetes in mice. These mice suffer progressive deterioration of glucose homeostasis and, at 10-16 weeks of age, develop severe NIDDM due to end-tissue insulin resistance and beta cell failure (Withers et al., 1998).

Mutations in insulin signaling at more than one level may contribute to the development of diabetes in some individuals. Despite much research, the genes responsible for the majority of NIDDM cases have not yet been identified (Kahn, 1998).

2.2 Insulin Signaling in the Brain

The presence of insulin in the CNS was first recognized two decades ago by immunohistochemical staining of the brain with anti-insulin antibodies (Havrankova et al., 1978). Later studies documented the expression of insulin in neurons (Dorn et al., 1981). The relevance

of insulin signaling in the brain suffered years of controversy however, primarily because the origin of this brain insulin was disputed. Substantial evidence now exists for the transport of peripheral insulin across the blood-brain barrier by GLUT1 and GLUT3 (Frank et al., 1986; Duffy and Pardridge, 1987; Pardridge et al., 1990) as well as for the local production of insulin in neurons (Clarke et al., 1986; Young, 1986; Wozniak et al., 1993). Today, the distributions of components of the insulin signaling pathways are being characterized, and the effects of insulin on the brain and on neuronal cells in culture are being dissected. The consequence of insulin in the brain has yet to be elucidated, however.

2.2.1 The Insulin Receptor in Brain

The presence of insulin receptors in the CNS is now well documented (Havrankova et al., 1978; Wozniak et al., 1993; Kenner et al., 1995; Smit et al., 1998). Immunocytochemistry, binding studies, and other experiments indicate that insulin receptors are dispersed throughout the brain. The highest densities of insulin receptor are in the olfactory bulb, cerebral cortex, hypothalamus, and hippocampus. In situ hybridization studies show insulin receptor mRNA distributed in various parts of the olfactory bulb, cerebral cortex, cerebellum, hypothalamus, and brain stem (Wozniak et al., 1993).

Two types of insulin receptors are found in brain. Studies in primary cell culture indicate the glial insulin receptor, like the insulin receptor in peripheral tissues, has a higher apparent molecular weight than the neuronal insulin receptor. Denaturing gel electrophoresis demonstrates that the apparent molecular weight of the neuronal insulin receptor about 5-10 kDa lower than those of their peripheral counterparts: 115 kDa for the α subunit and 85 kDa for the β subunit. This distinct feature of brain insulin receptors is conserved in mammals, birds, reptiles, and amphibians (Wozniak et al., 1993; Kenner et al., 1995).

Peripherally, two forms of the insulin receptor have been identified. These are generated by alternative splicing of exon 11,

which differ by a 12 amino acid insert at the C-terminus of the α subunit. This does not reflect the difference between peripheral and neural insulin receptors, however. Careful sequence analysis of the entire coding region of brain insulin pro-receptor cDNA has shown that neural and peripheral insulin receptors have identical primary structures, and has ruled out the possibility of alternative splicing as the origin of the lower apparent molecular weight of brain insulin receptors (Kenner et al., 1995)

Biochemical studies support the conclusion that the brain insulin receptor differences are due to distinct carbohydrate additions. The α subunit of the insulin receptor contains multiple N-linked glycosylation sites, and the β subunit contains a number of these sites as well. Whereas endoglycosidase H (cleavage of N-linked mannose) and endoglycosidase F (cleavage of N-linked mannose and complex carbohydrates) treatments affected both brain and peripheral insulin receptor α subunits equally, treatment of insulin receptors with neuraminidase, an enzyme that cleaves N-linked terminal sialic acid residues, had no effect on the molecular weight of brain insulin receptor α subunit but it reduced the molecular weight of the peripheral insulin receptor α subunit by approximately 10 kDa (Hendricks et al., 1984; McElduff et al., 1988; Wozniak et al., 1993).

Despite the structural difference between the glial and neuronal insulin receptor, the insulin binding characteristics and the ligand induced autophosphorylation of these receptors are the same. However, the insulin-induced cell biological response achieved by these cells is not the same (Wozniak et al., 1993). For example, chronic insulin exposure causes expression of the glial insulin receptor to be down-regulated, an effect not observed in neuronal cells (Clarke et al., 1984). In glial cells, insulin binding to its receptor stimulates glucose uptake, a biologic consequence that does not occur in neurons (Wozniak et al., 1993). Insulin has different effects on neurons. For example, insulin stimulates the uptake of serotonin, while it inhibits the uptake of norepinephrine. Although neurons express both insulin receptor and IGF-I receptor, this effect is not achieved with IGF-I

treatment. Similarly, immunodepletion of neuronal IGF-I receptors has no effect on insulin-stimulated insulin receptor kinase activity (Boyd et al., 1985). These results indicate that the neuronal effects of insulin are specifically mediated by the insulin receptor.

2.2.2 The Insulin Receptor Signaling Pathway in Brain

Since both insulin and insulin receptor are present in brain, and insulin binding appears to exact biological responses in neurons and glia, one expects to locate downstream elements of the insulin-signaling pathway to be present in the brain as well.

In situ hybridization reveals that the patterns of insulin receptor mRNA and IRS-1 mRNA are similar in both distribution and relative intensity. In most regions, hybridization is observed primarily in neuronal cell body layers. In olfactory bulb and hippocampus, IRS-1 and insulin receptor mRNA are also concentrated in synaptic layers (Baskin et al., 1994) suggesting that there may be a role for insulin signaling processes at synapses.

Significant amounts of IRS-1 and insulin receptor proteins are expressed in brain as well. Immunocytochemical studies ascertained that a large number of neurons in the adult CNS express IRS-1, insulin receptor and/or IGF-I receptor, and PI3-kinase. No staining for IRS-1 is detected in glial cells. Although IRS-1 and insulin receptor staining patterns tend to overlap, in a few areas of the brain the expression patterns of IRS-1 and PI3-K do not parallel the insulin receptor and/or IGF-I receptor expression patterns. In general, IRS-1 and insulin receptor immunoreactivity is restricted to cell bodies, although in certain regions including the cerebellar cortex, staining is appreciated in the initial portions of proximal dendrites (Baskin et al., 1994; Folli et al., 1994).

Although IRS-1 and the insulin receptor have been localized to neurons, it appears unlikely that IRS-1 acts discriminately in the brain as a substrate in the insulin signaling pathway. In cultured cerebral cortical neurons, IRS-1 and its close relative IRS-2 participate in the neurotrophin signaling pathway. In these cultures, IRS-1/2 are tyrosine

phosphorylated, and associated with PI3-kinase, in response to brain-derived neurotrophic factor (BDNF) treatment. This response is mediated by the BDNF/NT3 receptor tyrosine kinase TrkB. There is no direct interaction between TrkB and PI3-kinase in response to BDNF treatment, so the binding of BDNF to TrkB induces the activation of PI3-kinase in an IRS-1/2 dependent manner (Yamada et al., 1997).

2.2.3 Insulin Signaling at Synapses

Although the expression of insulin signaling proteins, including insulin receptor, IGF-I receptor, IRS-1/2, and PI3-kinase, is primarily concentrated at cell bodies, new experiments suggest a role for insulin at synapses.

Synaptosomal preparations, rich in sealed synaptic terminals, contain ~200 pg of insulin per mg of protein, a four-fold enrichment from whole brain extracts (Wei et al., 1990). The depolarization of synaptosomes (elicited by raising the extracellular K^+ concentration from 5 mM KCl to 60 mM KCl) induces a four-fold greater release of insulin than the amount of basal insulin release, measured by radioimmunoassay. Removing Ca^{++} from the medium, or blocking voltage-dependent Ca^{++} entry with elevated Mg^{++} or Co^{++} concentrations, inhibits this release. Synaptosomes can also be depolarized by the activation of neuronal voltage-gated Na^+ channels by the drug veratridine. This treatment induces an even greater increase in insulin release, eight-fold greater than basal levels. Tetrodotoxin treatment, which blocks Na^+ channels, inhibits this effect. It is well-established that depolarizing synaptosomes with high K^+ levels or with veratridine leads to increased intrasynaptosomal Ca^{++} levels and neurotransmitter release. Thus, elevated intra-synaptosomal Ca^{++} levels induce insulin release as well (Wei et al., 1990). A similar result occurs following the depolarization of cultured neuronal cells, but not of astrocyte or glial cells (Clarke et al., 1986). These authors propose that the brain is "capable of restricting and controlling the availability of insulin in a manner consistent with that of neurotransmitters and modulators (Wei et al., 1990)."

Theories about the biologic response to insulin at synapses converge on learning and memory. A recent *Science* note (Wickelgren, 1998) proposes a link between insulin and memory, citing several new publications. Rats that receive brain injections of streptozotocin, a drug that damages the insulin receptor, exhibit an impaired ability to remember the compartment in which they had received a shock (Hoyer, 1997). Further, a study in human subjects finds that insulin mediates improvements in verbal memory in both early stage Alzheimer's disease patients and controls (Craft et al., 1996). Experiments in neuronal cell cultures show that insulin inhibits the hyperphosphorylation of tau, a process that has been linked to the formation of neurofibrillary tangles, a hallmark of Alzheimer's disease (Hong and Lee, 1997).

Linking insulin's action to learning and memory is intriguing, yet direct evidence for this is scant. It must be first demonstrated that insulin receptor signaling elements are localized to synapses, and subsequently, that such signaling pathways play role in the mechanisms of synaptic plasticity. One compelling piece of evidence for a direct insulin effect at synapses establishes that insulin induces a rapid recruitment of functional type A GABA receptors, the principal neurotransmitter at inhibitory synapses, from intracellular to postsynaptic and dendritic membranes. Inhibition of protein tyrosine kinases by the drug genistein blocked this translocation, suggesting that an activated insulin receptor is required to execute insulin's effect. This translocation of $GABA_A$ receptors is observed in HEK cells, hippocampal neurons in culture, and neurons in hippocampal slices (Wan et al., 1997).

2.3 The Postsynaptic Density

It is becoming clear that, at excitatory synapses in particular, an elaborate signaling machine rests just below the postsynaptic membrane, in the form of the postsynaptic density. It is reasonable to propose that, if insulin has a role at excitatory synapses, then the

downstream effectors of the insulin signal are likely to be tethered at the PSD, positioned to transform the presynaptic insulin signal into a postsynaptic, biologic consequence.

2.3.1 History and description

The postsynaptic density, or PSD as it has since become known, was remarked upon in the 1950's by an electron microscopist, Sanford Palay. He stained CNS synapses with osmium tetroide and described what he saw, a prominent thickening on the cytoplasmic side of the postsynaptic membrane of synapses, as a 'postsynaptic density.' Microscopists observed that these PSDs varied in thickness, and a classification system developed wherein PSDs were subdivided morphologically, the thicker being classed as 'asymmetric,' or type I, and the thin, sparse PSD as 'symmetric,' or type II. This morphologic classification was later paired with the observation that the thicker, type I PSDs were at excitatory, or glutamatergic synapses, whereas the thinner, type II PSDs were correlated with inhibitory, or GABAergic, synapses (Kennedy, 1993).

In the 1970's, cell biologists advanced biochemical methods for the subcellular fractionation of brain tissue into fractions enriched for structures morphologically similar to type II PSDs. From brain homogenate, Philip Siekevitz' group purified synaptosomes (synaptic membranes), treated these with 0.5% Triton X-100, and purified this extract by further centrifugation. This PSD-enriched fraction, when separated by SDS-PAGE, appears to contain about 15 major and 10 minor protein bands. Carl Cotman used a similar technique, but extracted with 3% N-lauroyl sarcosinate, a harsher detergent. SDS-PAGE of this PSD fraction revealed about 10 major bands (Cotman et al., 1974)(Cotman et al., 1974(Kennedy, 1993)).

> The PSDs isolated with our procedure are apparently derived from the asymmetric type of synapse (type I). They are generally similar in size to the PSDs from cortical asymmetric synapses, and no structures in these fractions resemble the thin sparse PSDs often present at symmetric (type II) synapses. On this basis, the purified PSDs most likely arise predominantly from excitatory axodendritic synapses. Thus our PD fraction represents the distinctive

organelle of this specific synaptic type in isolation (Cotman et al., 1974).

These techniques are the basis of today's protocols for the preparation of PSD fractions. Often, a 0.5% Triton extraction is referred to as yielding a PSDI fraction, this followed by a second 0.5% Triton extraction as PSDII, or followed by a 3% N-lauroyl sarcosinate extraction as PSDIII, or 'core PSD' (Kennedy, 1997). Today, biochemically purified PSD fractions are generally believed to be enriched for the dense thickenings of proteins that lie apposed to excitatory, glutamatergic, active zones.

During the early days of PSD investigation, there were two major impediments to working with the PSD fraction. First, the PSD was regarded by some as a morphological entity that was not physiologically significant. Moreover, the PSD structure was technically challenging, disruptable only by treatment with SDS, a harsh detergent. Nonetheless, tubulin, actin, and fodrin (brain spectrin), as well as calmodulin were identified as PSD components. In the 1980's the 'major PSD protein' was identified as a subunit of the brain calcium/calmodulin dependent protein kinase (αCaMKII). This discovery ushered in growing support for the hypothesis that the PSD organizes signaling molecules.

Though some PSD characterization proceeded, it was not until the first half of the 1990's, when the techniques of peptide microsequencing were widely available, that biochemists were able to begin to identify individual components of the PSD. In many cases, the fraction was separated by SDS-PAGE, individual protein bands were excised and tryptically digested, and the peptide sequence obtained was used to identify or clone the abundant protein.

During this time, the first novel PSD protein was identified and cloned: PSD-95 (Cho et al., 1992; Kistner et al., 1993). The lack of known interactions for this protein spurred the utilization of a newly emerging technique for discovering protein-protein interactions, the yeast two hybrid assay. In 1995, using this technique, investigators selected regions of PSD-95 to use as 'bait' and uncovered an interaction between one portion of PSD-95 and the C-terminal tail of the 2B subunit

of the NMDA receptor (Kim et al., 1995; Kornau et al., 1995). Meanwhile, a biochemical approach had led to the discovery that a protein that had previously had been observed to be phosphorylated by kinase activity inherent to the PSD, the concavalin-A binding PSD protein gp180, was the 2B subunit of the NMDA receptor (Gurd, 1985).

Evidence of interactions between neurotransmitter receptors, kinases, and novel proteins at the PSD greatly advanced the appreciation of the PSD as a functional unit, as well as significantly modified the way in which researchers approached dissecting the components of the PSD. Today, due to the continued successes of the yeast two-hybrid technique, molecular biologists regularly fish the PSD and uncover new protein-protein interactions that occur within this clearly significant density of proteins.

2.3.2 The excitatory postsynaptic apparatus

Ion channels and a cohort of receptors dive through the postsynaptic membrane and are anchored to the PSD. Glutamate binds to and activates several types of receptors on the postsynaptic membrane of excitatory synapses. NMDA and AMPA receptors are ligand gated ion channels that transduce ligand binding into cation influx. Metabotropic glutamate receptors are G-protein coupled seven transmembrane receptors that mediate the slower action of glutamate by intracellular second messengers. Communication depends on these receptors being concentrated at the postsynaptic apparatus where they can respond to presynaptically released glutamate. Glutamate receptors maintain a specific topological relationship there: AMPA receptors are central, facing the presynaptic zone, and metabotropic receptors lie at the edges. The mechanisms that lead to their specific clustering are beginning to be understood (Sheng, 1997; Ziff, 1997).

One of the proteins that clusters glutamate receptors and connects them to cytoplasmic proteins is the above mentioned 95 kDa protein isolated from PSD fractions, PSD95 (Ziff, 1997). PSD95 is the prototype for a family of membrane associated guanylate kinase (MAGUK) proteins. These proteins contain at the N-terminus, three PDZ domains, an SH3

domain and a guanylate kinase domain at the C-terminus. The cloning of PSD95 revealed the existence of the PDZ domain, named after the three proteins in which it was first identified, PSD95, discs large (*dlg*), and zona occulens (ZO-1). PSD95 contains three PDZ domains that specifically bind to peptide sequences at the C-terminus of interacting proteins. The PDZ domain creates a hydrophobic pocket in which rests the C-terminal motif T/SXV-COOH. A diverse set of proteins bears this peptide motif at their C-terminus, including Fas.

The first 2 PDZ domains of PSD95 interact with the C-terminus of the NMDA receptor subunit NR2, as well as with the Shaker K^+ channel. MAGUK proteins also can link receptors to cell adhesion molecules that are concentrated at synapses. The third PDZ domain of PSD95 binds neuroligan, a cell surface protein (Ziff, 1997). PDZ domains have also been shown to bind intracellular proteins. PSD95 and chapsyn110/PSD93 interact with neuronal nitric oxide synthase (nNOS) through a PDZ-PDZ interaction. As mentioned in Chapter I, nNOS can similarly interact with a PDZ domain in syntrophin.

Following the identification of the PSD fraction protein PSD95, two other synapse-associated glutamate receptor interacting proteins were identified. The AMPA receptor subunits GluR2 and GluR3 bind the synaptic glutamate receptor interacting protein (GRIP) and AMPA binding protein (ABP). This theme continues for the metabotropic glutamate receptor. Homer, which contains a single PDZ-like domain, binds mGluR1α and mGluR5. The level of Homer expression is dramatically upregulated by synaptic activity. It appears likely that these types of proteins couple receptors to downstream signaling pathways (Sheng, 1997).

PSD95 and chapsyn110 not only bind, but also cluster NMDAR receptors and Shaker channels. It is now known that MAGUK proteins can multimerize through disulfide bridges between pairs of cysteines located at the N-terminus (Hsueh et al., 1997). It is likely that PSD95 and other MAGUKs use this mechanism to cluster their target proteins. Although GRIP and ABP represent a different class of PDZ proteins (they lack the SH3 and GK domains of MAGUK proteins) it is likely that they multimerize as do MAGUKs (Ziff, 1997). The existence of separate

proteins for the postsynaptic clustering of glutamate receptor types may allow for their differential distribution within the postsynaptic apparatus.

The GK domain enables MAGUK proteins to serve as intermediaries between channels and Guanylate Kinase domain Associated Proteins (GKAPs). While the GK domain exhibits high homology to guanylate kinases, and can bind GMP, it has no catalytic activity. The GK domain binds the PSD fraction associated protein GKAP, three other SAPAPs (SAP-associated proteins) and two DAP (hDLG and PSD95 associated protein) proteins. To date, no interactions have been found for MAGUK proteins' SH3 domain.

2.3.3 A postsynaptic signaling apparatus

The excitatory synapse rapidly obtains and transmits information. As scientists map the interconnections among postsynaptic proteins, it is becoming clear that the PSD is a relay station on this information highway that encompasses the synapse's elaborate signaling machine.

CaMKII, the major PSD protein, has been shown to be involved in synaptic plasticity, namely in LTP. Numerous regulatory molecules reside in the PSD, including calmodulin. Calmodulin binds to CaMKII until the kinase becomes autophosphorylated. CaMKII then translocates to the PSD and is poised to serine/threonine phosphorylate glutamate receptors. Although there is as yet no known functional role for the serine threonine phosphorylation of NMDA receptors by CaMKII, tyrosine phosphorylation of NMDA receptor has been shown to regulate ion channel function under certain conditions (Kennedy, 1997).

Other enzymes, including the non receptor tyrosine kinase Fyn, and the neurotrophin RTK TrkB, are found in PSD preparations. TrkB has been shown to binds its ligand BDNF at PSDs (Wu et al., 1996). The substrates of this RTK at the postsynaptic apparatus are not yet known. NMDA receptor subunits NR2A/B have been shown to bind SH2 domains in a tyrosine phosphorylation dependent manner, but the identity of such SH2 domain containing proteins are not known.

Several cytosolic serine/threonine kinases are tethered near to or within the PSD by adapter proteins. Type II PKA is anchored at the PSD by A kinase anchoring proteins AKAP79 and AKAP150. AKAP79 also anchors PKC, a cytoplasmic serine/threonine kinase found at the PSD (Ziff, 1997). Other types of signaling elements are found in PSD fractions, including protein phosphatase 1 (PP1) and G proteins. The Ras-GTPase activating protein Syn-GAP is a component PSD fractions. Syn-GAP binds to ras-GTP and decreases the signal by turning on ras' GTPase activity. PSD fractions also contain the downstream signaling component ERK2-type MAP Kinase and its substrates.

These signaling pathways are likely anchored by the cytoskeletal elements of the PSD. Actin and α-actinin-2 are abundant in PSD fractions, and fodrin (non-erythroid brain spectrin) is a major calmodulin binding protein in PSD preparations. Other less abundant cytoskeletal components that are found in the PSD fraction include dystrophin, amyloid precursor protein-like protein-1, and α-adducin. α-actinin-2 binds to the cytoplasmic tails of NR1 and NR2B through its central rod domain. This interaction is antagonized by Ca^{++}/calmodulin binding to NR1. Ca^{++} fluxes through the NMDAR may activate calmodulin and release the receptor from the cytoskeleton. The reduction in NMDAR channel currents that result from Ca^{++}/calmodulin binding to the NR1 C-term may occur due the channel dissociating from the cytoskeleton. In sum, a variety of discrete signaling pathways are woven into the PSD, placed to elicit the coordinated functions required at the synapse.

2.3.4 Synapse regulation

While the cytoplasm of most cells is filled with signaling pathways that coordinate and intersect to allow for diverse coordinated functions, it appears that these tools are specifically enriched locally, for short term plasticity, and are locally modified, for the construction of long term changes. How can the crucial structure of the postsynaptic apparatus change to reflect its active environment?

The latest hypothesis focuses on local mRNA regulation and translation. This type of self-contained mechanism would be necessary if

all of the synapse's signaling machinery was locally arranged. Perhaps at the postsynaptic signaling apparatus, the signal that originates in the synaptic cleft and migrates to the postsynaptic membrane, weaves about the PSD and induces, in conjunction with the PSD protein CPEB (cytoplasmic polyadenylation element binding protein), synthesis of new synaptic components. This inducible, local, new synthesis, allows for maintenance or modulation of the synaptic structure. Indeed, the polyadenylation of CaMKII mRNA is regulated in a CPEB dependent manner, and activity can induce CaMKII synthesis at the synaptic apparatus (Wu et al., 1998). Other PSD protein mRNAs also possess these 3'UTR CPEB binding consensus sequences, and thus may have the potential for local translation. Whether or not these mRNAs are locally translated remains to be tested.

The PSD, a small subcellular structure, is dense with the tools that cells use to elicit change and the potential to modify and modulate the strength of an individual synapse. As PSD proteins continue to be identified, the diverse signaling pathways that the postsynaptic signaling apparatus comprises can be carefully reconstructed, aiding our understanding of how mechanisms at this small structure lead to such complex biologic outcomes as learning and memory.

2.4 The Postsynaptic Density and Insulin Signaling

Indeed, it appears that insulin and its signaling pathways are at excitatory synapses. The experimental data that I proffer in this chapter implicate the insulin receptor and the insulin receptor substrate IRSp58/53 in insulin dependent signaling mechanisms at the synapse.

3. Methods

Brain Subcellular Fractions

Brain homogenate, synaptosome, and postsynaptic density (PSD) fractions were prepared as described in Chapter I, Section 3 (Methods). Frozen porcine brain tissue was provided by Susan Lacy (Children's Hospital, Boston, MA).

Antibodies

Ab98 antisera was raised by immunizing a rabbit with the peptide KAPLPPPEYPSQ (a sequence in the cytosolic domain of β-dystroglycan that was used for the production of antibody PA3a (Yoshida et al., 1993) and affinity purified (Quality Controlled Biochemicals, Hopkinton, MA). The anti-IRSp58/53 polyclonal antibody was raised by injecting a rabbit with the MAP-conjugated peptide DKDDLALPPPDYGT (Research Genetics, Inc., Huntsville, AL) and was affinity purified. Immunoabsorption experiments were performed by mixing the primary antibody with its corresponding peptide for 2 hours to overnight at 4°C then western blotting or immunostaining as described below. H720, an anti-IRSp53 monoclonal antibody, was generously provided by Dr. Roth and is described elsewhere (Yeh et al., 1996).

The anti-dystrophin monoclonal antibody DYS2 was obtained from Novocastra, the anti-αCaMKII (#6G9) and anti-synaptophysin monoclonal antibodies were obtained from Boehringer Mannheim, the anti-NMDAR1 monoclonal antibody was obtained from Pharmingen, and the polyclonal anti-mouse CPEB antibody was obtained from Joel Richter, University of Massachusetts, Worcester (Wu et al., 1998). Insulin Receptor β subunit polyclonal (C-19) antibody was obtained from Santa Cruz Antibodies. Fas Ligand monoclonal (33) antibody was obtained from Transduction Laboratories. Insulin Receptor β subunit polyclonal antibody (#C-19) was obtained from Santa Cruz Biotechnology, Inc. An anti-peptide antiserum to β-dystroglycan (12031C) was a generous gift of Lou Kunkel (HHMI, Children's Hospital, Boston, MA). Monoclonal anti-β-dystroglycan antibody NCL-43DAG was obtained from Novocastra.

Western Blotting

Protein concentrations were determined with the BCA protein assay (Pierce, Rockford, IL), using bovine serum albumin (BSA) as a standard. Equal quantities of homogenate, synaptosomal, and PSD proteins were separated on a 10% or a 5-15% gradient gel by SDS-PAGE, transferred onto nitrocellulose membranes, and incubated with primary antibodies followed by alkaline phosphatase-conjugated goat anti-rabbit or anti-mouse IgG (Boehringer Mannheim). Bound antibody was visualized using the BCIP/NBT substrate system (Promega, Madison, WI). In some experiments, lysates of CHO.T cells, which overexpress insulin receptors (generous provided by M. Czech, Univ. of Mass Medical Center), were also analyzed. For Western blotting with DYS2, horseradish peroxidase-conjugated anti-mouse IgG was used as the second layer, and bound antibodies were visualized by ECL chemiluminescence (Amersham).

2D gel electrophoresis

Isoelectric focusing (IEF) was performed essentially as instructed by the manufacturer (Pharmacia Biotech). Briefly, IEF strips (Immobiline Dry Strips, pH 3-10L, 11 cm) were rehydrated for 6 hours to overnight at room temperature in 2D sample/rehydration buffer (8M urea, 2% CHAPS, 2% IPG buffer 3-10L (Pharmacia), 0.3% DTT). Strips were stored at -20°C after rehydration. Samples were diluted or resuspended to 100 µl 2D sample buffer. The soluble fraction was loaded at the anodic end of the IEF strip (pH 3-10 linear gradient, Pharmacia). IEF was performed at 20°C on a Multiphor II apparatus (Pharmacia) for 1 hour at 300V, 15 hours at 1400V. Following IEF, the strips were equilibrated at room temperature for 10 minutes in 20 mg DTT per ml equilibration buffer (50 mM Tris-HCl, pH 6.8, 8M urea, 35% glycerol, 0.3% SDS), followed by 10 minutes in 25 mg iodoacetamide per ml equilibration buffer. Strips were then placed horizontally (cathode to anode, left to right) on a 0.5 mm thick 10% SDS-polyacrylamide gel and anchored with a stacking solution (0.5% agarose, 125 mM Tris, pH 6.8, 1% SDS). Sample or protein standard was loaded into one lane on the gel and was separated by SDS-PAGE only.

The samples were electrophoresed in the second (SDS-PAGE) dimension and gels were either silver stained (Morrissey, 1981), stained with commassie blue, or transferred to nitrocellulose (10 volts, 16 hours) for western blotting.

Hydrophobic Interaction Chromatography

For hydrophobic interaction chromatography (HIC), PSDs were solubilized overnight at 4°C in 8M urea, 1M NaCl, 5 mM dithiothreotol (DTT), 50 mM sodium phosphate buffer, pH 7.5. The soluble fraction was then made 4M in urea and incubated with HIC matrix (high performance phenyl sepharose, Pharmacia Biotech) for 3 hours at 4°C. The HIC matrix was then washed, pre-eluted in the same buffer with 0.8M NaCl, and eluted with the same buffer in 0.1M NaCl. Apomyoglobin (Sigma Chemicals, St. Louis, MO) was added to the eluate as a carrier protein, and the solubilized proteins were subsequently precipitated with trichloroacetic acid.

MALDI-TOF Mass Spectrometry and peptide sequencing

HIC eluates separated by 2D electrophoresis were visualized by commassie stain and the bands corresponding to p58 and p53 were excised from the gel. The polypeptides were recovered from the gel and subjected to trypsin digestion. Peptide masses were determined by Matrix Assisted Laser Desorption Ionization Time-of-flight Mass Spectrometry (MALDI-TOF MS). MS-Fit search software was then used to compare the p58 and p53 mass profiles to known proteins. Tryptic fragments from p58 and p53 were separated by HPLC and peptide sequence was obtained from 3 fragments of p58 (J. Leszyk, Worcester Foundation Protein Sequencing Facility, Worcester, MA).

In vitro phosphorylation of PSD fraction proteins

The method used is a modification of a procedure described elsewhere (Dosemeci et al., 1994). PSDs were pretreated on ice for 3 hours with occasional mixing in 20 mM HEPES, pH 7.4, 100 mM DTT. PSDs were diluted to a final concentration of 0.4 mg protein/ml in

phosphorylation solution (5 mM $MgCl_2$, 50 µg/ml leupeptin, 20 mM DTT, 20 mM HEPES, pH 7.4, 1 mM $CaCl_2$, 1 mM orthovanadate, +/- 100 µM ATP)), and incubated at 37°C for 5 minutes. The reaction was quenched by the addition of SDS sample buffer.

Northern blot hybridization

The ^{32}P labeled IRSp58/53 oligonucleotide probe was synthesized by PCR using the IRSp53 cloned DNA (provided by Roth, described in (Yeh et al., 1996)) as template and the primer pair:

F1: AAGAGCGTGACCCCGAAGAACAGC

R1: AACCAGCCCCGCATTTTG.

The rat Multiple Tissue Northern Blot (MTN; Clontech, Palo Alto, CA) was prehybridized in ExpressHyb for 1 hour at 55°C. The IRSp58/53 probe was denatured, diluted in ExpressHyb, and incubated with the blot overnight at 55°C. After hybridization, the blot was washed extensively; the most stringent wash performed was 0.1X SSC, 0.1% SDS, at 65°C for 40 minutes.

The ^{32}P labeled human βactin cDNA control probe was generated using random hexamer labeling (Gibco). The blot was prehybridized in ExpressHyb for 1 hour at 68°C. Hybridization with the βactin cDNA probe was performed overnight at 68°C. The blot was then washed extensively; the most stringent wash performed was 0.5X SSC, 0.1% SDS at 60°C for 60 minutes.

RNA isolation and RT-PCR

RNA was isolated from 20 mg of rat cerebral cortex by the RNeasy mini kit (Qiagen). cDNA was synthesized by reverse transcription of 30 µg of the RNA, using either oligo-(dT) or random primers and reverse transcriptase (Gibco). Conditions for reverse transcription were 40 X (3 minutes at 94°C, 1.2 minutes at 37°C, 4.3 minutes at 60°C). The product of this reaction was used as the template for PCR. The PCR conditions were 3 minutes at 94°C, 40X (30 sec. at 94°C, 1 minute at 55°C; 4 minutes at 68°C), 8 minutes at 68°C. The sequences of the primers used are as follows:

A (UTR/C): 5' GTGTAGCCGGGACCCAGGACCAT 3'
B (MIDF): 5' CGAGGAGCGGAGGAGGTTCTGC 3'
C (F1): 5' AAGAGCGTGACCCCGAAGAACAGC 3'
D (R1): 5' AACCAGCCCCGCATTTTG 3'
E (MIDR): 5' ACGGCCACACTGTAGGGTCTCTGC 3'
F (ENDR): 5' TCTAGTCAGGGGCAGCTCAAAATC 3'.

Tissue sections and immunohistochemistry

Brains were dissected out of adult female rats, and immersed in freezing isopentane, mounted in OCT embedding medium and equilibrated to -20°C. 8 μm frozen sections were cut, air-dried onto glass slides, fixed in MeOH at -20°C for 10 minutes, and rehydrated in PBST (PBS, 0.1% Triton-X 100). The sections were blocked for one hour at room temperature with PBST, 1% BSA, 10% horse serum, 1% goat serum. The primary antibodies, anti-IRSp58/53 (1 ug/ml +/- peptide (1 mg/ml)), rabbit anti-synapsin-I (1:3000, Pietro DeCamilli, HHMI (Malgaroli et al., 1989)), or control rabbit IgG (Sigma, 1 ug/ml) were diluted in blocking solution and were applied overnight at 4°C. The slides were washed at room temperature for 2 hours in PBST with stirring and one wash solution change. Cy3-conjugated goat anti-rabbit IgG (1:500-1:4000, Jackson ImmunoResearch) or FITC-conjugated goat anti-mouse IgG, rat absorbed (1:100, Vector Laboratories, Burlingame, CA) was applied for 3 hours at room temperature. The sections were washed as above, dehydrated in -20°C MeOH for 10 minutes , allowed to air dry, and mounted in Citifluor (Ted Pella Inc., Redding, CA). Immunostaining was visualized by indirect fluorescence using a Nikon E800 fluorescent microscope. Images were recorded with a Photometrics CCD camera using IP Lab systems software.

Hippocampal neuron cultures and immunohistochemistry

Low density cultures were maintained primarily by David Wells, a postdoctoral fellow in the lab (Wu et al., 1998)), as described in (Goslin and Banker, 1991). Briefly, the hippocampus was removed from E18 rat embryos, trypsinized (0.25%), dissociated by trituration, and plated

onto poly-L-lysine (1 mg/ml) coated glass coverslips in modified Eagle's medium (MEM, Gibco) with 10% horse serum for 4 hours. The coverslips were then transferred to dishes containing a monolayer of glial cells in growth medium consisting of MEM, ovalbumin (100 µg/ml) pyruvate (1.1 µg/ml), glucose (0.6%) and N2 supplement. The culture medium was changed weekly. After 19-21 days, the cells were fixed with 4% paraformaldehyde at 37°C for 20 minutes, covered with saponin (0.05%) for 5 minutes and then incubated in blocking solution (MEM, 10% horse serum, 1% goat serum, 1% BSA). The primary antibodies, mouse anti-synaptophysin (Boehringer, diluted 1:20), mouse anti-insulin receptor β subunit (Santa Cruz, diluted 1:100), and rabbit anti-IRSp58/53 (diluted 1:5) were applied overnight at 4°C and the second layer antibodies, directly conjugated to either FITC (Caltag) or Cy3 (Jackson ImmunoResearch), were applied for 1 hour at room temperature. The coverslips were mounted onto glass slides with Citifluor (Ted Pella).

In vitro transcription/translation and immunoprecipitation

IRSp53 was subcloned from the Bluescript vector into the BamH1 site of the expression vector pMGT. The clones C2797 and DP71 (in pMGT, provided by L. Kunkel (Ahn and Kunkel, 1995; Chan and Kunkel, 1997)), encode a dystrophin fragment from bp 2797 to the C-terminal end, and the small dystrophin isoform that is highly expressed in brain, respectively. The clone αDG is in the expression vector pMGT and encodes a dystroglycan fragment from bp 345 to 653. These plasmids were used for in vitro transcription/translation (TNT Quick Coupled In Vitro Transcription and Translation System, Promega) using ^{35}S-methionine. In vitro expressed proteins were diluted in TBST (10 mM Tris pH 7.8, 150 mM NaCl, 0.1% Tween-20) and incubated with each other on ice for 1 hour. The mixtures were then incubated with the immunoprecipitating monoclonal antibody (DYS2 or H720) for one hour. The sample-antibody mixture was then incubated with Protein G-sepharose (Sigma Chemicals) for 1 hour. The beads were washed with TBST and then incubated in protein sample buffer at 100°C for 10 minutes. The supernatants were analyzed by SDS-PAGE and autoradiography.

Biotinylation and solubilization of PSDs

Purified PSDs (2 mg) were resuspended in 1 ml 50 mM HCO_3, pH 8.8. Following the addition of 74 ul biotin (1 mg/ml), PSD proteins were incubated for 30 minutes at room temperature and then solubilized as described in (Blackstone et al., 1992). Briefly, PSDs were reisolated by centrifugation, and resuspended in 10 mM Tris, pH 7.4. 1/10 volume of 10% DOC, 500 mM Tris pH 9.0 was added to the PSD and the mixture was incubated at 37°C for 30 minutes with occasional vortexing. 1/10 volume of 1% Triton X-100, 50 mM Tris pH 9.0 was added, and the PSD solution was dialyzed overnight against 50 mM Tris pH 7.4, 0.1% Triton-X100. The following day, the PSD solution was centrifuged at 100K x *g* for 30 minutes This supernatant was used for immunoprecipitations and for incubation with GST-tagged proteins.

GST-tagged IRSp53

PCR mutagenesis was used to introduce EcoR1 sites that flanked the coding region of IRSp58/53 using the primers:

F= 5' CGGAATTCTCGCTCTCACGCTCGGAG 3'

R= 5' GGGAATTCAAAATCTGGCCACTT 3'.

The PCR product was gel-purified (Qiagen), and linearized pGEX-1λT (Pharmacia), was ligated with or without the insert (T4 ligase). BL21 (and DH10B cells for plasmid maintenance) were electroporated with the ligation products and screened for inserts. I isolated DNA isolated from several colonies, and performed PCR with a IRSp58/53 specific primer pair to determine the presence or absence of the IRSp58/53 insert. The restriction enzymes Sph1 and BamH1 were then used to determine the orientation of the insert. Identification of a clone with a correctly oriented IRSp58/53 insert was verified by sequencing the plasmid from each end of the ligation. Sequencing primers were:

F= 5' GGGCTGGCAAGCCACGTTTGGTG 3'

R= 5' CCGGGAGCTGCATGTGTCAGAGG 3'.

Fusion Proteins

BL21 cells were grown overnight in Luria broth with 1 μg/ml ampicillin (LBA). The overnight cultures were diluted 1:10 in fresh LBA and grown until the absorbance at OD_{600} = 0.8. Protein expression was induced by adding IPTG to the cultures to a final concentration of 1 mM. Induced cultures were incubated with agitation at 25°C for 3 hours. The cells were pelleted and resuspended in $1/100^{th}$ culture volume with 50 mM Tris, 150 mM NaCl. Triton X-100 was added to the resuspended cells to a final concentration of 1% and DTT was added to 1 mM. The cell suspension was sonicated for 3 x 10 seconds and the sonicate was centrifuged for 5 minutes at 14,000 rpm. The supernatant was collected and placed on ice. The pellet was resuspended as above and sonicated 2 x 10 seconds. The sonicate was centrifuged for 5 minutes at 14,000 rpm and the supernatant was pooled with above. The pooled supernatants were spun and the supernatant was incubated for 1.5 hours at 4°C with glutathione-sepharose beads that had been rinsed with 20 volumes of PBS. The beads were washed with 50 mM Tris, 150 mM NaCl, 1% Triton X-100 and packed for elution. Glutathione elution buffer (10 mM reduced glutathione, 50 mM Tris-HCl, pH 8.0) (1 ml) was added, the beads were incubated for 10 minutes at room temperature, the eluate was collected, and elution was repeated. Eluate fraction were pooled and dialyzed overnight at 4°C against 50 mM Tris pH 7.5, 0.1% Triton X-100. Following dialysis, salt was added to a final concentration of 150 mM NaCl. The purified GST protein solutions were then tumbled with an equal volume of solubilized, biotinylated PSDs or synaptosomes for 4 hours at 4°C. This mixture was then incubated with fresh, rinsed glutathione-sepharose beads for 1.5 hour incubation at 4°C, and subsequently washed thoroughly. GST-sample complexes were released from the glutathione sepharose by boiling the pellet for 10 minutes in sample buffer. Eluates were analyzed by western blot, and biotinylated PSD proteins were identified by incubating the blot in ABC reagent and visualizing the reaction with the BCIP/NBT system (Vector).

^{35}S labeled in vitro expressed IRSp58/53 blot overlay

The subcellular fractions were separated by SDS-PAGE and blotted to nitrocellulose. The blot was immediately rinsed in wash buffer (Hanks Buffered Saline Solution (HBSS), 0.1% BSA, pH 7.4) for 30 minutes with multiple wash changes. The blot was blocked for 3 hours at 4°C (HBSS, 1% BSA, 1 mM DTT, 5 mM HEPES, pH 7.4). ^{35}S-labeled proteins (IRSp58/53, αDG) were made as described above. The radiolabeled proteins were diluted in block and incubated with the blot overnight at 4°C. The blots were washed for 1 hour with multiple changes of wash buffer, dried, and exposed to film for 6 hours to overnight.

4. Results

The postsynaptic density is a structure that appears to be the morphological consequence of a complex scaffold of signaling molecules that rests just below the postsynaptic membrane of central synapses. I have identified a protein that is selectively enriched in the PSD fraction as the insulin receptor substrate IRSp58/53. The protein IRSp58/53 was recently identified in a non neuronal cell line and found to be an insulin receptor substrate (Danielsen and Roth, 1996; Yeh et al., 1996; Yeh et al., 1998). I have determined that the IRSp58/53 mRNA is most highly expressed in brain, and that alternative splicing of the transcript does not appear to account for IRSp58/53's appearance as a doublet following electrophoresis, nor do traditional post-translational modifications. Additionally, I have shown that IRSp58/53 is concentrated at synaptic sites: in cerebellar tissue and in cultured hippocampal neurons. I have found that the β subunit of the insulin receptor, IRSp58/53's functional partner, is a component of the PSD fraction as well. I have uncovered no interaction between IRSp58/53 and the potential binding partners dystrophin or FasL in vitro. I have identified a potential binding partner for IRSp58/53, PSD255. The results that I present here provide evidence for a synaptic insulin receptor signaling pathway.

4.1 Polypeptides p58 and p53 are enriched in the postsynaptic density fraction

While surveying adult rat brain homogenate, synaptosome, and PSD fractions to determine the relative enrichment of β-dystroglycan in subcellular fractions (see Chapter I), I discovered that one antiserum, Ab98, cross-reacted with a pair of polypeptides of 58 kDa and 53 kDa, termed p58 and p53, that were highly concentrated in the PSD fraction (Figure 4). p58 and p53 were highly enriched in the PSD fraction, since these polypeptides were not detected in blots of homogenate and

synaptosomes that contained the same amount of total protein (Figure 4A). p58 and p53 were enriched in PSD fractions isolated from rat cerebral cortex, cerebellum, and hippocampus (Figure 4B). In contrast, β-dystroglycan (migrating at 43 kDa) was present in brain homogenate and was modestly enriched in synaptosomes, but was not detected in the PSD fraction from cerebral cortex (Figure 4A) or other brain regions (not shown, see Chapter I).

Like other components of the PSD fraction, p58 and p53 were virtually insoluble in all non-ionic detergents tested. In addition, these polypeptides were not extracted in 3% N-lauroyl sarcosinate (not shown). Such solubility properties indicate tight association with the 'core' PSD (Kennedy, 1993). Relatively few proteins have been found specifically enriched in the postsynaptic density fraction. This feature of p58/53 suggested that it was a synapse specific protein. Since the identification of the components of the synapse is essential to understanding its structure and function, I was resolute to determine whether p58 and p53 were relatives of β-dystroglycan, proteins not yet localized to the PSD fraction, or novel proteins. Since p58 and p53 were observed as immunologically related to β-dystroglycan, I first pursued the identification of these polypeptides in that context. Although I found no evidence of alternative splice forms of β-dystroglycan in brain (see Chapter I), I concluded that, in order to positively discount the possibility that p58 and p53 were related to dystroglycan, and to make a conclusive identification, I must obtain peptide microsequence from these polypeptides.

4.2 Purification of p58 and p53

Protein staining of SDS-PAGE separated PSD fraction proteins demonstrated that, within the molecular weight range of 50-60 kDa, p58 and p53 were interdigitated among at least three major PSD proteins (Figure 4C). When I carefully extracted the p58 and p53 bands from blots of PSD fractions and obtained MALDI-TOF masses, it was clear that within

the bands there was overwhelming contamination from at least one of these major PSD proteins, tubulin. To achieve an improved gel separation of p58 and p53 from the 50-60 kDa major PSD proteins, and to further investigate their biochemical properties, I separated the PSD sample proteins by charge and by size using two-dimensional gel electrophoresis. This method yielded substantial improvement in the isolation of p58 and p53: unlike the majority of the PSD proteins, this doublet migrated to a basic isoelectric point (pI ~9), free from the bulk of PSD proteins (Figure 5A). The p58 and p53 bands each migrated as a series of closely spaced spots of differing isoelectric points, suggesting that these polypeptides may be post-translationally modified (see below).

Next, I established conditions for the solubilization of p58 and p53 in the absence of detergents. Many chromatographic methods did not contribute to the purification of p58 and p53. Affinity chromatography with the antibody Ab98 was far too inefficient to attain significant quantities of p58 and p53; anion and cation exchange chromatography, and fast performance liquid chromatography (FPLC) provided no separation of p58 and p53 from other components of the fraction. In contrast, hydrophobic interaction chromatography (HIC) provided an excellent separation of p58 and p53 from the majority of other PSD components. HIC yielded a protein fraction that was highly enriched in p58 and p53. Comparison of silver stained gels of HIC starting material (total PSD fraction proteins) and HIC eluate, both separated by 2D gel electrophoresis, demonstrated that the hydrophobic subpopulation of PSD proteins, including p58 and p53, is a small component of the total PSD fraction (Figure 5B). Ultimately, to obtain a quantity of p58 and p53 sufficient for peptide microsequencing, I exploited a purification scheme which combined subcellular fractionation, HIC, and 2D gel electrophoresis.

4.3 Mass Spectrometry Analysis and Peptide Microsequencing of p58 and p53

To identify p58 and p53, I used MALDI-TOF mass spectrometry to analyze tryptic digests of the purified polypeptides. Comparison of the profile of masses obtained from both p58 and p53 to computer-generated mass profiles of protein sequences in the NCBI database showed that p58 and p53 from rat were highly homologous to hamster Insulin Receptor Tyrosine Kinase Substrate p53 (IRSp58/53, Figure 6). This pair of polypeptides had been isolated from CHO cells by Yeh et al., and the cDNA encoding IRSp53 was cloned (Yeh et al., 1996). The precise relationship between IRSp58 and IRSp53 was not established in that study, but it seems likely that they are encoded by the same sequence (see below).

Sixty-five percent of both the p58 masses (15/23) and the p53 masses (13/20) matched the tryptic digest masses computed from the deduced IRSp53 amino acid sequence (Table 1). There were eight p58 masses that did not correspond to an IRSp53 mass, but six of these masses were shared by p53. Two p58 masses and one p53 mass were unique. Only slight differences were observed when the HPLC chromatograms of the p58 and p53 tryptic digests were compared (not shown). Together, these data indicate that the primary structures of p58 and p53 are very similar.

To verify the identification of p58 and p53 as IRSp53, I obtained amino acid sequence from three of the p58 tryptic fragments. Of the 33 amino acids obtained, all perfectly matched the published sequence of the IRSp53 cDNA (Table 1, Figure 6). I further confirmed the identification of p58 and p53 as IRSp53 by western analysis of PSD fractions with monoclonal antibody H720 (not shown). Hereafter, p58 and p53 will be referred to as IRSp58/53.

4.4 Relationship of IRSp58 and IRSp53

In the course of my biochemical studies of IRSp58/53, I have consistently encountered a ~5 kDa difference in the molecular weights of IRSp58 and IRSp53. However, neither mass spectrometry nor HPLC analysis indicated differences in the primary structures of these polypeptides. One modification that could potentially account for this difference is phosphorylation. Indeed, in vitro phosphorylation of PSD proteins caused an upward shift in the electrophoretic mobility of both IRSp58 and IRSp53, suggesting that they are substrates of a kinase(s) in the PSD fraction. However, this shift did not account for the 5 kDa difference (Figure 7A). Similarly, enzymatic deglycosylation did not yield any consolidation of the doublet (not shown). Thus, I found no evidence that these posttranslational modifications cause the 5 kDa apparent molecular weight difference between IRSp58 and IRSp53.

To further investigate the relationship between IRSp58 and IRSp53, I analyzed their expression in brain tissue from rat, mouse, and porcine PSD fractions. Western analysis revealed that in the rat and mouse PSD fractions, the IRSp58/53 pair was indistinguishable (not shown). However, in the porcine PSD fraction the IRSp58 species was prominent, and the IRSp53 species was barely detectable (Figure 7B). This observation raises the possibility that IRSp53 is a proteolytic cleavage product of IRSp58. However, it should be noted that the relative levels of IRSp58 and IRSp53 remains stable when PSD fractions are stored for prolonged periods at -80°C or incubated overnight at room temperature (not shown).

4.5 Distribution of IRSp58/53 mRNA

Hoping to learn more about the molecular relationship between IRSp58 and IRSp53, I investigated the possibility that IRSp58/53 represent alternative splice forms. To examine the distribution and configuration of the IRSp58/53 transcript, I probed rat tissue Northern

blots with a radiolabeled oligonucleotide probe that corresponded to the putative SH3 domain (see below) of the IRSp53 clone (Yeh et al., 1998). This probe hybridized predominantly to transcripts of two sizes, 2.4 and 3.5 kb (Figure 8). The mRNA tissue expression pattern revealed in this experiment is more extensive than the tissue expression of the IRSp58/53 protein. Yeh et al. showed that IRSp58/53 expression is significant in brain, and is undetectable in spleen, muscle or liver (Yeh et al., 1996). Brain contained the highest level of IRSp58/53 mRNA, with the 3.5 kb transcript predominating. Varying amounts of the two transcripts were observed in other tissues. Notably, neither transcript was detected in skeletal muscle. Thus, there appear to be at least two IRSp58/53 mRNAs, and the highest hybridization is to the 3.5 kb IRSp53 transcript, which is most prevalent in brain.

4.6 Organization of IRSp58/53 mRNA

Considering the possibility that the two transcripts observed in the Northern blots might correspond to alternatively spliced mRNAs, I then searched the EST database using the BLAST algorithm (Altshcul, 1990) for sequences that might represent IRSp53 homologues. I identified a large set of IRSp53-homologous ESTs that spanned the entire open reading frame of IRSp53 (not shown). However, this analysis revealed no divergences from the reported IRSp53 cDNA sequence, and thus provided no evidence for the existence of alternatively spliced transcripts.

To determine whether the size difference between the 3.5 kb and the 2.4 kb mRNAs was due to variation in their coding sequence, I performed RT-PCR. I isolated RNA from rat cortex and used random primers to reverse transcribe the RNA. I then used an array of primers that spanned the IRSp53 coding region for PCR analysis. Each of the generated RT-PCR products corresponded in size to a product obtained using IRSp53 cDNA as template: no major additional products were detected (Figure 9). Together, these RT-PCR products covered the entire coding region of IRSp53. Thus, in rat brain I found no evidence of alternative splicing

within the coding region of IRSp53 mRNA, suggesting that both IRSp58 and IRSp53 are products of a highly similar or identical mRNA.

4.7 Localization of IRSp58/53 to synapses

The enrichment of IRSp58/53 (p58 and p53) in the synaptic subcellular fractions suggested that IRSp58/53 is a component of the synapse. Since the antisera Ab98 cross-reacts with β-dystroglycan, and the IRSp58/53 monoclonal antibody H720 was unsuitable for immunohistochemistry, I raised and affinity purified a specific anti-IRSp58/53 antiserum. Importantly, this antiserum did not recognize β-dystroglycan. The specificity of this reagent for IRSp58/53 was verified by western blotting and immunoabsorption (Figure 10).

To determine it IRSp58/53 has a synaptic distribution in intact brain, I performed immunohistochemistry on frozen sections (Figure 11A). In the cerebellum, a zone of granule cells lies next to a band of Purkinje cells, whose synapse-laden dendrites lie in the adjacent molecular layer. Staining with this anti-IRSp58/53 antibody demonstrated that IRSp58/53 immunoreactivity is prominent in the synapse-rich molecular layer as well as in the granule cell layer of this tissue. The specificity of the IRSp58/53 antibody staining was demonstrated by peptide immunoabsorption. This pattern of staining suggested that IRSp58/53 may be expressed selectively at synaptic sites.

Therefore, to assess the distribution of IRSp58/53 in further detail, I exploited a system in which individual synapses can be resolved. Primary hippocampal neurons in low density cultures have well-differentiated axons and dendrites, and numerous functional synapses. These synapses can be reliably visualized using antibodies to synaptic vesicle proteins such as synaptophysin. Double labeling with anti-synaptophysin and anti-IRSp58/53 antibodies showed that IRSp58/53 immunoreactivity was localized at the majority of synapses on these cells (Figure 11B). Together, the findings from my biochemical and immunohistochemical studies indicate that IRSp58/53 is a component of

central synapses. I expect that this finding will verified by future immuno-electron microscopy studies.

4.8 IRSp58/53 binding partners

IRSp58/53 contains several potential protein-protein binding domains: an src homology 3 (SH3) domain, as well as an SH3-binding and a WW-binding domain (Figure 6) (Yeh et al., 1998). In light of IRSp58/53's potential for protein-protein interactions, I searched for binding partners for IRSp58/53. I both used a candidate partner approach and pursued novel protein binding interactions.

4.8.1 Fas Ligand Associated Factor 3 is a human homologue of IRSp53

A BLAST search with the IRSp53 cDNA reveals a NCBI database entry that is 95% identical to the N-terminal 320 amino acids (60%) of IRSp58/53 (Hachiya et al., 1997). The entry's annotation states that this cDNA, Fas Ligand Associated Factor 3 (FLAF3), encodes a large portion of a human homologue to IRSp53. The FLAF3 cDNA was obtained using the intracellular tail of Fas Ligand (FasL) as bait in a yeast two hybrid screen of a human placental cDNA library. FasL, a 37 kDa type II transmembrane protein, is known to wield the "death domain" which initiates Fas-mediated apoptosis. Whereas the extracellular portion of FasL and its role in apoptosis are well studied, little is known about the endodomain of this molecule.

To determine if FasL has a distribution that coincides with that of IRSp58/53, I probed western blots of brain subcellular fractions with an antibody directed against FasL. Following reducing gel electrophoresis of subcellular fractions proteins, FasL is observed in predominantly in brain homogenate and synaptosome fractions (Figure 12A). The immunogen against which this FasL antibody was made is the extracellular, C-terminal portion of FasL. This portion of FasL is often cleaved however, producing a soluble factor and presumably leaving behind a transmembrane "root." One explanation for the absence of FasL

in the PSD fraction is that the portion of FasL reported to interact with IRSp53, the intracellular "root" does in fact fractionate with the PSD, while the epitope containing extracellular portion is cleaved. The intracellular fragment is thus rendered virtually invisible, since antibodies directed against the less studied intracellular portion of FasL are currently unavailable. Such antibodies would be valuable for pursuing this potential interaction between FasL and IRSp58/53.

4.8.2 Dystrophin: a PSD protein with an available WW domain

The cytoskeletal PSD protein dystrophin (see Chapter I) is localized to the PSD and contains a WW domain (Bork and Sudol, 1994). The WW or WWP domain, identified in 1994, is a protein-protein interaction module which likely functions is a way analogous yet distinct from SH3 domains. This module contains approximately 40 amino acids and contains two highly conserved tryptophans and an invariant proline (Rotin, 1998). I hypothesized that at synapses, IRSp58/53 might interact with this protein-protein interaction domain within dystrophin's C-terminus. I attempted to co-immunoprecipitate in vitro expressed dystrophin fragments that contained the WW binding domain with vitro expressed IRSp58/53. I observed no interaction between these proteins, however (Figure 12B).

4.8.3 A search for novel IRSp58/53 protein-protein interactions

I continued to pursue IRSp58/53 interacting proteins by screening the conglomerate PSD fraction for binding proteins. First, to investigate the possibility that IRSp58/53 are tightly associated with other proteins in the PSD fraction, I immunoprecipitated IRSp58/53 under non-denaturing conditions from a preparation of biotin-labeled, solubilized PSD proteins. However, no PSD proteins co-immunoprecipitated with native IRSp58/53 (Figure 12C).

I next screened the PSD fraction for components that possessed affinity for IRSp58/53. I generated a glutathione s-transferase-tagged IRSp58/53 (GSTp53) and co-incubated GSTp53 with a preparation of biotin-labeled, solubilized PSD proteins. The GSTp53 precipitated a number of

biotinylated PSD proteins, while few PSD proteins bound to the GST control (Figure 13, left). To enhance this finding, I used an alternative approach and performed a blot overlay experiment. I probed a blot of subcellular fraction proteins with ^{35}S-methionine labeled in vitro expressed IRSp58/53. Again, IRSp58/53 appeared to bind a number of PSD proteins (Figure 13, right). To verify the specificity of these interactions, I also performed the overlay with an in vitro expressed fragment of α-dystroglycan, another synaptic protein. Each method revealed multiple binding proteins. However, by coordinating these two methods and directly comparing the results, I found one PSD-fraction protein, PSD225, that was identified by both fusion protein affinity and blot overlay. Thus, PSD225 is significantly more likely to be a true binding partner for IRSp58/53 than the many proteins identified using one of the two binding assays. If the interaction shown in this pair of experiments is shown to withstand increasingly stringent conditions, then this binding interaction should be pursued. Further studies will then be required to determine if PSD225 is a true IRSp58/53 binding partner in vivo.

4.9 Localization of the insulin receptor to synapses

Although a binding partner for IRSp58/53 has not yet been substantiated, a functional partnership has been established. IRSp58/53 has been shown to be an insulin receptor substrate in cultured fibroblasts. Further, IRSp58/53 isolated from brain can be tyrosine phosphorylated in vitro by insulin receptor (Yeh et al., 1996). Insulin receptor is known to be expressed in brain, and other components of insulin signaling pathways have been localized to brain regions as well (see above). I thus sought evidence for the presence of the insulin receptor at postsynaptic apparatus in vivo. Indeed, staining specific for the β subunit of the insulin receptor is concentrated at synapses in cultured hippocampal neurons (Figure 14A; David Wells, Brown University). This evidence is in agreement with recent findings of Beju

and Schechter. Using immuno-gold electron microscopy, they demonstrate insulin and insulin receptor within the axon and dendrites of hippocampal neurons in brains of rats 10 days old. They have localized insulin ultrastructurally to presynaptic regions, and the insulin receptor to presynaptic and postsynaptic membranes (Beju and Schechter, 1998).

4.10 The Insulin Receptor is a component of the PSD fraction

After determining that a population of inulin receptor is concentrated at synapses in culture, I was interested in whether the insulin receptor is associated with the pre- or postsynaptic specialization. I probed western blots of brain subcellular fractions with an antibody to the β subunit of the insulin receptor. The insulin receptor was detected in homogenate, and was enriched in both synaptosome and PSD fractions (Figure 14B). Thus, both the β subunit of the insulin receptor tyrosine kinase and its substrate IRSp58/53 are components of the PSD fraction. Indeed, using EM, Beju and Schechter have localized insulin ultrastructurally to the PSD structure itself (D. Beju, personal communication). Taken together with other data showing a functional relationship of the insulin receptor and IRSp58/53, this co-localization suggests that these molecules are part of an insulin-dependent signaling pathway at the postsynaptic apparatus.

The co-fractionation of the insulin receptor and its tyrosine kinase substrate IRSp58/53 strongly suggests that their established functional relationship is maintained within the synaptic signaling structure of the PSD.

5. Discussion

In this portion of my thesis work, I show that a substrate of the insulin receptor, and insulin receptors themselves, are localized at CNS synapses and are components of the postsynaptic density. Insulin is likely to have diverse roles in the CNS, including but not restricted to the regulation of glucose metabolism. Interestingly, there is a growing body of evidence that implicates insulin signaling in processes other than homeostasis (reviewed in (Wickelgren, 1998)). The multivariate downstream effects of insulin signaling may be coordinated through spatially regulated expression of the insulin receptor tyrosine kinase's substrate molecules. Signaling via a synapse-specific substrate, IRSp58/53, may define a subset of the insulin signaling pathway.

5.1 IRSp58/53 and Insulin Receptor are localized to synapses

I began my investigation of synaptic insulin signaling proteins at the level of the PSD, an electron-dense conglomeration of proteins that lies just below the postsynaptic membrane of central synapses. I have characterized and purified a pair of proteins of unknown identity, p58 and p53, that is selectively concentrated in the biochemical fraction enriched for PSDs. Using MALDI-TOF mass spectrometry, peptide sequencing, two-dimensional electrophoresis, and western blotting, I have identified these PSD proteins as the Insulin Receptor Substrate p58/53 (IRSp58/53). A small number of p58 and p53 peptide masses obtained by MALDI-TOF analysis do not match computed IRSp53 masses (Table 1). This presumably reflects species-dependent divergences (hamster versus rat) or posttranslational modifications. Notably, IRSp53 has sites for N-linked glycosylation, two potential tyrosine phosphorylation sites, and 25 potential serine/threonine phosphorylation sites.

I have shown that another key insulin signaling protein, the insulin receptor, is also a component of the PSD fraction. Generally,

transmembrane proteins such as the insulin receptor do not remain associated with the Triton X-100 insoluble PSD. There are significant exceptions however, and the most well-studied of these is the NMDA receptor. Specific subunits of the NMDA receptor are thought to be tethered to the PSD through an interaction between the NMDAR2 C-terminus and the second PDZ domain within PSD-95 (Kornau et al., 1995; Kim et al., 1996). The receptor tyrosine kinase TrkB has also been localized to the PSD fraction (Wu et al., 1996).

Although the PSD fraction is a powerful tool for identifying molecules that are specifically localized to the synaptic apparatus, this biochemical preparation can not precisely reflect the constitution of the synapse in vivo. Thus, with the help of David Wells (Brown University),, I demonstrated the presence of insulin signaling components at intact CNS synapses in culture. IRSp58/53 is expressed in the synapse-rich layers of the cerebellum, and both IRSp58/53 and insulin receptor are concentrated at synapses of hippocampal neurons.

5.2 Structure of IRSp58/53

I consistently observed that IRSp58/53 migrates as a pair of polypeptides. However, I could find little evidence that IRSp58 and IRSp53 differed in their primary sequences. HPLC chromatograms of tryptic fragments from p58 and p53 were virtually identical. MALDI-TOF analysis of purified p58 and p53 also revealed similar profiles - only two p58 masses and one p53 mass were unique. Although these masses could represent divergent primary sequences, they could also be due to posttranslational modification or proteolysis. Indeed, the relative expression of IRSp58 and IRSp53 is cell and tissue specific. Transfection of the IRSp53 cDNA into fibroblasts results in expression of only the IRSp53 species (Yeh et al., 1996). Further, I detected only IRSp58 in PSD fractions from porcine brain. Finally, using RT-PCR I detected only a single species of IRSp53 mRNA in the brain, and a survey of the EST database yielded no evidence of multiple mRNA species.

However, my comparative analysis of the IRSp53 cDNA to total rat brain cDNA does not exclude the possibility that differences exist 5' or 3' to the IRSp53 coding region. Such differences could be uncovered by performing 3' and 5' rapid amplification of cDNA ends (RACE).

The IRSp53 cDNA clone was the only cDNA isolated from a CHO library screened for cDNAs that encoded amino acid sequences matching two peptides obtained from IRSp58. It encodes a predicted protein with a molecular weight of 57.6 kDa. However, transfection of this cDNA into fibroblast cell lines induces overexpression of only the IRSp53 species, so Yeh and colleagues reached the conservative conclusion that the cDNA encoded only IRSp53, and surmised that IRSp58 was a related splice form of IRSp53 (Yeh et al., 1996). In contrast, I used a rabbit reticulocyte system to in vitro translate IRSp53, and observed that the product was a tight doublet of approximately 60 kDa (see Figure 12B).

Analysis of the IRSp53 cDNA reveals an open reading frame that encodes for a predicted protein of 57.6 kDa (Yeh et al., 1996). Interestingly, downstream of this first ATG codon are at least six subsequent potential start sites. Utilization of one of these in particular would yield a polypeptide with a predicted molecular weight of 53.6 kDa. Therefore, it is possible that use of alternative initiation sites is the basis for the observation of this pair of polypeptides of 58 kDa and 53 kDa. Nevertheless, my data are most likely to fit scenario whereby IRSp58 and IRSp53 derive from an identical mRNA coding region, and the difference in these polypeptides is the result of a species and cell background-dependent, posttranslational process.

This investigation of IRSp58/53 was a outgrowth of my use of an antiserum directed against β-dystroglycan (Ab98). Comparison of the IRSp53 and β-dystroglycan sequences revealed that these proteins have little to no homology. The immunological cross-reactivity that Ab98 demonstrated for IRSp58/53 is presumably due to a proline-rich stretch of amino acids within its amino acid sequence (KPLPVPPELAPF) that is similar to the β-dystroglycan peptide used to generate Ab98 (KAPLPPPEYPSQ). Notably, another group has reported a PSD fraction protein (not IRSp58/53) that is immunologically related β-dystroglycan

(Mummery et al., 1996). To date however, neither the identity of this 164 kDa PSD fraction protein, nor its homology/relationship to β-dystroglycan, have been shown.

5.3 Interactions of IRSp58/53

There is compelling evidence in support of the functional classification of IRSp58/53 as an insulin receptor substrate. Yeh and colleagues demonstrated that IRSp58/53 isolated from brain can be in vitro tyrosine phosphorylated by insulin receptors isolated from CHO.T cells (Yeh et al., 1996). I have found that, following in vitro phosphorylation of the insulin receptor-containing PSD fraction, IRSp58/53 experiences a gel shift consistent with phosphorylation by an endogenous kinase(s). These data implicate IRSp58/53 as a brain-derived substrate of the insulin receptor.

The downstream molecules that orchestrate insulin's potential action at the synapse are unknown. The predicted domain structure of IRSp53 (Figure 6) indicates many potential sites for protein-protein interactions including an SH3 domain, an SH2-binding domain, and a proline-rich WW-binding domain (Yeh et al., 1998). I asked whether IRSp58/53 interacts with the WW domain of dystrophin, a PSD-enriched cytoskeletal protein, but I was unable to co-immunoprecipitate in vitro expressed dystrophin fragments and IRSp58/53. I noted a report of a human homologue of IRSp53 (FLAF3) that interacts with the intracellular domain of Fas Ligand (FasL) in a yeast two hybrid assay, and I found that FasL is expressed in brain, but I found no evidence of IRSp58/53 binding to native brain FasL. Lastly, I did not detect co-immunoprecipitation of any native PSD fraction proteins with IRSp58/53. Other investigators have similarly been unable to demonstrate binding partners for IRSp58/53 (Yeh et al., 1996).

5.4 Insulin signaling at synapses

Insulin is likely to have many roles in the brain. One expects insulin signaling in the brain to play a role in glucose metabolism as well as in currently unidentified processes. Insulin signaling pathways may in fact be implicated in the progression of some disease states, including Alzheimer's disease (Hong and Lee, 1997; Frolich et al., 1998; Hoyer, 1998; Qiu et al., 1998). Key components of the insulin signaling mechanism, such as insulin receptor, phosphatidyl inositol-3 kinase, and IRS-1, are widely expressed and often co-distributed throughout the brain. These elements are found in various regions of the brain, in neurons and in some synapse-rich regions (Baskin et al., 1994; Folli et al., 1994; Yamada et al., 1997). Recent data, including those presented here, strongly support the tenet that insulin signaling occurs throughout the brain, as well as specifically at synapses.

One compelling piece of evidence for a direct insulin effect at synapses is the finding that insulin induces a rapid recruitment of functional type A GABA receptors, the principal neurotransmitter at inhibitory synapses, from intracellular to postsynaptic and dendritic membranes (Wan et al., 1997). Inhibition of protein tyrosine kinases blocks this translocation, suggesting that an activated insulin receptor is required to execute insulin's effect. This translocation of $GABA_A$ receptors is observed in HEK cells, hippocampal neurons in culture, and neurons in hippocampal slices (Wan et al., 1997).

5.5 IRSp58/53 may define a synapse-specific insulin signaling pathway

The expression of the insulin receptor is neither restricted to the brain nor restricted to the synaptic apparatus. Similarly, IRS-1 and IRS-2 are expressed both in the periphery and in the CNS: brain IRS-1 (and perhaps IRS-2) is localized in neuronal cell bodies, and some proximal dendrites (Baskin et al., 1994; Folli et al., 1994; Yamada et

al., 1997). In contrast, IRSp58/53 expression is restricted to brain, to neurons, and specifically to the PSD-enriched biochemical fraction. Interestingly, IRSp58/53 is not the first example of an insulin receptor substrate that displays a subcellularly restricted expression pattern. In adipocytes, another substrate of the insulin receptor IRS-3, has been shown to have a subcellular distribution pattern that distinguishes it from IRS-1 and IRS-2 (Anai et al., 1998). The spatial coordination of IRS proteins may contribute to the determination of tissue, cell, or subcellular variations in insulin's action.

Thus, the selective expression of different insulin receptor substrates may facilitate a careful control of insulin-activated signaling. Indeed, IRSp58/53 may define a special type of insulin signaling in the brain. The discovery that IRSp58/53 is a synapse-specific substrate for the insulin receptor tyrosine kinase provides the first evidence for an insulin signaling mechanism at synapses. It is likely that other elements of this synaptic insulin signaling pathway will soon emerge. One expects that the effect of insulin at synapses is distinct from its global, metabolic control. However, the nature of this effect, and its effectors, remain to be elucidated.

5.6 Future Directions

Work focused at the PSD has to date provided many insights into the complexity of the synapse. Using the PSD biochemical preparation, I have found two components of an insulin-dependent signaling pathway at synapses. IRSp58/53 and the insulin receptors are components of the PSD fraction. The protein IRSp58/53 exists in two forms (IRSp58 and IRSp53) which have similar primary structure and may not differ in posttranslational additions. Most likely, IRSp58 and IRSp53 are products of two different start sites. There are at least two mRNA transcripts that encode IRSp58/53 that are likely to be different in their noncoding regions. Levels of IRSp58/53 mRNA are highest in brain and testis.

IRSp58/53 is at synapses in vivo in cerebellum and cultured hippocampal neurons.

The discovery that IRSp58/53 is a synapse-specific substrate for the insulin receptor tyrosine kinase provides the first evidence for insulin-dependent signaling at central synapses. Localization of the insulin receptor to the PSD fraction supports this hypothesis. It is likely that other elements of this synaptic insulin signaling pathway are buried in the postsynaptic density as well; some may diverge from the components that have been identified and characterized in peripheral tissues, while others may be known components of this signaling pathway.

Future studies are required to determine the role of insulin signaling at synapses. Technologies such as the yeast two hybrid assay (see Chapter I) should now be exploited to uncover the other crucial synapse-specific effectors of insulin's synaptic signal. Once a backbone of signaling elements has been identified, a role for insulin in learning and memory can be sought. There are numerous pharmacologic methods that can be used to affect many levels of signaling pathways. Enzymes that work downstream of the insulin receptor tyrosine kinase can be inhibited and the effect of this treatment on the healthy development and function of a synapse can be monitored. For example, the compounds wortmannin and LY294002 specifically inhibit the kinase activity of PI3K. Many mouse models with null mutations in various elements of the traditional insulin signaling pathway have been and are being created (Araki et al., 1994; Tamemoto et al., 1994; Bruning et al., 1997). Little attention has been paid to CNS function in these mice. Careful evaluation of neuronal physiology and synaptic morphology and functionality in these models and in future "knockouts" would contribute substantially to the understanding of insulin's role in the brain.

The relationship between FasL and IRSp58/53 must be examined further. An interaction between these proteins will suggest a role, perhaps in intracellular signaling, for the little studied endodomain of FasL. A protein-protein interaction between these two might be demonstrated using in vitro expressed molecules. Similarly, colocalization of FasL and IRSp58/53 might be appreciated upon co-

transfection of these proteins in heterologous cells. If a relationship is found, the domain of IRSp58/53 that mediates this interaction should then be mapped, since no protein-protein interaction domains have been identified within the region of IRSp58/53's putative FasL interaction. A direct way to asses the role of IRSp58/53 in vivo is to generate IRSp58/53 null mice. Analysis of brain (and other tissues) from these animals is likely to indicate what types of biologic functions require the work of this signaling molecule.

Discovering the focus of insulin signaling elements at synapses would be a launching pad for future study. It is likely that insulin's role in the brain is important in homeostasis and, as suggested by these data, in synaptic function. Results from the experiments proposed above would contribute to dissecting this compelling synaptic signaling pathway.

6. Tables and Figures

6.1 Figure Legends

Figure 1. Insulin Receptor and Relatives (see Introduction)

Figure 2. Insulin Receptor Signaling (see Introduction)

Figure 3. Insulin Receptor activation, GLUT4 translocation (see Introduction)

Figure 4. A 58 kDa and a 53 kDa polypeptide are enriched in PSDs
A. Homogenate, synaptosome, and PSD fractions from rat brain were separated by SDS-PAGE, transferred to nitrocellulose, and probed with Ab98 (left) or Ab98 that had been pre-incubated with peptide (right). β-dystroglycan is observed in the homogenate and synaptosomal fractions (β-DG) and a pair of polypeptides of 58 and 53 kDa is specifically detected in the PSD fraction (p58 and p53). Binding of Ab98 to all three polypeptides is eliminated when the antibody was preabsorbed (Ab98 + peptide). Mobilities of molecular weight standards are indicated. (H, homogenate; SX, synaptosomes; PSD, postsynaptic density fraction.)
B. Western blots of homogenate, synaptosomes, and PSD fractions from the indicated brain regions were probed with antibody Ab98. p58 and p53 are selectively enriched in the PSD fractions from all areas examined.
C. Comparison of PSD blots stained for protein (Ponceau S, PS) or western blots (WB) probed with Ab98 indicates that p58 and p53 (arrows) are interdigited between three major PSD proteins (*).

Figure 5. Purification of p58 and p53 by 2D gel electrophoresis and hydrophobic interaction chromatography (HIC)
A. Two-dimensional gel electrophoresis was used to separate PSD fraction proteins. Gels of equivalent samples were silver stained (left) or blotted to nitrocellulose and probed with Ab98 (right). Comparison of

these reveals that p58 and p53 are minor components of the complex PSD fraction. The migration of p58 and p53 in the first dimension indicates that these polypeptides are basic (pI ~9).

B. The PSD fraction proteins were solubilized in urea, loaded onto a HIC column in 1M NaCl buffer, and then eluted in 0.1M NaCl salt buffer. 2D gels of the HIC eluates were either silver stained (left) or blotted to nitrocellulose and probed with Ab98 (right). p58 and p53 are readily visualized in silver stained gels of HIC eluate (arrows), indicating that they are highly enriched by this procedure.

Figure 6. Structure of Insulin Receptor Tyrosine Kinase Substrate p53 IRSp53 is predicted to contain several protein-protein interaction domains: one SH3 domain (SH3), one SH3 binding domain, and one WW binding domain (Yeh et al., 1998). Additionally, there are 25 potential serine/threonine phosphorylation sites (protein kinase A, protein kinase C, and casein kinase; not shown) and two potential tyrosine phosphorylation sites (pY). The positions of the peptide microsequences obtained from purified p58 are noted. The positions of the epitope that is likely to be recognized by Ab98, and of the peptide used to generate the polyclonal anti-IRSp58/53 antiserum are indicated. The region that corresponds to the IRSp53 DNA fragment used as a probe for Northern blots is also shown.

Figure 7. Relationship of IRSp58 and IRSp53 from PSDs

A. PSD fractions from rat brain were incubated under conditions promoting in vitro phosphorylation in the either the absence (left) or presence (right) of added ATP (100 uM), as described in Methods. Western blotting with Ab98 shows that IRSp58 and IRSp53 undergo similar gel shifts following in vitro phosphorylation.

B. Species differences in the expression of IRSp58 and IRSp53 in PSD fractions. PSD fractions from rat (left) and pig (right) were probed with antibody Ab98. Although similar amounts of IRSp58 and IRSp53 are detected in rat PSDs, only IRSp58 is detected in porcine PSDs.

Figure 8. Tissue distribution of IRSp58/53 mRNAs

A. A multiple rat tissue Northern blot was probed with a radiolabeled IRSp58/53 oligonucleotide probe (248 bp; see Fig. 3) as described in Methods. Transcripts of 2.4, 3.5, and 8 kb are observed. The highest level of IRSp58/53 mRNA is detected in brain, with the 3.5 kb transcript predominating.

B. The blot was rehybridized with a probe for βactin to verify the integrity and quantity of the RNA from each tissue.

Figure 9. Structural analysis of brain IRSp58/53 mRNA

A. RNA isolated from rat cerebral cortex was reverse transcribed using random primers. The resulting cDNA was amplified by PCR using seven sets (1-7) of six primers (A-F; see B.). PCR products from the cerebral cortex cDNA ('RT') are equivalent in size to those produced using the cloned IRSp53 cDNA as a template ('c') .

B. The PCR products (numbered 1-7) were generated using a set of three forward and three reverse primers (A-F, arrows) that spanned the entire coding region (thick line) of IRSp53.

Figure 10. Characterization of anti-IRSp58/53

Rabbits were immunized with a 13 amino acid peptide from the predicted amino acid sequence of IRSp58/53 and the resulting antiserum was affinity purified. On western blots, anti-IRSp58/53 antibody recognizes polypeptides of 58 and 53 kDa, which are also bound by Ab98. However, anti-IRSp58/53 does not recognize β-dystroglycan. All anti-IRSp58/53 immunoreactivity is abolished if the antibody is preabsorbed with peptide.

Figure 11. Localization of IRSp58/53 at intact synapses

A. Localization of IRSp58/53 in the molecular layer of the cerebellum

Sections of rat cerebellum were immunostained with the affinity purified anti-IRSp58/53 or with anti-synapsin-I antiserum (to reveal the distribution of synapses). IRSp58/53 immunoreactivity is observed in the synapse-rich molecular layer as well as in the granule cell layer. Anti-

IRSp58/53 immunoreactivity is greatly reduced when the antibody was preabsorbed with peptide. (Scale bar: 50 μm; M, molecular layer; PC, Purkinje cell layer; GC, granule cell layer)

B. Localization of IRSp58/53 at synapses in culture

Cultured rat hippocampal neurons were immunostained with the affinity purified anti-IRSp58/53 antiserum (left). IRSp58/53 immunoreactivity is distributed in a punctate pattern along the dendrites of the neurons. The distribution of synapses in the same dendrite was visualized by double-labeling with anti-synaptophysin (right). IRSp58/53 immunoreactivity is selectively concentrated at synapses (arrows).

Figure 12. Candidate IRSp58/53 binding partners

A. Western blots of subcellular fractions were probed for Fas Ligand. FasL is present in all brain fractions, and is not concentrated in the PSD fraction.

B. ^{35}S labeled in vitro translated proteins (DYS, DP71, and IRSp53) were co-incubated as indicated and immunoprecipitated with appropriate antibodies as indicated (DYS2 and H720). The WW domain of dystrophin (present in the DYS in vitro translated protein, shortened in the DP71 protein) does not coimmunoprecipitate IRSp58/53 (or vice versa). Probe that was not labeled with ^{35}S is indicated as ~.

C. A panel of antibodies was used to immunoprecipitate selected proteins from the PSD fraction (biotin labeled). Only H720 (and neither Ab98 nor anti-IRSp58/53) immunoprecipitates native IRSp58/53. PY99 and 4G10 are anti-phosphotyrosine antibodies (Santa Cruz). No proteins co-immunoprecipitate with native IRSp58/53 (arrows).

Figure 13. A potential IRSp58/53 binding partner

Biotin-labeled PSDs were incubated with a GST-tagged IRSp53 column. A group of PSD proteins specifically bound the IRSp53 column (left). Adjacent blots of equivalent PSD samples were probed with in vitro expressed ^{35}S-labeled IRSp58/53, or αDG as control (right). Comparison of the two experiments reveals one band, PSD225, that binds both the GST-IRSp53 column and in vitro expressed IRSp53 ligand.

Figure 14. Localization of Insulin Receptor at synapses and in PSD fractions

A. Localization of insulin receptor at synapses

Cultured rat hippocampal neurons were immunostained with anti-insulin receptor β subunit antibody (right). Immunoreactivity is distributed in a punctate pattern along the dendrites of the neurons. The distribution of synapses in the same dendrite was visualized by double-labeling with anti-synaptophysin (left). Insulin receptor β subunit immunoreactivity is selectively concentrated at synapses (David Wells, Brown University).

B. The Insulin Receptor β subunit is a component of the PSD fraction

A western blot of rat brain subcellular fractions (homogenate, synaptosome, PSD) and CHO.T (cell line engineered to overexpress insulin receptors) cell lysate was probed with an anti-insulin receptor β subunit antibody. The β subunit of the insulin receptor is detected in brain homogenate, synaptosome, and PSD fractions. High levels of insulin receptor β subunit are seen in CHO.T cell lysate.

6.2 Tables and Figures

Table 1. Mass Spectrometry and Peptide Microsequence Analysis of p58/53

p58 and p53 tryptic fragments		predicted IRSp53 tryptic fragments†		peptide microsequence††
p58 masses	p53 masses	IRSp53 masses*	position**	
788.5	788.4	788.9	6 - 11	
1336.5	1336.4	1336.6	19 - 29	
912.7		913.1	51 - 58	GYFDALVK
	1645.3	1644.9	71 - 84	
1374.2		1374.6	85 - 95	
1009.3		1010.1	123 - 130	
912.7		913.9	129 - 136	
1788.2	1789.7	1788.0	157 - 171	YSDKELQYIDAISNK
1374.2		1374.4	161 - 171	
1502.8	1502.9	1502.6	172 - 184	
1788.2	1789.7	1789.7	201 - 214	
877.5		877.9	207 - 214	
2023.5	2023.9	2023.3	223 - 239	
1352.6	1352.5	1352.5	334 - 345	
1480.6		1480.7	334 - 346	
1009.3		1009.1	365 - 374	
1336.5	1336.4	1336.5	365 - 377	
	1426.7	1426.7	399 - 411	
1208.1	1208.4	1208.2	412 - 421	DGWHYGESEK
1042.5	1042.4	1044.0	435 - 443	
1042.5	1042.4	1042.3	444 - 452	
	2298.5	2298.5	489 - 509	
	1426.7	1427.3	510 - 521	
804.2	804.1			
824.8	824.9			
842.6	842.7			
942.0				
952.4				
1155.3	1155.0			
	1572.6			
1754.2	1754.2			
2607.4	2607.6			

† Calculated masses of IRSp53 tryptic fragments that correspond to p58 or p53 masses are listed.

* All masses are in Daltons.

** Amino acid positions of the fragments are based on the numbering system of Yeh et. al., 1996.

†† Peptide microsequences were obtained from three p58 tryptic fragments (underlined). These were identical to deduced IRSp53 amino acid sequences.

Figure 1. Insulin Receptor and Relatives

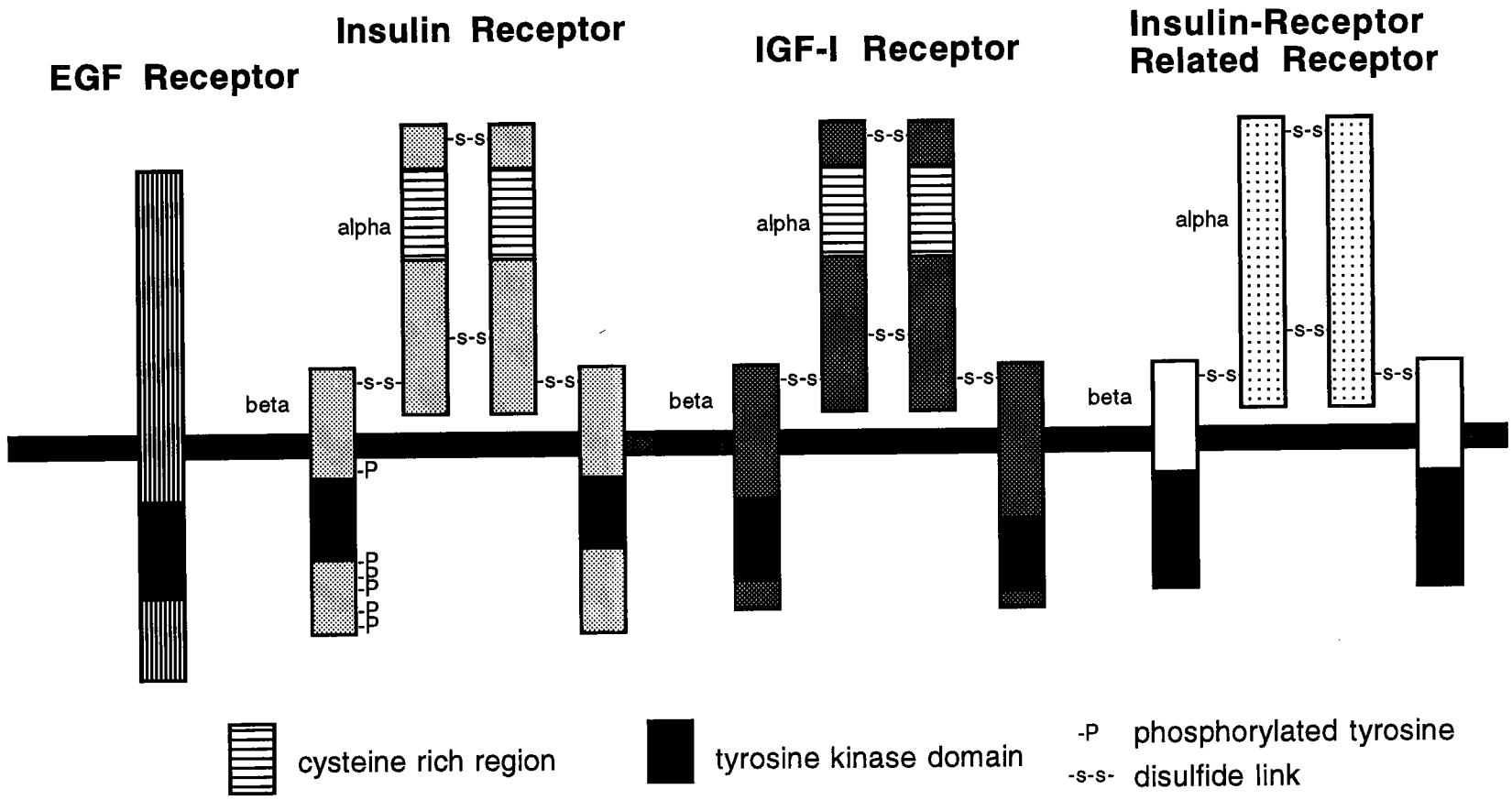

Figure 2. Insulin Receptor Signaling

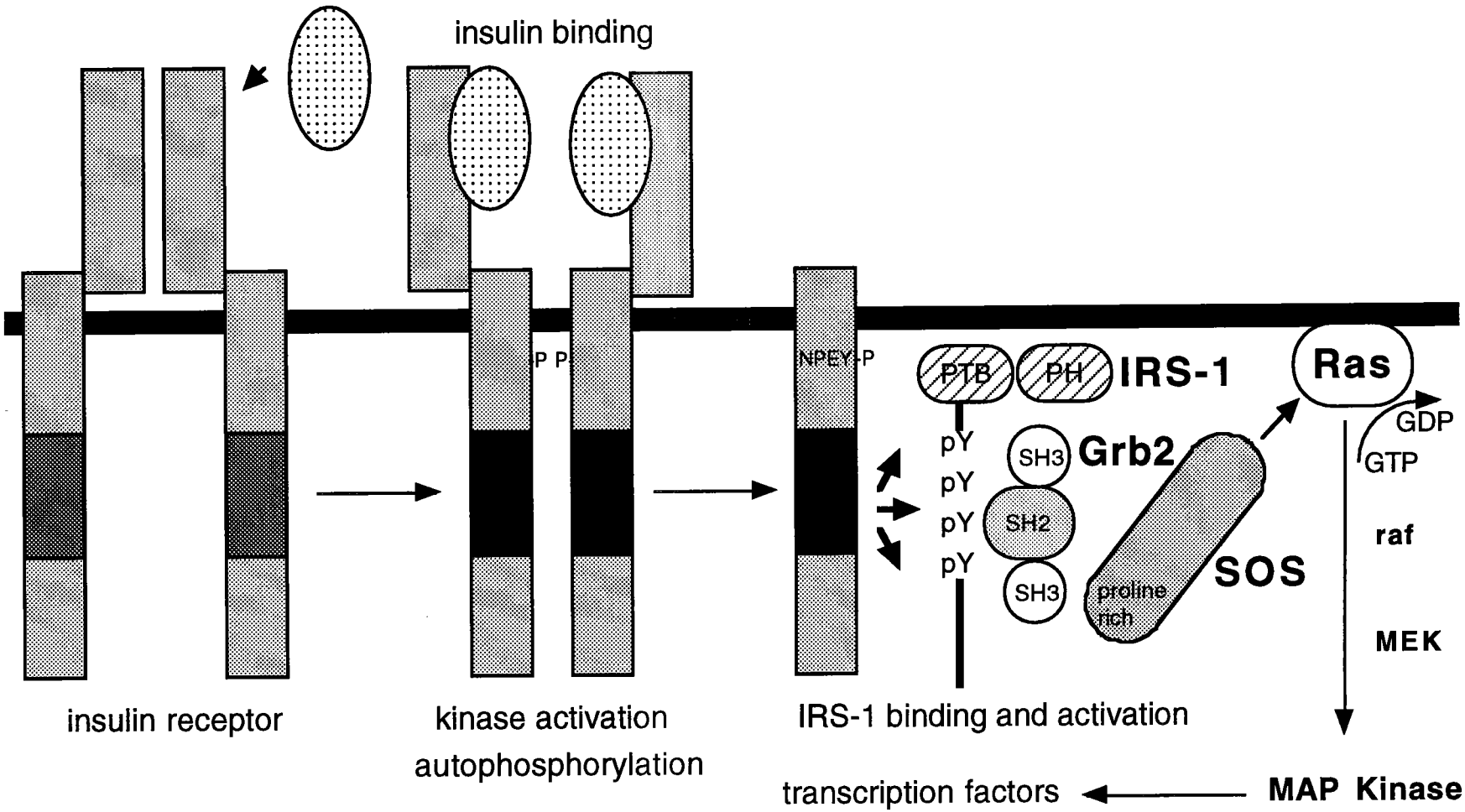

Figure 3. IR activation, GLUT4 translocation

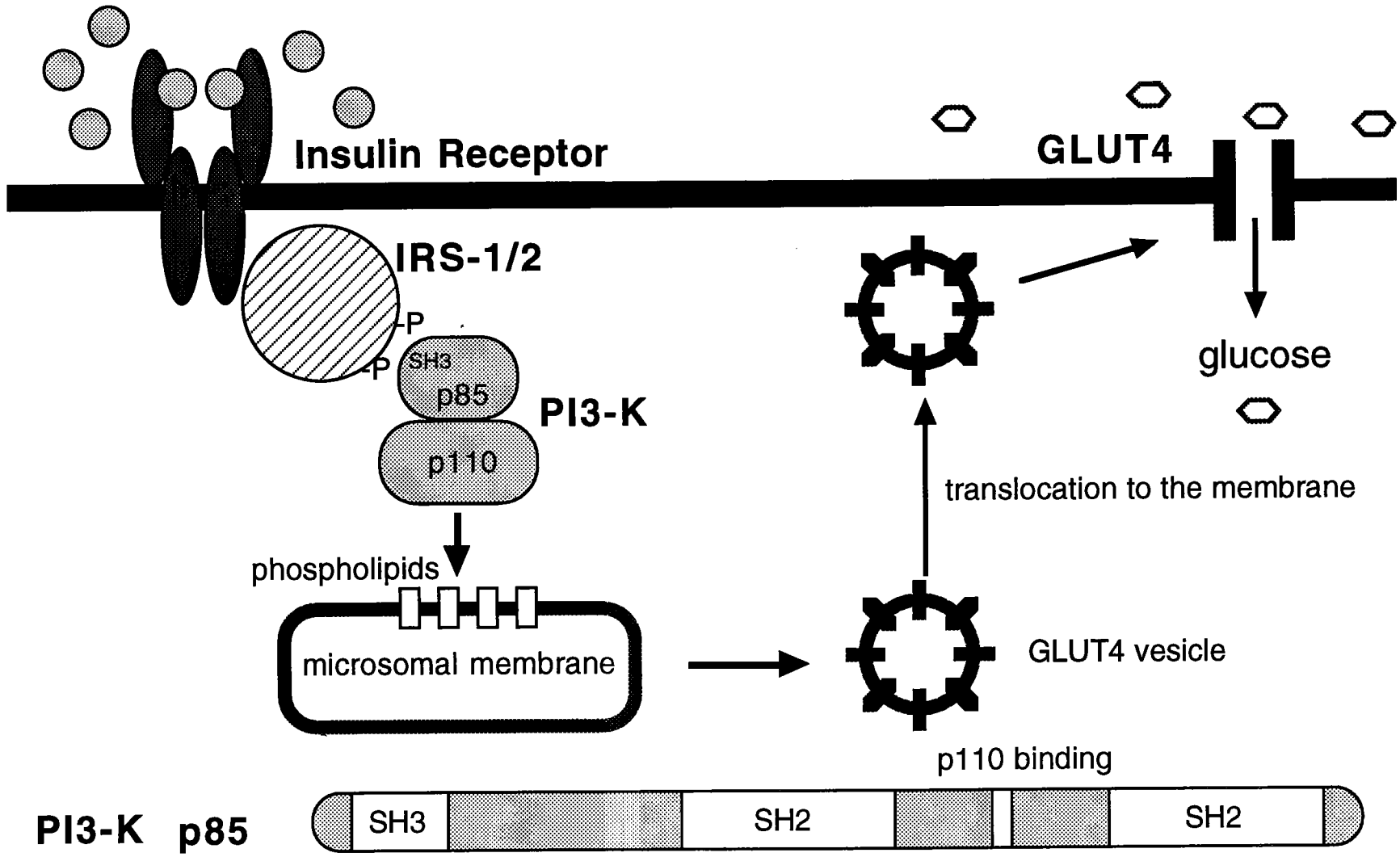

Figure 4.

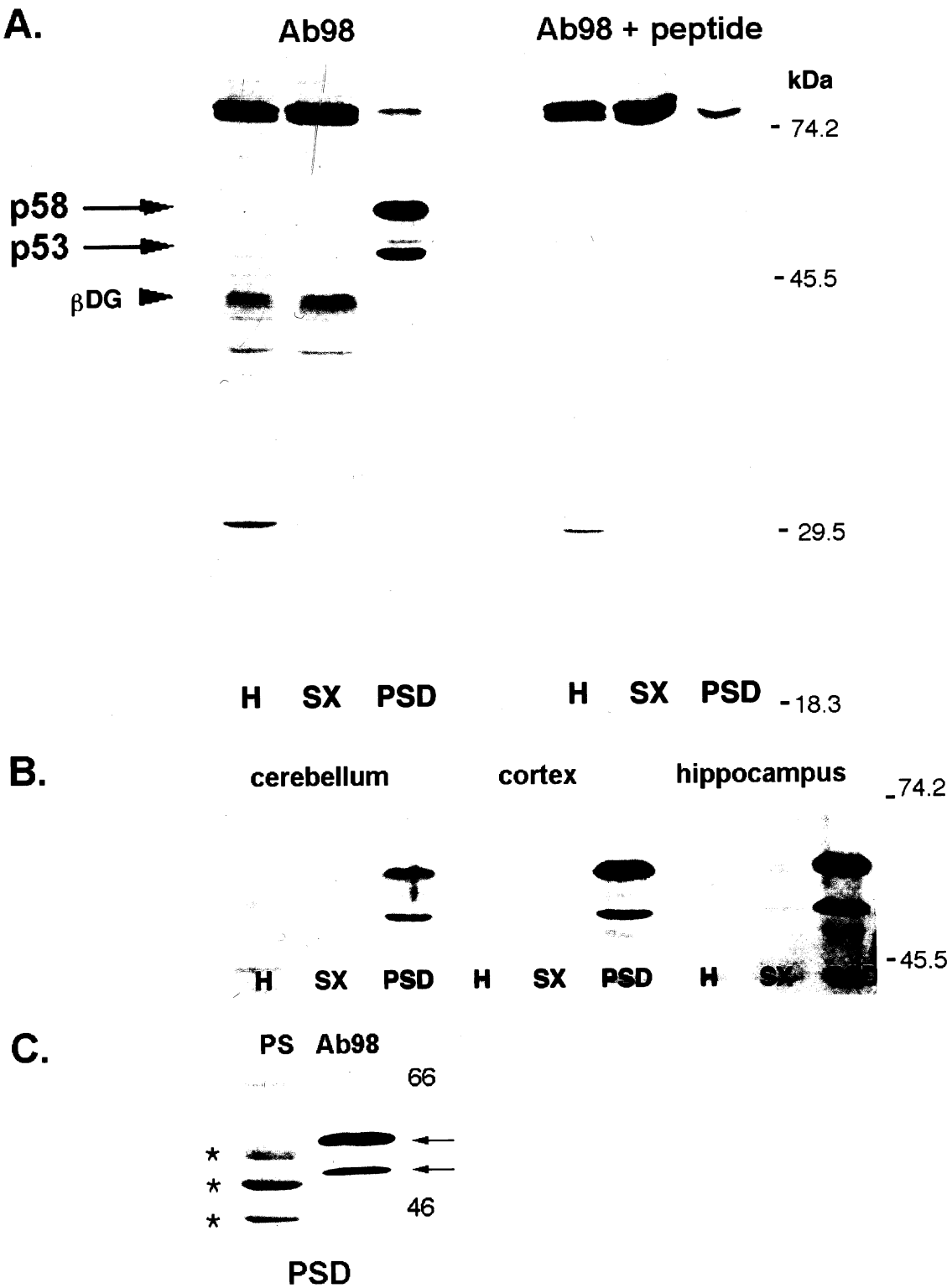
A.
Ab98
Ab98 + peptide
kDa
- 74.2
p58
p53
βDG
- 45.5
- 29.5
H SX PSD
H SX PSD
- 18.3
B.
cerebellum
cortex
hippocampus
- 74.2
- 45.5
H SX PSD H SX PSD H SX
C.
PS Ab98
66
46
PSD

Figure 5.

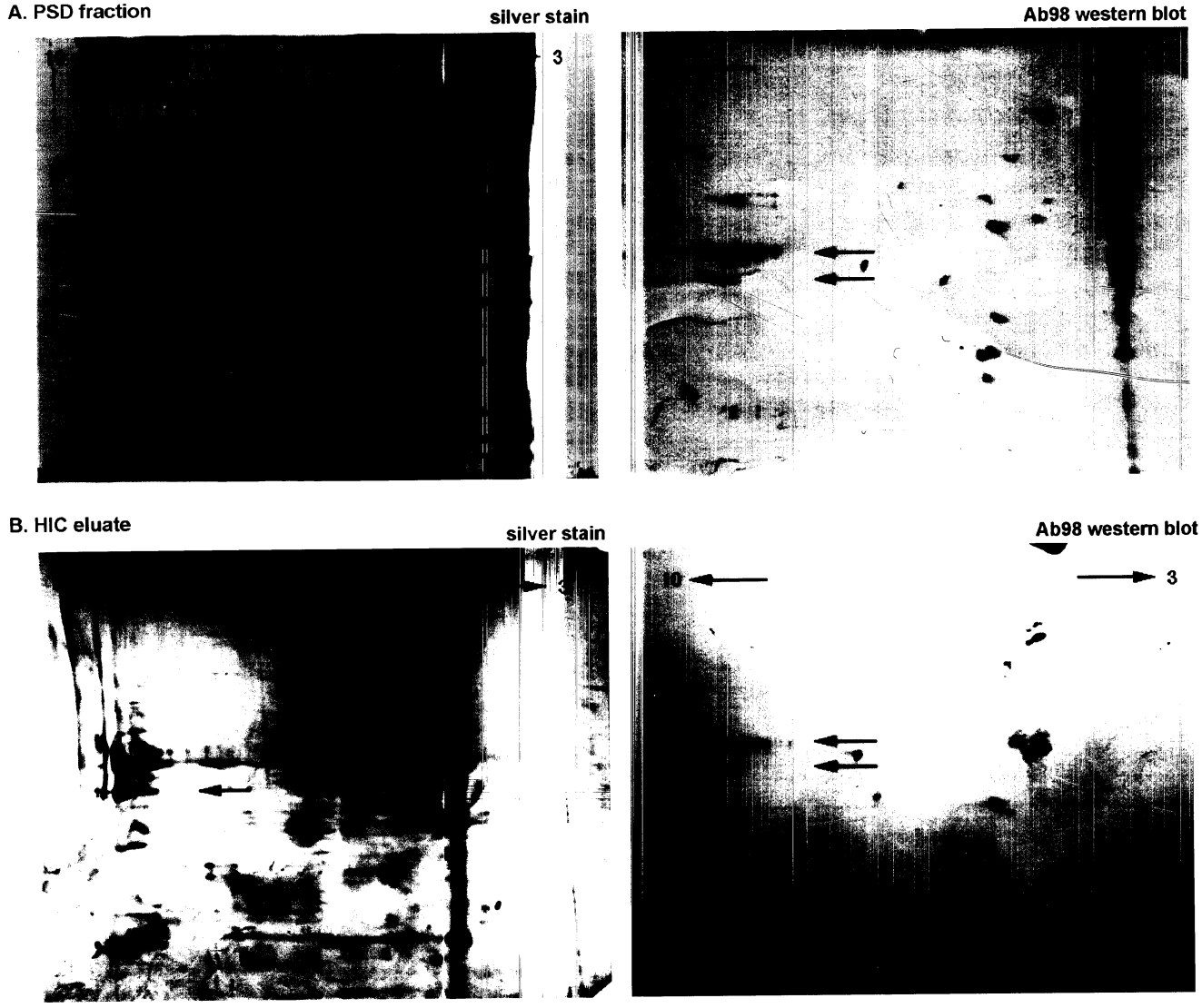
A. PSD fraction
silver stain
3
Ab98 western blot
B. HIC eluate
silver stain
Ab98 western blot
3

Figure 6. Insulin Receptor Substrate p53 (IRSp53)

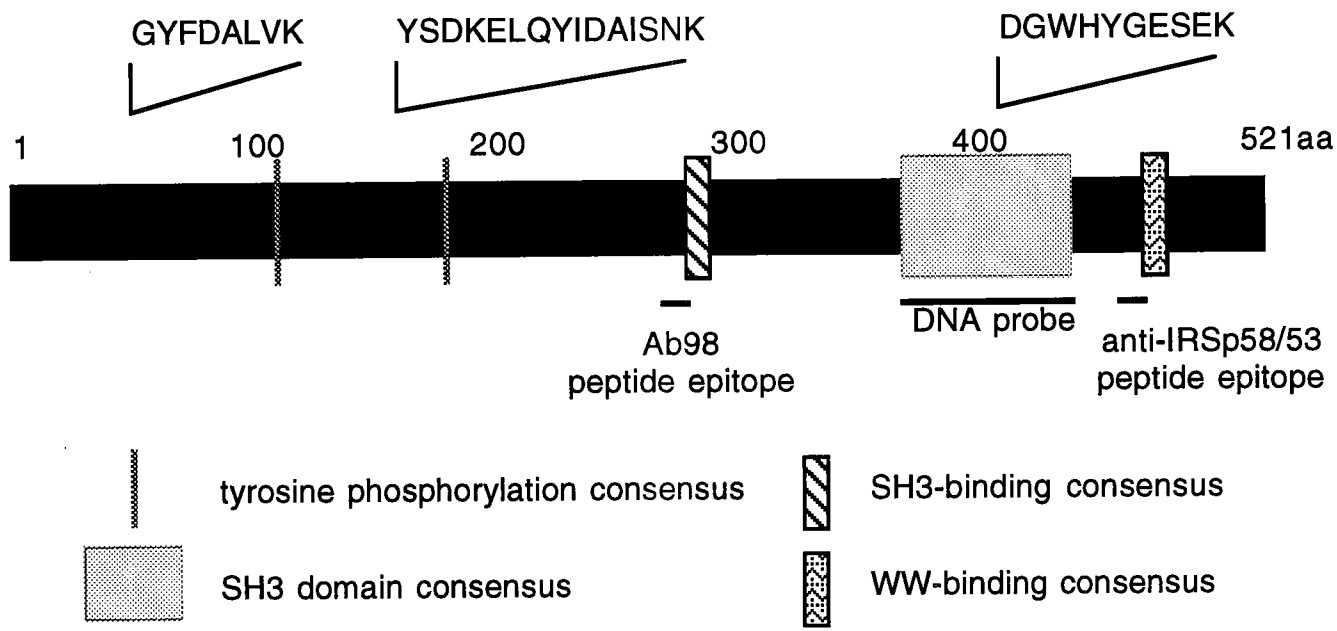

Figure 7.

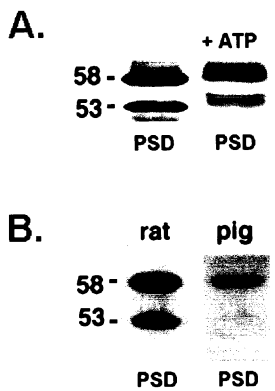

Figure 8.

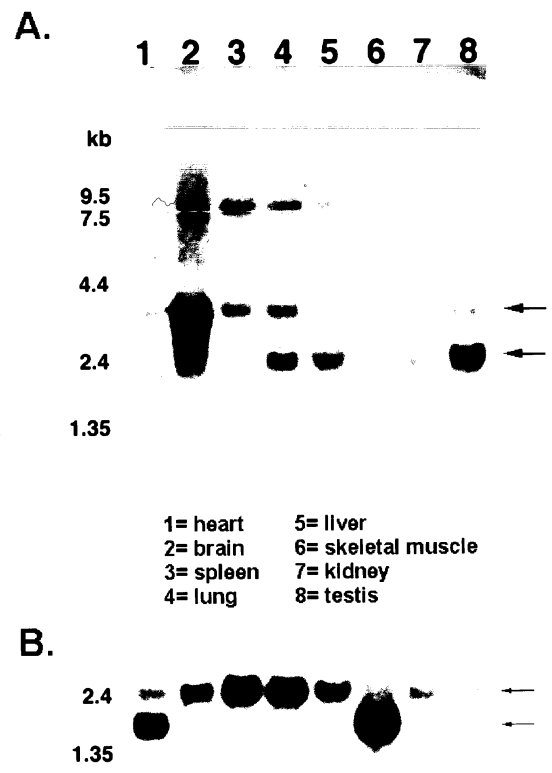

Figure 9.

A.

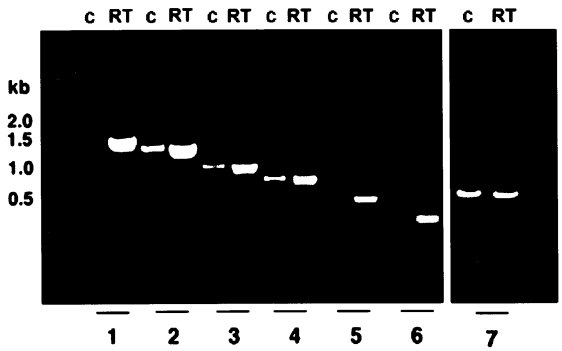

B.

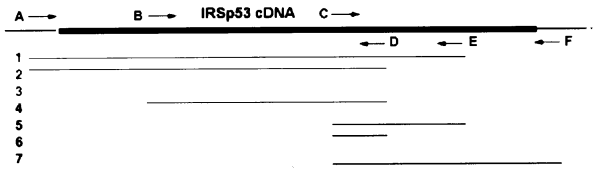

Figure 10.

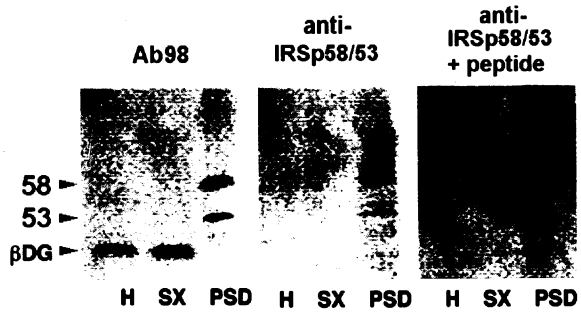

Figure 11.

A.

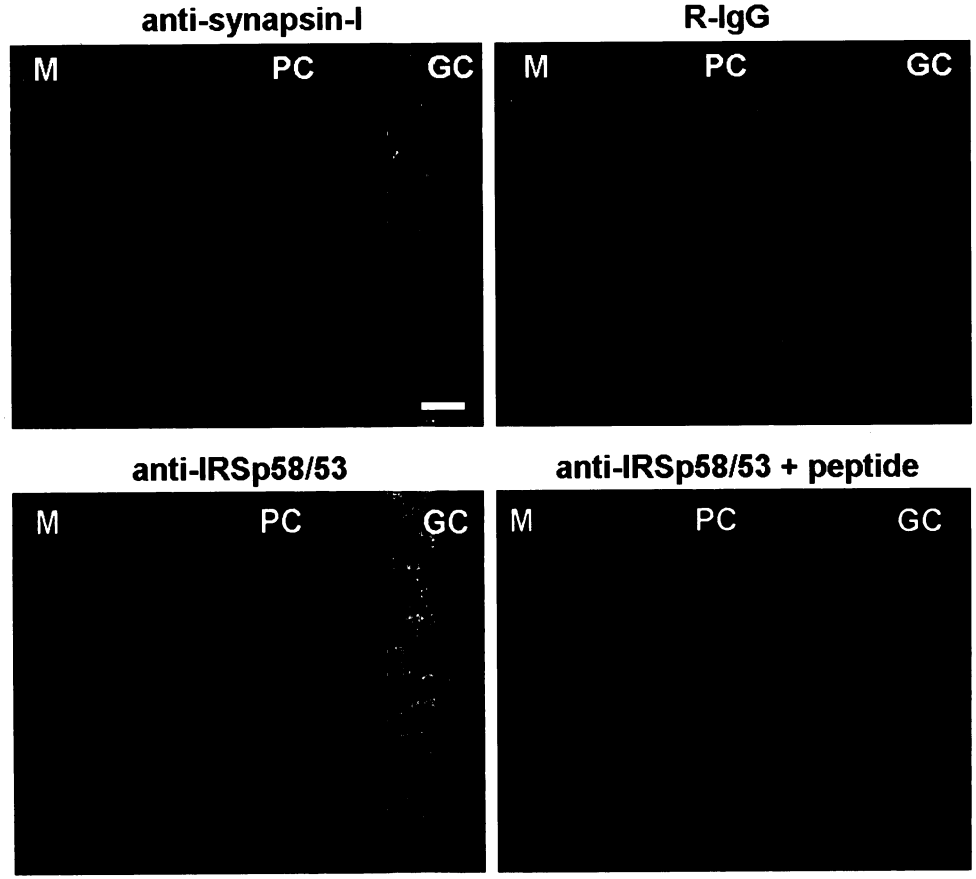
anti-synapsin-I
M
PC
GC
R-IgG
M
PC
GC
anti-IRSp58/53
M
PC
GC
anti-IRSp58/53 + peptide
M
PC
GC

B.


anti-IRSp58/53
anti-synaptophysin

Figure 12.

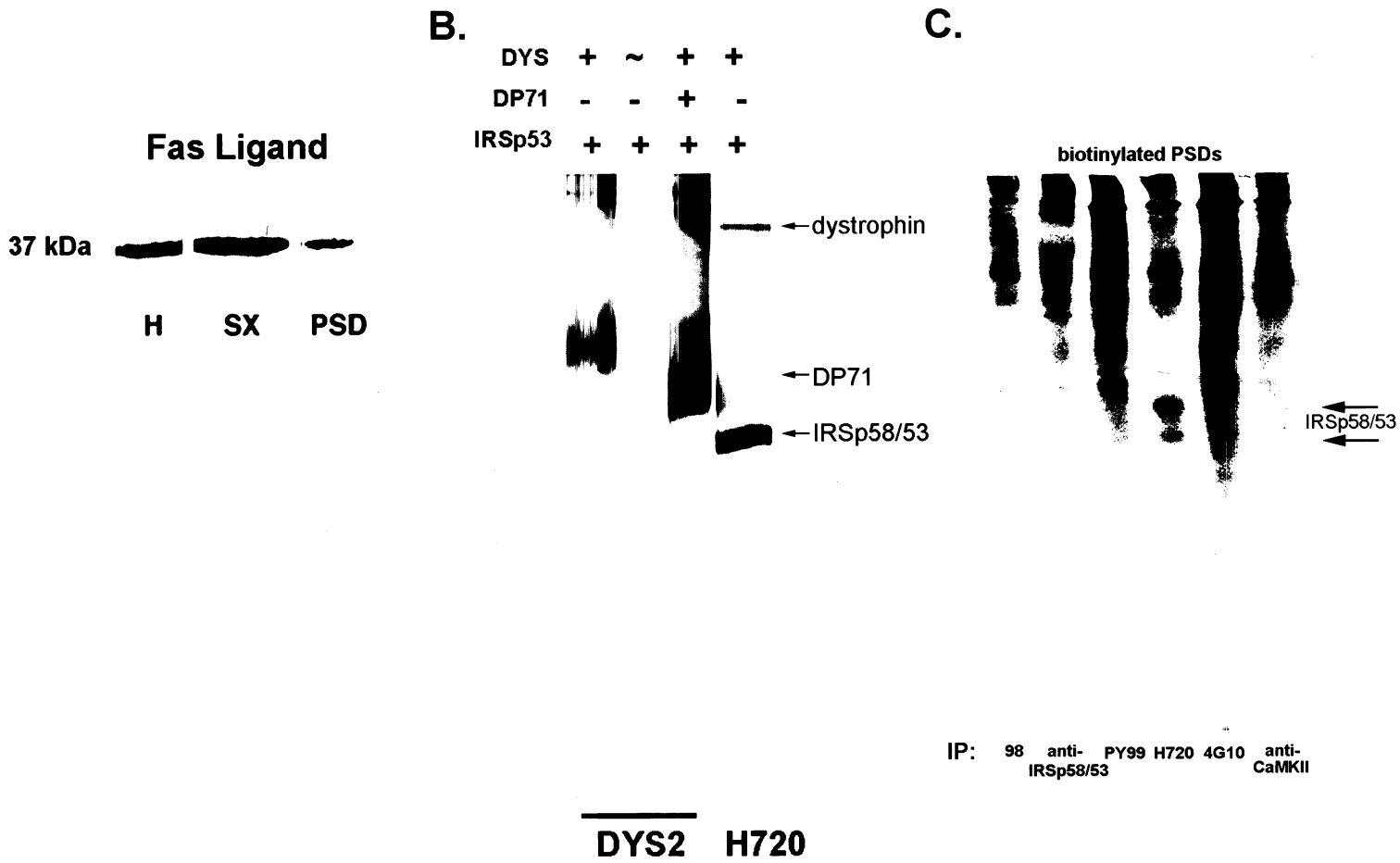
A.
Fas Ligand
37 kDa
H
SX
PSD
B.
DYS + ~ + +
DP71 - - + -
IRSp53 + + + +
dystrophin
DP71
IRSp58/53
C.
biotinylated PSDs
IRSp58/53
IP: 98 anti-IRSp58/53 PY99 H720 4G10 anti-CaMKII
DYS2 H720

Figure 13.

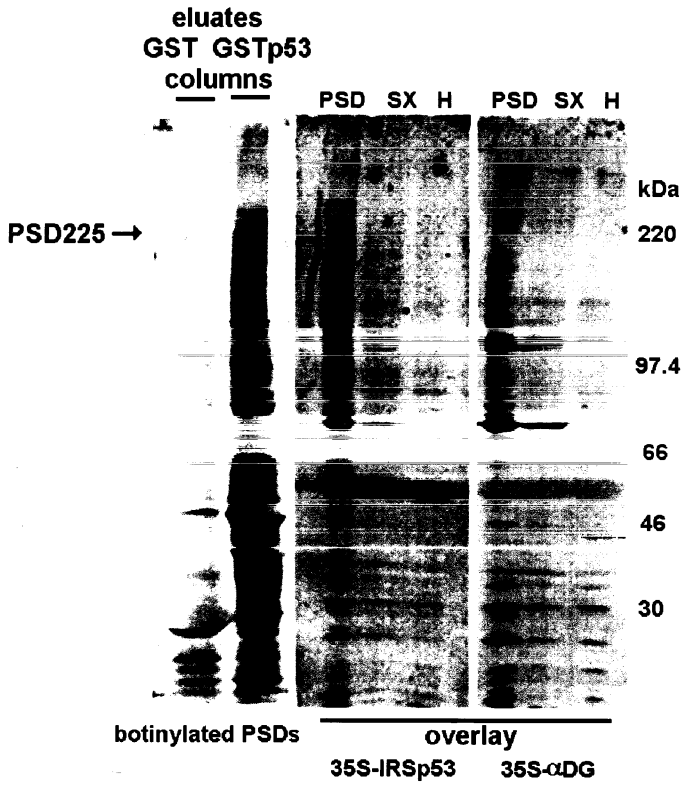
eluates
GST GSTp53
columns
PSD SX H
PSD SX H
kDa
PSD225
220
97.4
66
46
30
botinylated PSDs
overlay
35S-IRSp53
35S-αDG

Figure 14.

A.

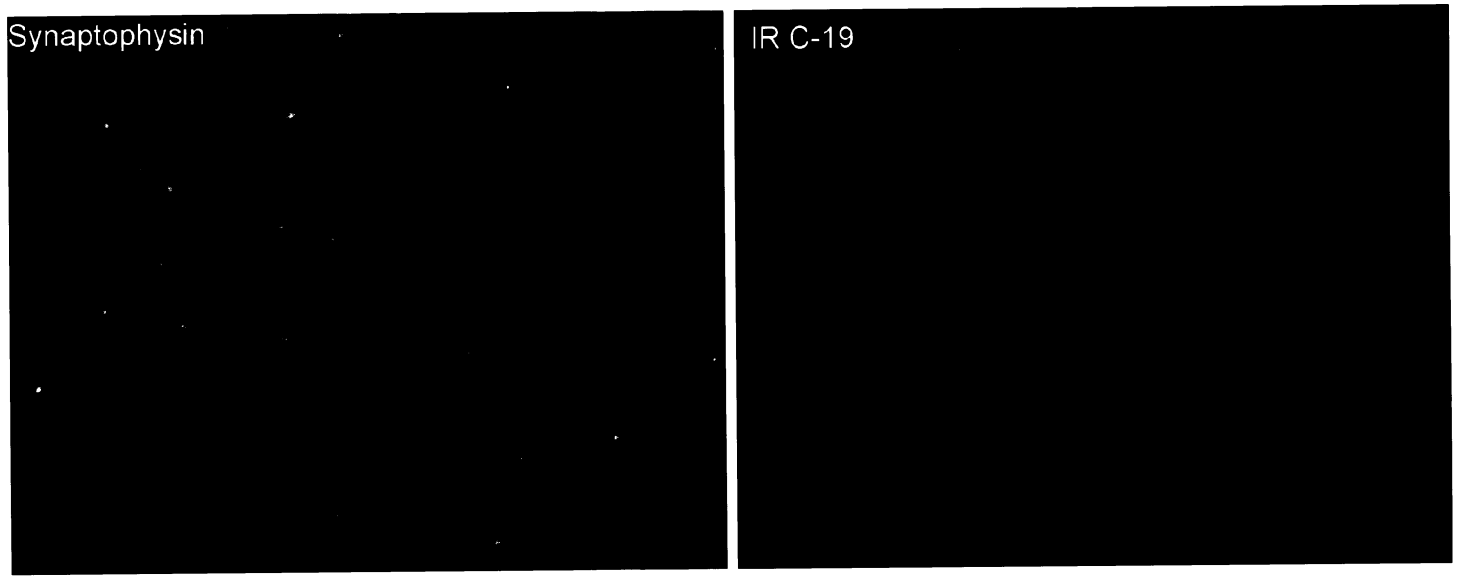
Synaptophysin
IR C-19

B.

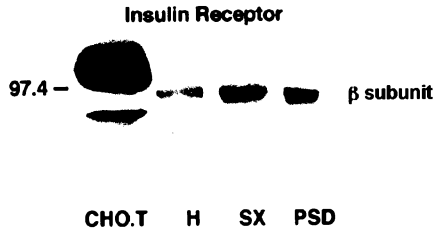
Insulin Receptor
97.4 –
β subunit
CHO.T
H
SX
PSD

Chapter I References

Balasubramanian S, Fung ET, Huganir RL (1998) Characterization of the tyrosine phosphorylation and distribution of dystrobrevin isoforms. FEBS Lett 432: 133-40.

Blake DJ, Love DR, Tinsley J, Morris GE, Turley H, Gatter K, Dickson G, Edwards YH, Davies KE (1992) Characterization of a 4.8kb transcript from the Duchenne muscular dystrophy locus expressed in Schwannoma cells. Hum Mol Genet 1: 103-9.

Bonnemann CG, McNally EM, Kunkel LM (1996) Beyond dystrophin: current progress in the muscular dystrophies [published erratum appears in Curr Opin Pediatr 1997 Apr;9(2):196]. Curr Opin Pediatr 8: 569-82.

Bowe MA, Deyst KA, Leszyk JD, Fallon JR (1994) Identification and purification of an agrin receptor from *Torpedo* postsynaptic membranes: A heteromeric complex related to the dystroglycans. Neuron 12: 1173-1180.

Bowe MA, Fallon JR (1995) The role of agrin in synapse formation. Annu Rev Neurosci 18: 443-462.

Bushby KM, Appleton R, Anderson LV, Welch JL, Kelly P, Gardner MD (1995) Deletion status and intellectual impairment in Duchenne muscular dystrophy. Dev Med Child Neurol 37: 260-9.

Campanelli JT, Roberds SL, Campbell KP, Scheller RH (1994) A role for dystrophin-associated glycoproteins and utrophin in agrin-induced AChR clustering. Cell 77: 663-74.

Carlin RK, Grab DJ, Cohen RS, Siekevitz P (1980) Isolation and characterization of postsynaptic densities from various brain regions: enrichment of different types of postsynaptic densities. J Cell Biol 86: 831-45.

Cartaud A, Coutant S, Petrucci TC, Cartaud J (1998) Evidence for in situ and in vitro association between beta-dystroglycan and the subsynaptic 43K rapsyn protein. Consequence for acetylcholine receptor clustering at the synapse. J Biol Chem 273: 11321-6.

Cibis GW, Fitzgerald KM, Harris DJ, Rothberg PG, Rupani M (1993) The effects of dystrophin gene mutations on the ERG in mice and humans. Investigative Ophthalmology & Visual Science 34: 3646-52.

Cox GA, Philps SF, Chapman VM, Chamberlain JS (1993) New mdx mutation disrupts expression of muscle and nonmuscle isoforms of dystrophin. Nature Genetics 4: 87-93.

Cox GA, Sunada Y, Campbell KP, Chamberlain JS (1994) DP71 can restore the dystrophin associated glycoprotein complex in muscle but fails to prevent dystrophy. Nat Genet 8: 333-339.

Cullen MJ, Walsh J, Stevenson SA, Rothery S, Severs NJ (1998) Co-localization of Dystrophin and beta-Dystroglycan Demonstrated in En Face View by Double Immunogold Labeling of Freeze-fractured Skeletal Muscle. J Histochem Cytochem 46: 945-54.

D'Souza VN, Nguyen TM, Morris GE, Karges W, Pillers DA, Ray PN (1995) A novel dystrophin isoform is required for normal retinal electrophysiology. Hum Mol Genet 4: 837-42.

DeChiara TM, Bowen DC, Valenzuela DM, Simians MV, Poueymirou WT, Thomas S, Kinetz E, Compton DL, Rojas E, Park JS, Smith C, DiStefano PS, Glass DJ, Burden SJ, Yancopoulos GD (1996) The Receptor Tyrosine Kinase MuSK is Required for Neuromuscular Junction Formation In Vivo. Cell 85: 501-512.

Deyst KA, Bowe MA, Leszyk JD, Fallon JR (1995) The alpha-dystroglycan-beta-dystroglycan complex. Membrane organization and relationship to an agrin receptor. J Biol Chem 270: 25956-9.

Dosemeci A, Reese TS (1993) Inhibition of endogenous phosphatase in a postsynaptic density fraction allows extensive phosphorylation of the major postsynaptic density protein. J Neurochem 61: 550-5.

Durbeej M, Henry MD, Ferletta M, Campbell KP, Ekblom P (1998) Distribution of dystroglycan in normal adult mouse tissues. J Histochem Cytochem 46: 449-57.

Durbeej M, Jung D, Hjalt T, Campbell KP, Ekblom P (1997) Transient expression of Dp140, a product of the Duchenne muscular dystrophy locus, during kidney tubulogenesis. Dev Biol 181: 156-67.

Durbeej M, Larsson E, Ibraghimov-Beskrovnaya O, Roberds SL, Campbell KP, Ekblom P (1995) Non-muscle alpha-dystroglycan is involved in epithelial development. J Cell Biol 130: 79-91.

Emery AEH (1993) *Duchenne Muscular Dystrophy*. Oxford monographs on medical genetics. Oxford University Press: New York.

Ervasti JM, Ohlendieck K, Kahl SD, Gaver MG, Campbell KP (1990) Deficiency of a glycoprotein component of the dystrophin complex in dystrophic muscle. Nature 345: 315-9.

Finn DM, Culligan KG, Ohlendieck K (1998) Decreased expression of brain beta-dystroglycan in Duchenne muscular dystrophy but not in the mdx animal model. Biochem Biophys Res Commun 249: 231-5.

Gautam M, Noakes PG, Moscoso L, Rupp F, Scheller RH, Merlie JP, Sanes JR (1996) Defective Neuromuscular Synaptogenesis in Agrin Deficient Mutant Mice. Cell 85 :525-35.

Gesemann M, Brancaccio A, Schumacher B, Ruegg MA (1998) Agrin is a high-affinity binding protein of dystroglycan in non-muscle tissue. J Biol Chem 273: 600-5.

Glass DJ, Bowen DC, Stitt TN, Radziejewski C, Bruno J, Ryan TE, Gies DR, Shah S, Mattssin K, Burden SJ, DiStefano PS, Valenzuela DM, DeChiara TM, Yancopoulos GD (1996) Agrin Acts via a MuSK Receptor Complex. Cell 85: 1-20.

Gorecki DC, Barnard EA (1995) Specific expression of G-dystrophin (Dp71) in the brain. Neuroreport 6: 893-6.

Gorecki DC, Derry J, Barnard EA (1994) Dystroglycan: Brain localization and chromosome mapping in the mouse. Hum Mol Genet 3: 1589-1597.

Gorecki DC, Monaco AP, Derry JM, Walker AP, Barnard EA, Barnard PJ (1992) Expression of four alternative dystrophin transcripts in brain regions regulated by different promoters. Hum Mol Genet 1: 505-10.

Goslin K, Banker G. (1991) Rat hippocampal neurons in low-density culture. *Culturing Nerve Cells*. Cambridge, MIT Press.

Greenberg DS, Schatz Y, Levy Z, Pizzo P, Yaffe D, Nudel U (1996) Reduced levels of dystrophin associated proteins in the brains of mice deficient for Dp71. Hum Mol Genet 5: 1299-303.

Greenberg DS, Sunada Y, Campbell KP, Yaffe D, Nudel U (1994) Exogenous Dp71 restores the levels of dystrophin associated proteins but does not alleviate muscle damage in mdx mice. Nat Genet 8: 340-344.

Hayashi YK, Engvall E, Arikawa HE, Goto K, Koga R, Nonaka I, Sugita H, Arahata K (1993) Abnormal localization of laminin subunits in muscular dystrophies. Journal of the Neurological Sciences 119: 53-64.

Ibraghimov BO, Ervasti JM, Leveille CJ, Slaughter CA, Sernett SW, Campbell KP (1992) Primary structure of dystrophin-associated glycoproteins linking dystrophin to the extracellular matrix. Nature 355: 696-702.

Ibraghimov-Beskrovnaya O, Milatovich A, Ozcelik T, Yang B, Koepnick K, Francke U, Campbell KP (1993) Human dystroglycan: skeletal muscle cDNA, genomic structure, origin of tissue specific isoforms and chromosomal localization. Human Molecular Genetics 2: 1651-7.

Ishii H, Hayashi YK, Nonaka I, Arahata K (1997) Electron microscopic examination of basal lamina in Fukuyama congenital muscular dystrophy. Neuromuscul Disord 7: 191-7.

Jung D, Yang B, Meyer J, Chamberlain JS, Campbell KP (1995) Identification and characterization of the dystrophin anchoring site on beta-dystroglycan. J Biol Chem 270: 27305-27310.

Kanoff RJ, Curless RG, Petito C, Falcone S, Siatkowski RM, Pegoraro E (1998) Walker-Warburg syndrome: neurologic features and muscle membrane structure. Pediatr Neurol 18: 76-80.

Khurana TS, Watkins SC, Kunkel LM (1992) The subcellular distribution of chromosome 6-encoded dystrophin-related protein in the brain. J. Cell Biol. 119: 357-66.

Kim T-w, Wu K, Xu J-l, Black IB (1992) Detection of dystrophin in the postsynaptic density of rat brain and deficiency in a mouse model of Duchenne muscular dystrophy. Proc. Natl. Acad. Sci. USA 89: 11642-11644.

Kobayashi K, Nakahori Y, Miyake M, Matsumura K, Kondo-Iida E, Nomura Y, Segawa M, Yoshioka M, Saito K, Osawa M, Hamano K, Sakakihara Y, Nonaka I, Nakagome Y, Kanazawa I, Nakamura Y, Tokunaga K, Toda T (1998) An ancient retrotransposal insertion causes Fukuyama-type congenital muscular dystrophy. Nature 394: 388-92.

Kroger S, Horton SE, Honig LS (1996) The developing avian retina expresses agrin isoforms during synaptogenesis. J Neurobiol 29: 165-182.

Lederfein D, Yaffe D, Nudel U (1993) A housekeeping type promoter, located in the 3' region of the Duchenne muscular dystrophy gene, controls the expression of Dp71, a major product of the gene. Hum Mol Genet 2: 1883-8.

Lenk U, Oexle K, Voit T, Ancker U, Hellner KA, Speer A, Hubner C (1996) A cysteine 3340 substitution in the dystroglycan-binding domain of dystrophin associated with Duchenne muscular dystrophy, mental retardation and absence of the ERG b-wave. Hum Mol Genet 5: 973-5.

Lidov H (1996) Dystrophin in the nervous system. Brain Pathol 6: 63-77.

Lidov H, Selig S, Kunkel LM (1995) Dp140: A novel 140 kDa CNS transcript from the dystrophin locus. Hum Mol Genet 4: 329-335.

Lidov HGW, Byers TJ, Kunkel LM (1993) The distribution of dystrophin in the murine central nervous system: an immunocytochemical study. Neuroscience 54: 167-187.

Matsumura K, Nonaka I, Campbell K (1993) Abnormal expression of dystrophin-associated proteins in Fukuyama-type congenital muscular dystrophy. The Lancet 341: 521-22.

Monaco AP, Bertelson CJ, Liechti-Gallati S, Moser H, Kunkel LM (1988) An explanation for the phenotypic differences between patients bearing partial deletions of the DMD locus. Genomics 2: 90-5.

Monaco AP, Neve RL, Colletti FC, Bertelson CJ, Kurnit DM, Kunkel LM (1986) Isolation of candidate cDNAs for portions of the Duchenne muscular dystrophy gene. Nature 323: 646-50.

Montanaro F, Carbonetto S, Campbell KP, Lindenbaum M (1995) Dystroglycan expression in the wild type and mdx mouse neural retina: synaptic colocalization with dystrophin, dystrophin-related protein but not laminin. J Neurosci Res 42: 528-38.

Mummery R, Sessay A, Lai FA, Beesley PW (1996) Beta-dystroglycan: Subcellular localisation in rat brain and detection of a novel immunologically related, postsynaptic density-enriched protein. J Neurochem 66: 2455-2459.

Muntoni F, Mateddu A, Marchei F, Clerk A, Serra G (1993) Muscular weakness in the mdx mouse. J Neurol Sci 120: 71-7.

Muntoni F, Mateddu A, Serra G (1991) Passive avoidance behaviour deficit in the mdx mouse. Neuromuscular Disorders 1: 121-3.

O'Toole JJ, Deyst KA, Bowe MA, Nastuk MA, McKechnie BA, Fallon JR (1996) Alternative splicing of agrin regulates its binding to heparin alpha-dystroglycan, and the cell surface. Proc Natl Acad Sci U S A 93: 7369-74.

Ohlendieck K, Campbell KP (1991) Dystrophin-associated proteins are greatly reduced in skeletal muscle from mdx mice. J Cell Biol 115: 1685-94.

Petrof BJ (1998) The molecular basis of activity-induced muscle injury in Duchenne muscular dystrophy. Mol Cell Biochem 179: 111-23.

Pillers DM, Weleber RG, Woodward WR, Green DG, Chapman VM, Ray PN (1995) mdxCv3 mouse is a model for electroretinography of Duchenne/Becker muscular dystrophy. Invest Ophthalmol Vis Sci 36: 462-6.

Schmitz F, Drenckhahn D (1997) Localization of dystrophin and beta-dystroglycan in bovine retinal photoreceptor processes extending into the postsynaptic dendritic complex. Histochem Cell Biol 108: 249-55.

Smalheiser NR, Kim E (1995) Purification of cranin, a laminin binding membrane protein - Identity with dystroglycan and reassessment of its carbohydrate moieties. J Biol Chem 270: 15425-15433.

Stevenson S, Rothery S, Cullen MJ, Severs NJ (1998) Spatial relationship of the C-terminal domains of dystrophin and beta-dystroglycan in cardiac muscle support a direct molecular interaction at the plasma membrane interface. Circ Res 82: 82-93.

Tian M, Jacobson C, Gee SH, Campbell KP, Carbonetto S, Jucker M (1996) Dystroglycan in the cerebellum is a laminin alpha 2-chain binding protein at the glial-vascular interface and is expressed in Purkinje cells. Eur J Neurosci 8: 2739-47.

Ueda H, Gohdo T, Ohno S (1998) Beta-dystroglycan localization in the photoreceptor and Muller cells in the rat retina revealed by immunoelectron microscopy. J Histochem Cytochem 46: 185-91.

Vaillend C, Rendon A, Misslin R, Ungerer A (1995) Influence of dystrophin-gene mutation on mdx mouse behavior. 1. Retention deficits at long delays in spontaneous alternation and bar-pressing tasks. Behav Genet 25: 569-579.

Wells DG, Fallon JR (1996) The state of the union. Neuromuscular junction. Curr Biol 6: 1073-5.

Williamson RA, Henry MD, Daniels KJ, Hrstka RF, Lee JC, Sunada Y, Ibraghimov-Beskrovnaya O, Campbell KP (1997) Dystroglycan is essential for early embryonic development: disruption of Reichert's membrane in Dag1-null mice. Hum Mol Genet 6: 831-41.

Worton R (1995) Muscular dystrophies: Diseases of the Dystrophin-Glycoprotein Complex. Science 270: 755-756.

Wu L, Wells D, Tay J, Mendis D, Abbott MA, Barnitt A, Quinlan E, Heynen A, Fallon JR, Richter JD (1998) CPEB-mediated cytoplasmic polyadenylation and the regulation of experience-dependent translation of alpha-CaMKII mRNA at synapses. Neuron 21: 1129-39.

Yang B, Jung D, Motto D, Meyer J, Koretzky G, Campbell KP (1995) SH3 domain-mediated interaction of dystroglycan and Grb2. J Biol Chem 270: 11711-11714.

Yoshida M, Mizuno Y, Nonaka I, Ozawa E (1993) A dystrophin-associated glycoprotein, A3a (one of 43DAG doublets), is retained in Duchenne muscular dystrophy muscle. J Biochem (Tokyo) 114: 634-9.

Yotsumoto S, Fujiwara H, Horton JH, Mosby TA, Wang X, Cui Y, Ko MS (1996) Cloning and expression analyses of mouse dystroglycan gene: specific expression in maternal decidua at the peri-implantation stage. Hum Mol Genet 5: 1259-67.

Chapter II References

Ahn AH, Kunkel LM (1995) Syntrophin binds to an alternatively spliced exon of dystrophin. J Cell Biol 128: 363-71.

Anai M, Ono H, Funaki M, Fukushima Y, Inukai K, Ogihara T, Sakoda H, Onishi Y, Yazaki Y, Kikuchi M, Oka Y, Asano T (1998) Different Subcellular Distribution and Regulation of Expression of Insulin Receptor Substrate (IRS)-3 from Those of IRS-1 and IRS-2. J Biol Chem 273: 29686-29692.

Araki E, Lipes MA, Patti ME, Bruning JC, Haag B 3rd, Johnson RS, Kahn CR (1994) Alternative pathway of insulin signalling in mice with targeted disruption of the IRS-1 gene. Nature 372: 186-90.

Baskin DG, Schwartz MW, Sipols AJ, D'Alessio DA, Goldstein BJ, White MF (1994) Insulin receptor substrate-1 (IRS-1) expression in rat brain. Endocrinology 134: 1952-5.

Beju D, Schechter R. 1998. Brain endogenous insulin and insulin receptor ultrastructural localization [abstract]. Society for Neuroscience Annual Meeting. 24: 1298.

Blackstone CD, Moss SJ, Martin LJ, Levey AI, Price DL, Huganir RL (1992) Biochemical characterization and localization of a non-N-methyl-D- aspartate glutamate receptor in rat brain. J Neurochem 58: 1118-26.

Bork P, Sudol M (1994) The WW domain: a signalling site in dystrophin? Trends Biochem Sci 19: 531-3.

Boyd FT Jr., Clarke DW, Muther TF, Raizada MK (1985) Insulin receptors and insulin modulation of norepinephrine uptake in neuronal cultures from rat brain. J Biol Chem 260: 15880-4.

Bruning JC, Winnay J, Bonner-Weir S, Taylor SI, Accili D, Kahn CR (1997) Development of a novel polygenic model of NIDDM in mice heterozygous for IR and IRS-1 null alleles. Cell 88: 561-72.

Chan Y, Kunkel LM (1997) In vitro expressed dystrophin fragments do not associate with each other. FEBS Lett 410: 153-9.

Cho KO, Hunt CA, Kennedy MB (1992) The rat brain postsynaptic density fraction contains a homolog of the Drosophila discs-large tumor suppressor protein. Neuron 9: 929-42.

Clarke DW, Boyd FT Jr., Kappy MS, Raizada MK (1984) Insulin binds to specific receptors and stimulates 2-deoxy-D-glucose uptake in cultured glial cells from rat brain. J Biol Chem 259: 11672-5.

Clarke DW, Mudd L, Boyd FT Jr., Fields M, Raizada MK (1986) Insulin is released from rat brain neuronal cells in culture. J Neurochem 47: 831-6.

Cotman CW, Banker G, Churchill L, Taylor D (1974) Isolation of postsynaptic densities from rat brain. J Cell Biol 63: 441-55.

Craft S, Newcomer J, Kanne S, Dagogo-Jack S, Cryer P, Sheline Y, Luby J, Dagogo-Jack A, Alderson A (1996) Memory improvement following induced hyperinsulinemia in Alzheimer's disease. Neurobiol Aging 17: 123-30.

Danielsen AG, Roth RA (1996) Role of the juxtamembrane tyrosine in insulin receptor-mediated tyrosine phosphorylation of p60 endogenous substrates. Endocrinology 137: 5326-31.

Dorn A, Bernstein HG, Hahn HJ, Ziegler M, Rummelfanger H (1981) Insulin immunohistochemistry of rodent CNS: apparent species differences but good correlation with radioimmunological data. Histochemistry 71: 609-16.

Dosemeci A, Gollop N, Jaffe H (1994) Identification of a major autophosphorylation site on postsynaptic density-associated Ca2+/calmodulin-dependent protein kinase. J Biol Chem 269: 31330-3.

Duffy KR, Pardridge WM (1987) Blood-brain barrier transcytosis of insulin in developing rabbits. Brain Res 420: 32-8.

Folli F, Bonfanti L, Renard E, Kahn CR, Merighi A (1994) Insulin receptor substrate-1 (IRS-1) distribution in the rat central nervous system. J Neurosci 14: 6412-22.

Frank HJ, Pardridge WM, Morris WL, Rosenfeld RG, Choi TB (1986) Binding and internalization of insulin and insulin-like growth factors by isolated brain microvessels. Diabetes 35: 654-61.

Frolich L, Blum-Degen D, Bernstein HG, Engelsberger S, Humrich J, Laufer S, Muschner D, Thalheimer A, Turk A, Hoyer S, Zochling R, Boissl KW, Jellinger K, Riederer P (1998) Brain insulin and insulin receptors in aging and sporadic Alzheimer's disease. J Neural Transm 105: 423-38.

Fujita-Yamaguchi Y (1984) Characterization of purified insulin receptor subunits. J Biol Chem 259: 1206-11.

Goslin K, Banker G. 1991. Rat hippocampal neurons in low-density culture. *Culturing Nerve Cells*. Cambridge, MIT Press.

Gurd JW (1985) Phosphorylation of the postsynaptic density glycoprotein gp180 by endogenous tyrosine kinase. Brain Res 333: 385-8.

Hachiya T, Kobayasi A, Touji S, Tamai K. (1997) Human Fas-ligand associated factor 3 mRNA, partial cds [GenBank Accession Number U70669, NCBI database].

Havrankova J, Roth J, Brownstein M (1978) Insulin receptors are widely distributed in the central nervous system of the rat. Nature 272: 827-9.

Hendricks SA, Agardh CD, Taylor SI, Roth J (1984) Unique features of the insulin receptor in rat brain. J Neurochem 43: 1302-9.

Hong M, Lee VM (1997) Insulin and insulin-like growth factor-1 regulate tau phosphorylation in cultured human neurons. J Biol Chem 272: 19547-53.

Hoyer S (1997) Models of Alzheimer's disease: cellular and molecular aspects. J Neural Transm Suppl 49: 11-21.

Hoyer S (1998) Is sporadic Alzheimer disease the brain type of non-insulin dependent diabetes mellitus? A challenging hypothesis. J Neural Transm 105: 415-22.

Hsueh YP, Kim E, Sheng M (1997) Disulfide-linked head-to-head multimerization in the mechanism of ion channel clustering by PSD-95. Neuron 18: 803-14.

Kahn BB (1998) Type 2 diabetes: when insulin secretion fails to compensate for insulin resistance. Cell 92: 593-6.

Kennedy MB (1993) The postsynaptic density. Curr Opin Neurobiol 3: 732-7.

Kennedy MB (1997) The postsynaptic density at glutamatergic synapses. Trends Neurosci 20: 264-8.

Kenner KA, Kusari J, Heidenreich KA (1995) cDNA sequence analysis of the human brain insulin receptor. Biochem Biophys Res Commun 217: 304-12.

Kim E, Cho KO, Rothschild A, Sheng M (1996) Heteromultimerization and NMDA receptor-clustering activity of Chapsyn-110, a member of the PSD-95 family of proteins. Neuron 17: 103-13.

Kim E, Niethammer M, Rothschild A, Jan YN, Sheng M (1995) Clustering of Shaker-type K+ channels by interaction with a family of membrane-associated guanylate kinases. Nature 378: 85-8.

Kistner U, Wenzel BM, Veh RW, Cases-Langhoff C, Garner AM, Appeltauer U, Voss B, Gundelfinger ED, Garner CC (1993) SAP90, a rat presynaptic protein related to the product of the Drosophila tumor suppressor gene dlg-A. J Biol Chem 268: 4580-3.

Kornau HC, Schenker LT, Kennedy MB, Seeburg PH (1995) Domain interaction between NMDA receptor subunits and the postsynaptic density protein PSD-95. Science 269: 1737-40.

Laakso M, Malkki M, Kekalainen P, Kuusisto J, Deeb SS (1994) Insulin receptor substrate-1 variants in non-insulin-dependent diabetes. J Clin Invest 94: 1141-6.

Lewin B (1997) *Genes VI*. New York, Oxford University Press, Inc.

Lieberman S (1996) Diabetes Mellitus. *Medicine*. Philadelphia, Lipincott-Raven.

Malgaroli A, DeCamilli P, Meldolesi J (1989) Distribution of alpha latrotoxin receptor in the rat brain by quantitative autoradiography: comparison with the nerve terminal protein, synapsin I. Neuroscience 32: 393-404.

McElduff A, Poronnik P, Baxter RC, Williams P (1988) A comparison of the insulin and insulin-like growth factor I receptors from rat brain and liver. Endocrinology 122: 1933-9.

Miele C, Caruso M, Calleja V, Auricchio R, Oriente F, Formisano P, Condorelli G, Cafieri A, Sawka-Verhelle D, Van Obberghen E, Beguinot F (1999) Differential role of insulin receptor substrate (IRS)-1 and IRS-2 in L6 skeletal muscle cells expressing the Arg1152 --> Gln insulin receptor. J Biol Chem 274: 3094-102.

Morrissey JH (1981) Silver stain for proteins in polyacrylamide gels: a modified procedure with enhanced uniform sensitivity. Anal Biochem 117: 307-10.

Mummery R, Sessay A, Lai FA, Beesley PW (1996) beta-dystroglycan: Subcellular localisation in rat brain and detection of a novel immunologically related, postsynaptic density-enriched protein. J Neurochem 66: 2455-2459.

Pardridge WM, Boado RJ, Farrell CR (1990) Brain-type glucose transporter (GLUT-1) is selectively localized to the blood-brain barrier. Studies with quantitative western blotting and in situ hybridization. J Biol Chem 265: 18035-40.

Qiu WQ, Walsh DM, Ye Z, Vekrellis K, Zhang J, Podlisny MB, Rosner MR, Safavi A, Hersh LB, Selkoe DJ (1998) Insulin-degrading enzyme regulates extracellular levels of amyloid beta- protein by degradation. J Biol Chem 273: 32730-8.

Rotin D (1998) WW (WWP) Domains: From Structure to Function. Curr Top Microbiol Immunol 228: 115-133.

Sheng M (1997) Excitatory synapses. Glutamate receptors put in their place. Nature 386: 221, 223.

Smit AB, van Kesteren RE, Li KW, Van Minnen J, Spijker S, Van Heerikhuizen H, Geraerts WP (1998) Towards understanding the role of

insulin in the brain: lessons from insulin-related signaling systems in the invertebrate brain. Prog Neurobiol 54: 35-54.

Tamemoto H, Kadowaki T, Tobe K, Yagi T, Sakura H, Hayakawa T, Terauchi Y, Ueki K, Kaburagi Y, Satoh S, et al. (1994) Insulin resistance and growth retardation in mice lacking insulin receptor substrate-1. Nature 372: 182-6.

Ullrich A, Bell JR, Chen EY, Herrera R, Petruzzelli LM, Dull TJ, Gray A, Coussens L, Liao YC, Tsubokawa M, et al. (1985) Human insulin receptor and its relationship to the tyrosine kinase family of oncogenes. Nature 313: 756-61.

Wan Q, Xiong ZG, Man HY, Ackerley CA, Braunton J, Lu WY, Becker LE, MacDonald JF, Wang YT (1997) Recruitment of functional GABA(A) receptors to postsynaptic domains by insulin. Nature 388: 686-90.

Wei LT, Matsumoto H, Rhoads DE (1990) Release of immunoreactive insulin from rat brain synaptosomes under depolarizing conditions. J Neurochem 54: 1661-5.

White MF, Yenush L (1998) The IRS-signaling system: a network of docking proteins that mediate insulin and cytokine action. Curr Top Microbiol Immunol 228: 179-208.

Wickelgren I (1998) Tracking insulin to the mind. Science 280: 517-9.

Withers DJ, Gutierrez JS, Towery H, Burks DJ, Ren JM, Previs S, Zhang Y, Bernal D, Pons S, Shulman GI, Bonner-Weir S, White MF (1998) Disruption of IRS-2 causes type 2 diabetes in mice. Nature 391: 900-4.

Wozniak M, Rydzewski B, Baker SP, Raizada MK (1993) The cellular and physiological actions of insulin in the central nervous system. Neurochem Int 22: 1-10.

Wu K, Xu JL, Suen PC, Levine E, Huang YY, Mount HT, Lin SY, Black IB (1996) Functional trkB neurotrophin receptors are intrinsic components of the adult brain postsynaptic density. Brain Res Mol Brain Res 43: 286-90.

Wu L, Wells D, Tay J, Mendis D, Abbott MA, Barnitt A, Quinlan E, Heynen A, Fallon JR, Richter JD (1998) CPEB-mediated cytoplasmic polyadenylation and the regulation of experience-dependent translation of alpha-CaMKII mRNA at synapses. Neuron 21: 1129-39.

Yamada M, Ohnishi H, Sano S, Nakatani A, Ikeuchi T, Hatanaka H (1997) Insulin receptor substrate (IRS)-1 and IRS-2 are tyrosine-phosphorylated and associated with phosphatidylinositol 3-kinase in response to brain-derived neurotrophic factor in cultured cerebral cortical neurons. J Biol Chem 272: 30334-9.

Yeh TC, Li W, Keller GA, Roth RA (1998) Disruption of a putative SH3 domain and the proline-rich motifs in the 53-kDa substrate of the insulin receptor kinase does not alter its subcellular localization or ability to serve as a substrate. J Cell Biochem 68: 139-50.

Yeh TC, Ogawa W, Danielsen AG, Roth RA (1996) Characterization and cloning of a 58/53-kDa substrate of the insulin receptor tyrosine kinase. J Biol Chem 271: 2921-8.

Yoshida M, Mizuno Y, Nonaka I, Ozawa E (1993) A dystrophin-associated glycoprotein, A3a (one of 43DAG doublets), is retained in Duchenne muscular dystrophy muscle. J Biochem (Tokyo) 114: 634-9.

Young WSd (1986) Periventricular hypothalamic cells in the rat brain contain insulin mRNA [published erratum appears in Neuropeptides 1986 Nov-Dec;8(4):401]. Neuropeptides 8: 93-7.

Ziff EB (1997) Enlightening the postsynaptic density. Neuron 19: 1163-74.

The Journal of Neuroscience, September 1, 1999, 19(17):7300–7308

The Insulin Receptor Tyrosine Kinase Substrate p58/53 and the Insulin Receptor Are Components of CNS Synapses

Mary-Alice Abbott,[1,2] David G. Wells,[1] and Justin R. Fallon[1]

[2]*University of Massachusetts Graduate School of Biomedical Sciences, Worcester, Massachusetts 01655, and* [1]*Department of Neuroscience, Brown University, Providence, Rhode Island 02912*

The synapse is the primary locus of cell–cell communication in the nervous system. It is now clear that the synapse incorporates diverse cell signaling modalities in addition to classical neurotransmission. Here we show that two components of the insulin pathway are localized at CNS synapses, where they are components of the postsynaptic density (PSD). An immunochemical screen revealed that polypeptides of 58 and 53 kDa (p58/53) were highly enriched in PSD fractions from rat cerebral cortex, hippocampus, and cerebellum. These polypeptides were purified and microsequenced, revealing that p58/53 is identical to the insulin receptor tyrosine kinase substrate p58/53 (IRSp53). Our analysis of IRSp58/53 mRNA suggests that within rat brain there is one coding region for IRSp58 and IRSp53; we find no evidence of alternative splicing. We demonstrate that IRSp58/53 is expressed in the synapse-rich molecular layer of the cerebellum and is highly concentrated at the synapses of cultured hippocampal neurons, where it colocalizes with the insulin receptor. Together, these data suggest that insulin signaling may play a role at CNS synapses.

Key words: insulin receptor; postsynaptic density; insulin receptor substrate; hippocampal neurons; brain; IRSp53

The synapse is the predominant site of cell–cell communication in the nervous system. In both the central and peripheral nervous systems, synapses are characterized by the precise apposition of the presynaptic nerve terminal and postsynaptic apparatus. Fast synaptic transmission relies on the coordinated localization of synaptic vesicles and neurotransmitter receptors at this site (Salpeter, 1987; Peters et al., 1991). Synapses are also distinguished by the presence of specialized molecular machinery for regulated exocytosis, neurotransmitter receptor clustering, and signal transduction (Hall and Sanes, 1993; Sheng and Wyszynski, 1997; Somogyi et al., 1998). Notably, synapses also support a range of other cell–cell signaling modalities. For example, neurotrophins and growth factors can modulate synaptic growth, plasticity, and function (Lohof et al., 1993; Kang and Schuman, 1995).

Insulin and its receptor are expressed in the brain, where they are likely to regulate glucose homeostasis and gene expression (Wozniak et al., 1993). Moreover, a number of findings have also suggested a relationship between insulin and Alzheimer's disease (Craft et al., 1996; Frolich et al., 1998; Hoyer, 1998; Wickelgren, 1998). For example, insulin action inhibits tau hyperphosphorylation and thus may block the formation of neurofibrillary tangles (Hong and Lee, 1997). In addition, insulin and its receptor may also play a role at synapses (Unger et al., 1989; Wozniak et al., 1993; Schechter et al., 1996). Destruction of insulin receptors by intracerebroventricular injection of streptozotocin leads to long-term deficits in learning and memory (Lannert and Hoyer, 1998). Insulin can be released from both cultured neuronal cells and synaptosomes in an activity-dependent fashion (Clarke et al., 1986; Wei et al., 1990). Moreover, insulin can recruit $GABA_A$ receptors to postsynaptic domains (Wan et al., 1997), suggesting a role for this hormone in synaptic plasticity.

The insulin receptor is a tyrosine kinase, but many of its actions require accessory molecules known as insulin receptor substrates (e.g., IRS-1, IRS-2, and IRS-3) (White and Yenush, 1998). In peripheral tissues, these substrates become phosphorylated by the insulin receptor and then coordinate flexible and diverse signaling pathways (Shepherd et al., 1998). In addition, IRS proteins exhibit distinct subcellular localizations, raising the possibility that they subserve spatially and qualitatively distinct intracellular signaling events (Anai et al., 1998). Therefore, characterizing insulin receptor substrates and determining their localization in the CNS may provide insights into diverse insulin actions in the brain.

In the CNS, many synaptic signaling molecules are concentrated in the postsynaptic density (PSD) (for review, see Sheng, 1997; Ziff, 1997). In the current study, we show that the insulin receptor substrate IRSp58/53 is highly enriched in PSD fractions. Microsequencing of IRSp58 and IRSp53 polypeptides suggests they differ only in some post-translational modification. A survey of several tissues revealed that IRSp58/53 and its mRNA are most highly expressed in the brain. IRSp58/53 is localized in the dendritic layers of the cerebellum and is concentrated at synapses in cultured hippocampal neurons. Finally, we show that the insulin receptor is both concentrated at synapses and is a component of the PSD fraction. Together, these data suggest that the synapse is an important site of specialized insulin signaling in the brain.

MATERIALS AND METHODS

Brain subcellular fractions. PSD fractions were prepared according to the method described elsewhere (Carlin et al., 1980; Dosemeci and Reese, 1993; Wu et al., 1998). The absence of presynaptic contaminants and enrichment of PSD proteins in this fraction was confirmed by Western

Received April 8, 1999; revised June 7, 1999; accepted June 15, 1999.

This work was supported in part by an MD/PhD predoctoral fellowship from the American Heart Association (M.-A.A.), an individual National Research Scientist postdoctoral award (NS10343; D.G.W.), the Muscular Dystrophy Association, and National Institutes of Health Grants HD23924 and MH53571. We acknowledge the generous gifts of reagents from E. Ozawa, R. Roth, and M. Czech. We also thank A. Dosemeci for providing initial PSD fractions.

Correspondence should be addressed to Justin Fallon, Department of Neuroscience, Brown University, Box 1953, 190 Thayer Street, Providence, RI 02912.

blotting with antibodies to NMDA receptor subunit 1, α-Ca^{2+}/calmodulin-dependent kinase II (α-CaMKII), and synaptophysin (Wu et al., 1998).

Antibodies. Ab98 antiserum was raised by immunizing a rabbit with the peptide KAPLPPPEYPSQ (a sequence in the cytosolic domain of β-dystroglycan that was used for the production of antibody PA3a; Yoshida et al., 1993) and was affinity-purified (Quality Controlled Biochemicals, Hopkinton, MA). The anti-IRSp58/53 polyclonal antibody was raised by injecting a rabbit with the MAP-conjugated peptide DKDDLALPPPDYGT (Research Genetics, Inc., Huntsville, AL) and was affinity-purified. Immunoabsorption was performed by mixing the primary antibody with its corresponding peptide for 2 hr to overnight at 4°C. The IRSp53 monoclonal antibody H720 is described elsewhere (Yeh et al., 1996).

Insulin receptor β-subunit polyclonal antibody (C-19) was obtained from Santa Cruz Biotechnology (Santa Cruz, CA). An anti-peptide antiserum to β-dystroglycan (12031C) was a generous gift of L. Kunkel (Howard Hughes Medical Institute, Harvard Medical School). Monoclonal anti-β-dystroglycan antibody NCL-43DAG was obtained from Vector Laboratories (Burlingame, CA). Monoclonal antibodies to synaptophysin (SY38) and to α-CaMKII (6G9) were obtained from Boehringer Mannheim (Irvine, CA). Antibody to NMDA receptor subunit NR1 (54.1) was obtained from PharMingen (San Diego, CA).

Western blotting. Protein concentrations were determined with the BCA protein assay (Pierce, Rockford, IL) using BSA as a standard. Equal quantities of homogenate, synaptosomal, and PSD fraction proteins were separated on 10 or 5–15% gradient gels by SDS-PAGE, transferred onto nitrocellulose membranes, and incubated with primary antibodies followed by alkaline phosphatase-conjugated goat anti-rabbit or anti-mouse IgG (Boehringer Mannheim, Indianapolis, IN). Bound antibody was visualized using the 5-bromo-4-chloro-3-indolyl phosphate/nitro blue tetrazolium substrate system (Promega, Madison, WI). In some experiments, lysates of Chinese hamster ovary (CHO).T cells, which overexpress insulin receptors (generously provided by M. Czech, University of Massachusetts Medical Center; Baltensperger et al., 1996), were also analyzed.

Hydrophobic interaction chromatography. For hydrophobic interaction chromatography (HIC), PSDs were solubilized overnight at 4°C in 8 M urea, 1 M NaCl, 5 mM dithiothreitol (DTT), 50 mM sodium phosphate buffer, pH 7.5. The soluble fraction was then made 4 M in urea and incubated with HIC matrix (high-performance phenyl-Sepharose; Pharmacia Biotech, Piscataway, NJ) for 3 hr at 4°C. The HIC matrix was then washed, preeluted in the same buffer with 0.8 M NaCl, and eluted with the same buffer in 0.1 M NaCl. Apomyoglobin (Sigma, St. Louis, MO) was added as a carrier to the eluate, and the proteins were precipitated with trichloroacetic acid.

Two-dimensional gel electrophoresis. Isoelectric focusing (IEF) strips (Immobiline Dry Strips, pH 3–10, 11 cm; Pharmacia) were rehydrated for 6 hr to overnight at room temperature in two-dimensional (2D) sample–rehydration buffer [8 M urea, 2% 3-[(3-cholamidopropyl)dimethylammonio]-1-propanesulfonic acid, 2% immobilized pH gradient buffer 3-10L (Pharmacia), and 0.3% DTT. Samples were loaded at the anodic end of the IEF strip, and IEF was performed at 20°C on a Multiphor II apparatus (Pharmacia) for 1 hr at 300 V and 15 hr at 1400 V. The strips were then equilibrated and electrophoresed in the second dimension (10% gel, SDS-PAGE), as per the manufacturer's instructions. The 2D gels were stained with either silver (Morrissey, 1981) or Coomassie blue or transferred (10 V, 16 hr) to nitrocellulose for Western blotting.

Matrix-assisted laser desorption ionization time-of-flight mass spectrometry and peptide sequencing. HIC eluates separated by 2D electrophoresis were visualized by Coomassie blue stain, and the bands corresponding to p58 and p53 were excised from the gel. The polypeptides were recovered from the gel and subjected to trypsin digestion. Peptide masses were determined by matrix-assisted laser desorption ionization time-of-flight mass spectrometry (MALDI-TOF MS). MS-Fit search software was then used to compare the p58 and p53 mass profiles to known proteins. Tryptic fragments from p58 and p53 were separated by HPLC, and peptide sequence was obtained from three fragments of p58 (J. Leszyk, Worcester Foundation Protein Sequencing Facility, Worcester, MA).

In vitro *phosphorylation of PSD fraction proteins.* The method used is a modification of a procedure described elsewhere (Dosemeci et al., 1994). PSDs were pretreated on ice for 3 hr with occasional mixing in 20 mM HEPES, pH 7.4, and 100 mM DTT. PSDs were diluted to a final concentration of 0.4 mg of protein/ml in phosphorylation solution (5 mM $MgCl_2$, 50 μg/ml leupeptin, 20 mM DTT, 20 mM HEPES, pH 7.4, 1 mM $CaCl_2$, and 1 mM orthovanadate, with or without 100 μM ATP), and incubated at 37°C for 5 min. The reaction was quenched by the addition of SDS sample buffer.

Northern blot hybridization. A ^{32}P-labeled probe was synthesized by PCR using the IRSp53 cDNA clone (provided by R. Roth, Stanford University School of Medicine; described by Yeh et al., 1996) as template, and the primer pair F1, AAGAGCGTGACCCCGAAGAACAGC; and R1, AACCAGCCCCGCATTTTG.

The rat Multiple Tissue Northern Blot (Clontech, Palo Alto, CA) was probed as instructed by the manufacturer. The most stringent wash performed was 0.1× SSC and 0.1% SDS at 65°C for 40 min.

RNA isolation and RT-PCR. RNA was isolated from 20 mg of rat cerebral cortex by the RNeasy mini kit (Qiagen, Chatsworth, CA). The total RNA (30 μg) was reverse-transcribed using random primers, and this reaction product was used as the template for PCR. The PCR conditions were 3 min at 94°C, 40 cycles (30 sec at 94°C, 1 min at 55°C, and 4 min at 68°C), and 8 min at 68°C. The sequences of the primers used are as follows, 5′ to 3′: A, GTGTAGCCGGGACCCAGGACCAT; B, CGAGGAGCGGAGGAGGTTCTGC; C, AAGAGCGTGACCCCGAAGAACAGC; D, AACCAGCCCCGCATTTTG; E, ACGGCCACACTGTAGGGTCTCTGC; and F, TCTAGTCAGGGGCAGCTCAAAATC.

Tissue sections and immunohistochemistry. Brains from adult rats were immersed in freezing isopentane, mounted in OCT embedding medium, and equilibrated to −20°C. Frozen sections (8 μm) were cut, air-dried onto glass slides, fixed in MeOH at −20°C for 10 min, and rehydrated in PBS with 0.1% Triton X-100 (PBST). The sections were blocked for 1 hr at room temperature with PBST, 1% BSA, 10% horse serum, and 1% goat serum. The primary antibodies anti-IRSp58/53 (with or without peptide) and rabbit anti-synapsin-I (1:3000; provided by Pietro DeCamilli, Howard Hughes Medical Institute, Yale University School of Medicine; Malgaroli et al., 1989) were diluted in block and were applied overnight at 4°C. The slides were washed at room temperature for 2 hr in PBST with stirring and one wash solution change. Cy3-conjugated goat anti-rabbit IgG (1:500–1:4000; Jackson ImmunoResearch, WestGrove, PA) or FITC-conjugated goat anti-mouse IgG, rat-absorbed (1:100; Vector Laboratories, Burlingame, CA) was applied for 3 hr at room temperature. The sections were washed as above, dehydrated in −20°C MeOH for 10 min, allowed to air dry, and mounted in Citifluor (Ted Pella, Redding, CA). Immunostaining was visualized by indirect immunofluorescence using a Nikon E800 microscope. Images were captured with a Photometrics CCD camera using IP Lab systems software.

Hippocampal neuron cultures and immunohistochemistry. Low-density cultures were created as previously described (Goslin and Banker, 1991; Wu et al., 1998). After 19–21 d, the cells were fixed with 4% paraformaldehyde at 37°C for 20 min, covered with saponin (0.05%) for 5 min. and then incubated in blocking solution (MEM, 10% horse serum, 1% goat serum, and 1% BSA). The primary antibodies, mouse anti-synaptophysin (1:20; Boehringer Mannheim), rabbit anti-IRSp58/53 (1:5), and mouse insulin receptor β-subunit (1:40, C-19; Santa Cruz Biotechnology) were applied overnight at 4°C. Species-specific secondary antibodies, directly conjugated to either FITC or Cy3, were applied for 1 hr at room temperature. Coverslips were mounted onto glass slides with Citifluor.

RESULTS

Polypeptides p58 and p53 are enriched in the postsynaptic density fraction

We were initially interested in determining the distribution of a known protein (β-dystroglycan) in the rat brain. We performed Western blot analysis on homogenate, synaptosomes, and PSD-enriched fractions. Antiserum Ab98 recognized a polypeptide of ~43 kDa in brain homogenate and synaptosome fractions (Fig. 1*A*). This polypeptide co-migrated with β-dystroglycan from muscle and was also bound by the anti-β-dystroglycan antibodies NCL-43DAG and 12031-C (data not shown). Thus we identified this 43 kDa polypeptide as β-dystroglycan.

Ab98 also recognized a pair of polypeptides, termed p58 and p53, in the PSD fraction (Fig. 1). p58 and p53 were highly enriched in the PSD fraction, because they were not detected in

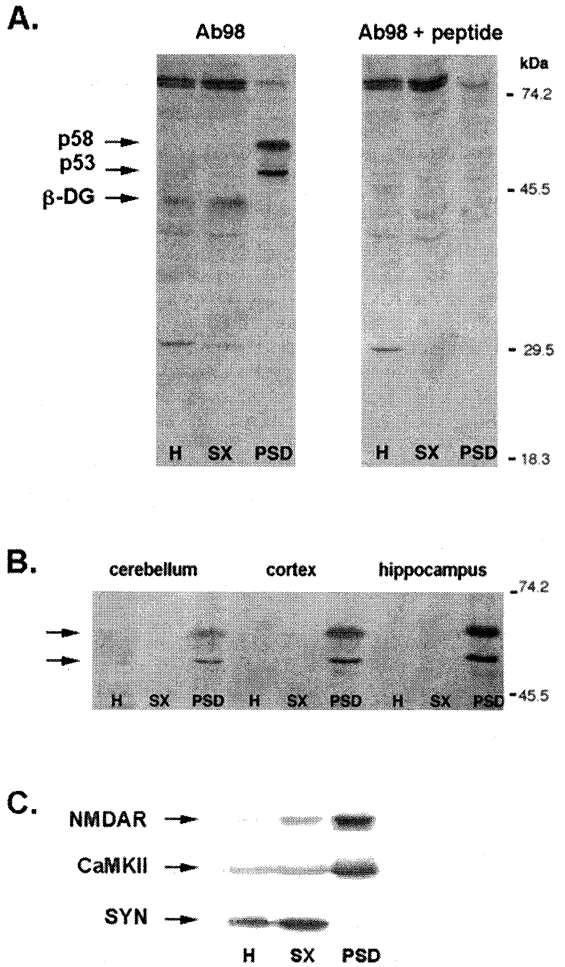

Figure 1. Polypeptides of 58 kDa and 53 kDa are enriched in the PSD fraction. *A*, Homogenate, synaptosome, and PSD fractions from rat brain were separated by SDS-PAGE, transferred to nitrocellulose, and probed with Ab98 (*left*) or Ab98 that had been preabsorbed with peptide (*right*). β-Dystroglycan is observed in the homogenate and synaptosomal fractions (*β-DG*). A pair of polypeptides of 58 and 53 kDa is specifically detected in the PSD fraction (*p58*, *p53*). Binding of Ab98 to all three polypeptides is eliminated when the antibody was preabsorbed (*Ab98 + peptide*). Mobilities of molecular weight standards are indicated. *H*, Homogenate; *SX*, synaptosomes; *PSD*, postsynaptic density fraction. *B*, Western blots of homogenate, synaptosomes, and PSD fractions from the indicated brain regions were probed with antibody Ab98. p58 and p53 are selectively enriched in the PSD fractions from all areas examined. *C*, Western blot of homogenate, synaptosome, and PSD fractions from cerebral cortex probed with antibodies to NMDA receptor subunit NR1, α-CaMKII, and synaptophysin.

blots of homogenate or synaptosomes that contained the same amount of total protein (Fig. 1*A*). p58 and p53 were enriched in PSD fractions isolated from rat cerebral cortex, cerebellum, and hippocampus (Fig. 1*B*). The selective enrichment of p58 and p53 closely parallels that of known PSD constituents such as α-CaMKII and the NMDA receptor subunit NR1 (Fig. 1*C*). In contrast, β-dystroglycan (migrating at 43 kDa) was present in brain homogenate and was modestly enriched in synaptosomes, but was not detected in PSD fractions from cerebral cortex (Fig. 1*A*) or other brain regions (data not shown). Antibodies NCL-43DAG and 12031-C revealed a similar distribution of β-dystroglycan in these fractions. However, neither of these reagents bound either p58 or p53 (data not shown).

Purification of p58 and p53

We purified p58 and p53 to determine whether they were related to β-dystroglycan or were unrelated yet immunologically cross-reactive. Protein staining of one-dimensional SDS gels showed that p58 and p53 are minor components of the PSD fraction; moreover, they were not well resolved from other, more abundant polypeptides (data not shown). To achieve improved separation of p58 and p53 and to further investigate their biochemical properties, we separated the PSD fraction proteins by charge and size using 2D gel electrophoresis (Fig. 2*A*). This method yielded substantial improvement in the isolation of p58 and p53: unlike the majority of the PSD proteins, the doublet migrated to a basic isoelectric point (pI, ~9) free from the bulk of PSD proteins. The p58 and p53 bands migrated as a series of closely spaced spots of differing isoelectric points, suggesting that these polypeptides may be post-translationally modified (see below).

p58 and p53 were virtually insoluble in all nonionic detergents tested. Furthermore, they were not extracted in 3% *N*-lauroyl sarcosinate (data not shown). Such solubility properties indicate that these polypeptides are tightly associated with the "core" PSD (Kennedy, 1997). However, p58 and p53 could be efficiently solubilized in 8 M urea. Thus, we fractionated the urea-solubilized PSD proteins by HIC. p58 and p53 bound to the HIC matrix, whereas the majority of the PSD proteins did not. Elution of the HIC column thus yielded a fraction that was highly enriched in p58 and p53. We then used 2D electrophoresis to achieve the final purification of p58 and p53 (Fig. 2*B*).

Mass spectrometry analysis and peptide microsequencing of p58 and p53

To identify p58 and p53, we used MALDI-TOF mass spectrometry to obtain mass profiles of the gel-purified polypeptides. Comparison of these profiles with computer-generated mass profiles of protein sequences in the National Center for Biotechnical Information database showed that rat p58 and p53 were highly homologous to hamster IRSp58/53 (Table 1, Fig. 3). This pair of polypeptides was first identified in CHO cells, and the cDNA encoding IRSp53 was subsequently cloned (Yeh et al., 1996). However, the precise relationship between IRSp58 and IRSp53 was not established in that study.

Sixty-five percent of both the p58 masses (15 of 23) and the p53 masses (13 of 20) we obtained by mass spectrometry matched the tryptic digest masses computed from the deduced IRSp53 amino acid sequence (data not shown). There were eight p58 masses that did not correspond to a computed IRSp53 mass, but six of these masses were shared by p53. Two p58 masses and one p53 mass were unique. Only slight differences were observed when the HPLC chromatograms of the p58 and p53 tryptic digests were compared (data not shown). Together, these data indicate that the primary structures of p58 and p53 are very similar to the polypeptide encoded by IRSp53 and to each other.

To verify the identification of p58 and p53 as IRSp53, we obtained amino acid sequence from three of the p58 tryptic fragments. Of the 33 amino acids obtained, all perfectly matched the published sequence of the IRSp53 cDNA (Table 1, Fig. 3; data not shown). The predicted pI of IRSp53 is 8.8, which corresponds well to the basic pI we determined for p58 and p53. Western blots of PSD fractions probed with monoclonal antibody H720 further confirmed the identification of p58 and p53 as IRSp58/53 (data not shown). We will hereafter refer to p58 and p53 as IRSp58/53.

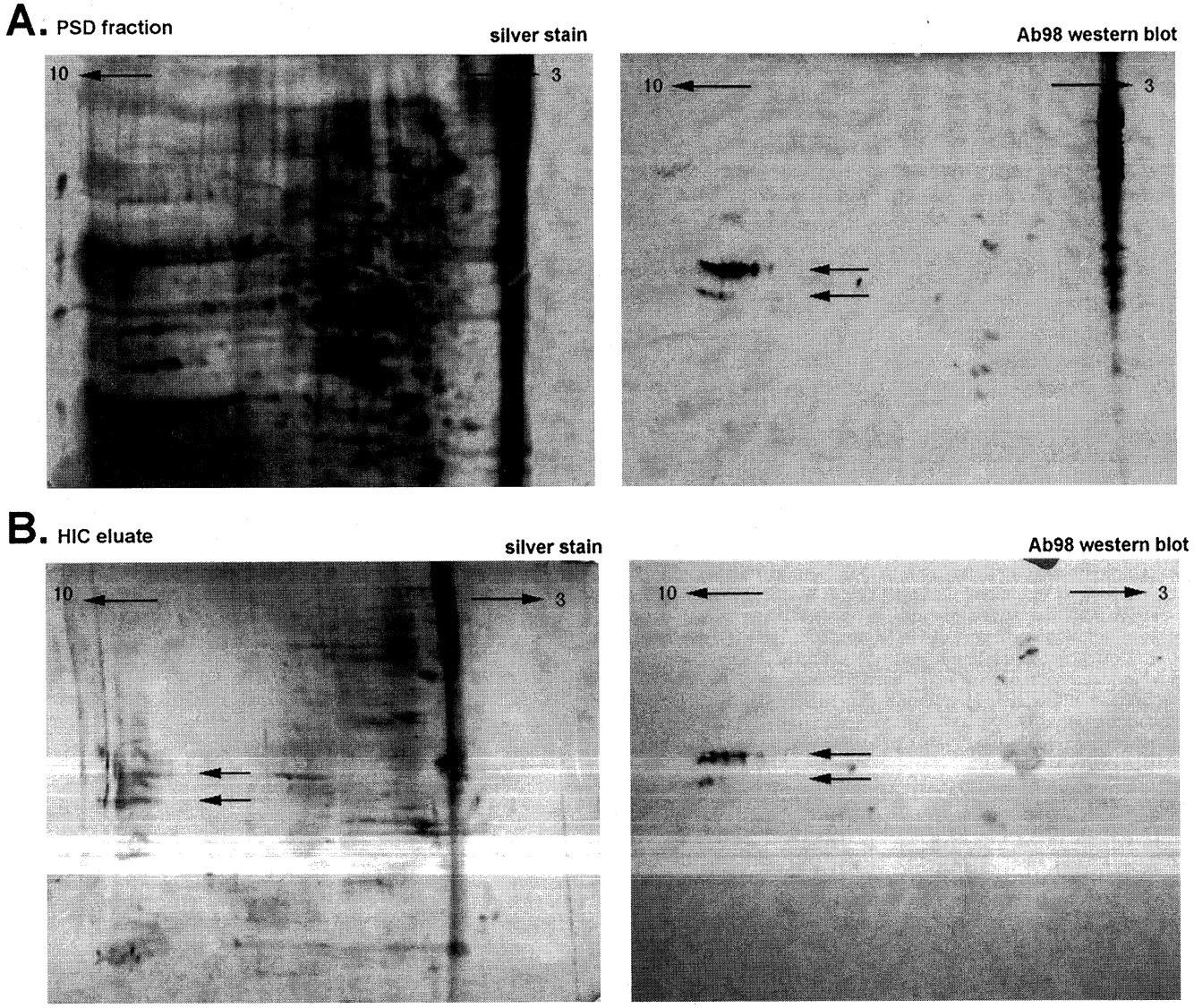

Figure 2. Purification of p58 and p53 by 2D gel electrophoresis and hydrophobic interaction chromatography. *A*, Two-dimensional gel electrophoresis was used to separate PSD fraction proteins. Gels of equivalent samples were silver-stained (*left*) or blotted to nitrocellulose and probed with Ab98 (*right*). The positions of p58 and p53, as visualized by Western blotting, are indicated by the pair of *arrows*. The migration of p58 and p53 in the first dimension indicates that these polypeptides are basic (pI, ~9). Comparison of silver stain and Western blot shows that p58 and p53 are minor components of the PSD fraction. *B*, The PSD fraction proteins were solubilized in urea, loaded onto a HIC column in 1 M NaCl buffer, and then eluted in 0.1 M NaCl salt buffer. 2D gels of the HIC eluates were either silver-stained (*left*) or blotted to nitrocellulose and probed with Ab98 (*right*). p58 and p53 are readily visualized in silver-stained gels of HIC eluate (*arrows*), indicating that they are highly enriched by this procedure.

Relationship of IRSp58 and IRSp53

In the course of our biochemical studies of IRSp58/53, we consistently encountered an ~5 kDa difference between the molecular weights of IRSp58 and IRSp53. However, neither mass spectrometry nor HPLC analysis yielded any indication that the primary structure of these polypeptides differed. Western analysis revealed that IRSp58/53 was identical in rat and mouse (data not shown). However, in the porcine PSD fraction the IRSp58 species was prominent, and the IRSp53 species was barely detectable (Fig. 4). *In vitro* phosphorylation of rat PSD proteins resulted in an upward shift in the mobility of both polypeptides, suggesting that they are substrates of a kinase(s) in the PSD fraction. However, this shift could not account for the 5 kDa difference between IRSp58 and IRSp53 (Fig. 4). Similarly, enzymatic deglycosylation did not yield any consolidation of the doublet (data not shown). Thus, we could find no evidence that these post-translational modifications are the basis for the difference in the apparent molecular weights of IRSp58 and IRSp53.

Distribution of IRSp58/53 mRNA

We next examined the distribution and configuration of the IRSp58/53 transcript. We probed Northern blots to determine the tissue distribution of IRSp58/53 mRNA. Transcripts of 2.4 and 3.5 kb were detected (Fig. 5). Brain contained the highest level of IRSp58/53 mRNA, with the 3.5 kb transcript predominating. Varying amounts of these transcripts were observed in other tissues. Neither transcript was detected in skeletal muscle.

Table 1. Mass spectrometry and peptide microsequence analysis of PSD58/53

p58 and p53 tryptic fragments		Predicted IRSp53 tryptic fragments[a]		
p58 masses	p53 masses	IRSp53 masses[b]	Position[c]	Peptide microsequence[d]
912.7		913.1	51–58	GYFDALVK
1788.2	1789.7	1788.0	157–171	YSDKELQYIDAISNK
1208.1	1208.4	1208.2	412–421	DGWHYGESEK

[a]The calculated masses of the IRSp53 tryptic fragments that correspond to p58 or p53 masses are listed.

[b]All masses are in daltons.

[c]The amino acid positions of these fragments are based on the numbering system of Yeh et al (1996).

[d]Peptide microsequences obtained from the three p58 tryptic fragments were identical to deduced IRSp53 amino acid sequences.

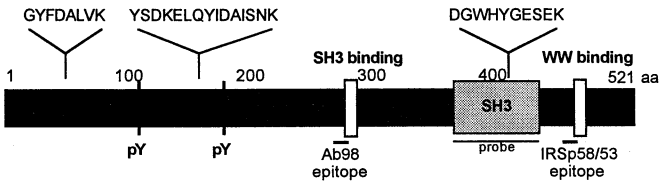

Figure 3. Structure of IRSp53. IRSp53 is predicted to contain several protein-protein interaction domains: one SH3 domain, one SH3 binding domain, and one WW binding domain (Yeh et al., 1998). Additionally, there are 25 potential serine/threonine phosphorylation sites (protein kinase A, protein kinase C, and casein kinase; data not shown) and two potential tyrosine phosphorylation sites (*pY*). The positions of the peptide microsequences obtained from purified p58 are noted. The positions of the epitope that is likely to be recognized by Ab98 and the peptide used to generate the polyclonal anti-IRSp58/53 antiserum are indicated. The region that corresponds to the IRSp53 DNA fragment used as a probe for Northern blots is also shown.

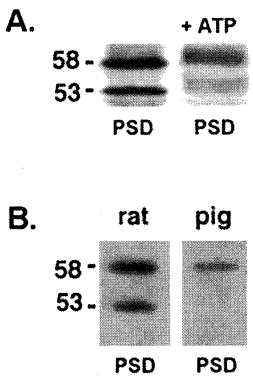

Figure 4. Relationship of IRSp58 and IRSp53 from PSDs. *A*, PSD fractions from rat brain were incubated under conditions promoting *in vitro* phosphorylation (see Materials and Methods) in either the absence (*left*) or presence (*right*) of exogenous ATP. Western blotting with Ab98 shows that IRSp58 and IRSp53 undergo similar gel shifts after *in vitro* phosphorylation. *B*, Blots of PSD fractions from rat (*left*) and pig (*right*) were probed with antibody Ab98. Comparison of these reveals species differences in the expression of PSD fraction IRSp58 and IRSp53. Although similar amounts of IRSp58 and IRSp53 are detected in rat PSDs, only IRSp58 is detected in pig PSDs.

Organization of IRSp58/53 mRNA

We next considered the possibility that the multiple transcripts observed in the Northern blots could correspond to alternatively spliced mRNAs. We searched the Expressed Sequence Tag (EST) database using the BLAST algorithm (Altschul et al., 1990) for sequences that might represent IRSp53 homologs. We identified a large set of IRSp53-homologous ESTs that spanned the entire open reading frame of IRSp53 (data not shown).

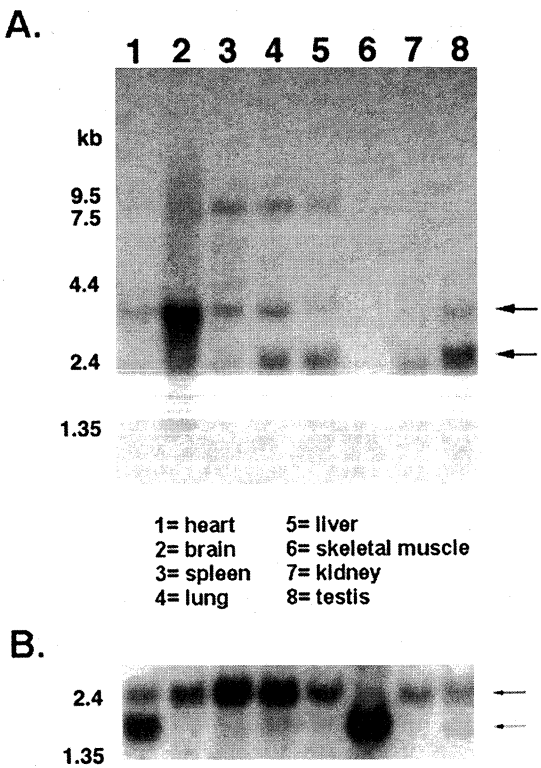

Figure 5. Tissue distribution of IRSp58/53 mRNAs. *A*, A multiple rat tissue Northern blot was probed with a radiolabeled IRSp58/53 oligonucleotide probe (248 bp; see Fig. 3) as described in Materials and Methods. Transcripts of 2.4, 3.5, and 8 kb are observed. The highest level of IRSp58/53 mRNA is detected in brain, with the 3.5 kb transcript predominating. *B*, The blot was rehybridized with a probe for β-actin to verify the integrity and quantity of the RNA from each tissue.

However, this analysis revealed no divergences from the reported IRSp53 cDNA sequence and thus provided no evidence for alternatively spliced transcripts.

As a further test for variations in the coding sequence of the IRSp58/53 mRNAs, we performed RT-PCR. We isolated total RNA from rat cerebral cortex and reverse-transcribed it using random primers. We then used an array of specific primers that spanned the IRSp53 coding region for PCR analysis. Each of the RT-PCR products generated corresponded in size to a product obtained using IRSp53 cDNA as template; no major additional products were detected (data not shown). Together, these PCR products covered the entire coding region of IRSp53. Thus, in rat brain we find no evidence of alternative splicing within the coding region of IRSp53, suggesting that both IRSp58 and IRSp53 are products of a highly similar or identical mRNA.

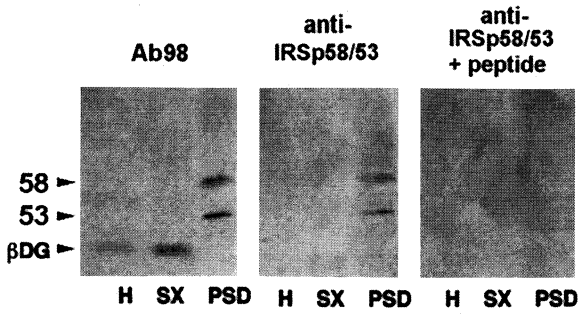

Figure 6. Characterization of the anti-IRSp58/53 antibody. Rabbits were immunized with a 13 amino acid peptide from the predicted amino acid sequence of IRSp58/53, and the resulting antiserum was affinity-purified. On Western blots, anti-IRSp58/53 antibody recognizes polypeptides of 58 and 53 kDa, which are also bound by Ab98. However, anti-IRSp58/53 does not recognize β-dystroglycan. All anti-IRSp58/53 immunoreactivity is abolished if the antibody is preabsorbed with peptide. *H*, Homogenate; *SX*, synaptosomes; *PSD*, postsynaptic density fraction.

Localization of IRSp58/53 to synapses

To determine whether IRSp58/53 is expressed at intact synapses, we raised and affinity purified a specific anti-IRSp58/53 antiserum. The specificity of this reagent for IRSp58/53 was verified by Western blotting and immunoabsorption (Fig. 6). In contrast to Ab98, this antiserum did not recognize β-dystroglycan.

To determine the distribution of IRSp58/53 in intact brain, we performed immunohistochemistry on frozen sections. The cytoarchitecture of the cerebellum consists of granular and pyramidal cell soma layers and a synapse-rich molecular layer. Staining with the anti-IRSp58/53 antibody demonstrated that IRSp58/53 immunoreactivity is prominent in the synapse-rich molecular layer as well as in the granule cell layer of this tissue (Fig. 7*A*). The specificity of the IRSp58/53 antibody staining was demonstrated by peptide immunoabsorption.

To assess the distribution of IRSp58/53 in further detail, we exploited a system in which individual synapses can be resolved. Primary hippocampal neurons in low density cultures have well differentiated axons and dendrites and numerous synapses. These synapses can be reliably visualized using antibodies to synaptophysin (Fletcher et al., 1991). Double labeling with anti-synaptophysin and anti-IRSp58/53 showed that IRSp58/53 immunoreactivity was localized at the majority of synapses on these cells (Fig. 7*B*). Little nonsynaptic localization was observed. Together, these studies indicated that IRSp58/53 is a component of CNS synapses.

Localization of insulin receptors at synapses

IRSp58/53 has been shown to be an insulin receptor substrate in cultured fibroblasts. Furthermore, IRSp58/53 isolated from brain can be tyrosine-phosphorylated *in vitro* by the insulin receptor (Yeh et al., 1996). To determine whether the insulin receptor is localized at synapses, we immunostained cultured hippocampal neurons with an antibody directed against the insulin receptor β-subunit and with an anti-synaptophysin antibody. Figure 8, *A* and *B*, shows that insulin receptors are highly concentrated at synapses on these cells. Insulin receptors are also localized at nonsynaptic regions of the dendrite (Fig. 8*B*).

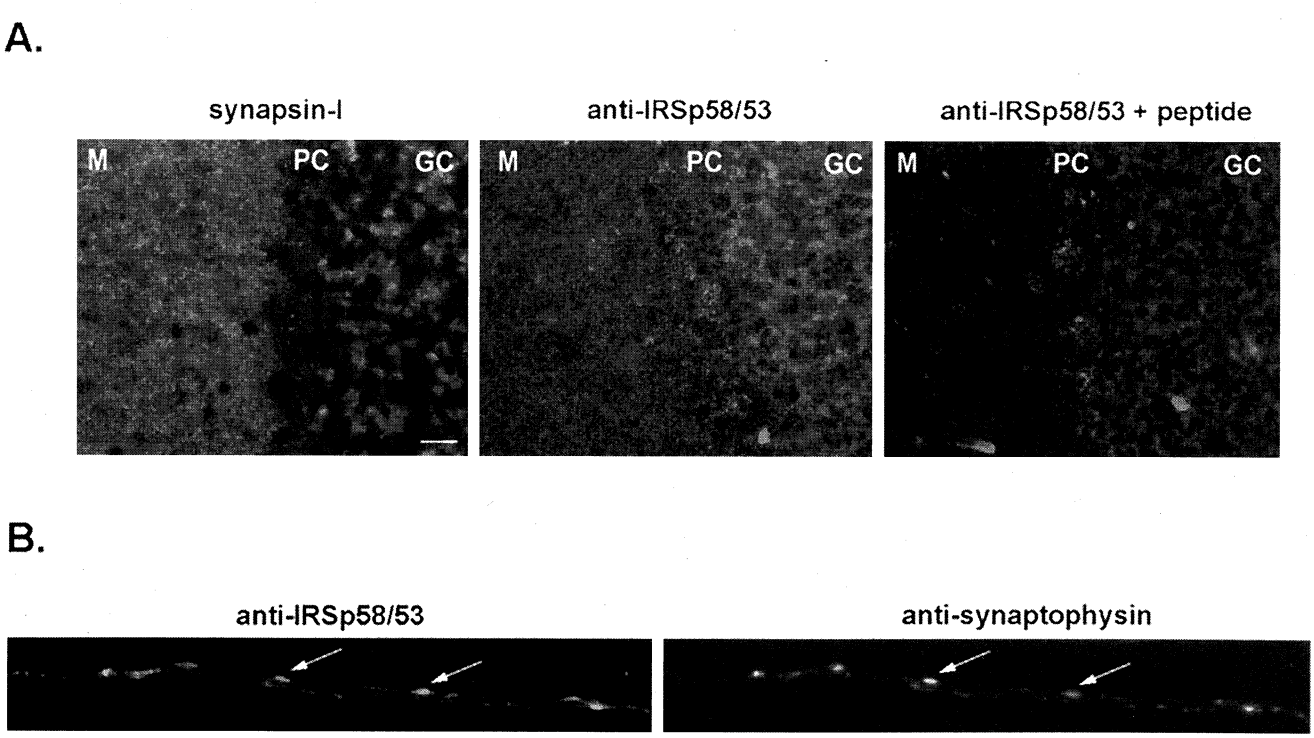

Figure 7. *A*, Localization of IRSp58/53 in the cerebellar cortex. Sections of rat cerebellum were immunostained with the affinity-purified anti-IRSp58/53 or with anti-synapsin-I antiserum. The synapsin-I immunoreactivity reveals the distribution of synapses. IRSp58/53 immunoreactivity is observed in the synapse-rich molecular layer as well as in the granule cell layer. Anti-IRSp58/53 immunoreactivity is greatly reduced when the antibody was preabsorbed with peptide. Scale bar, 50 μm. *M*, Molecular layer; *PC*, Purkinje cell layer; *GC*, granule cell layer. *B*, Localization of IRSp58/53 at synapses. Cultured rat hippocampal neurons were immunostained with the affinity-purified anti-IRSp58/53 antiserum (*left*). IRSp58/53 immunoreactivity is distributed in a punctate pattern along the dendrites of the neurons. The distribution of synapses in the same dendrite was visualized by double labeling with anti-synaptophysin (*right*). IRSp58/53 immunoreactivity is selectively concentrated at synapses (*arrows*).

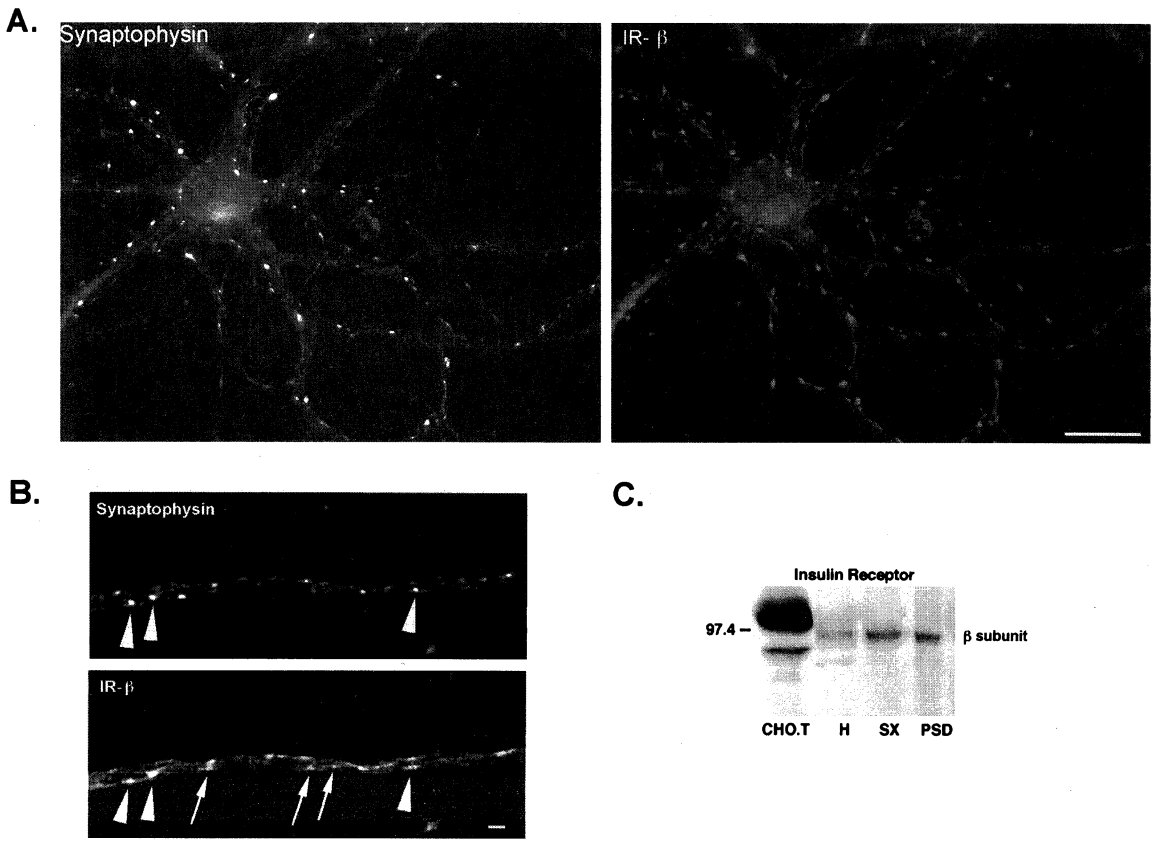

Figure 8. Insulin receptor localization in cultured neurons and brain subcellular fractions. *A*, Cultured rat hippocampal neurons were double-immunostained with anti-synaptophysin and anti-insulin receptor β-subunit antibody (*IR-β*). Insulin receptor immunoreactivity is distributed in a punctate pattern along dendrites. Note that insulin receptor β-subunit immunoreactivity is concentrated at synapses. Scale bar, 20 μM. *B*, High-magnification view of a single dendrite of a cultured hippocampal neuron double labeled with antibodies to the insulin receptor β-subunit and synaptophysin. IR-β immunoreactivity is concentrated at both synaptophysin-positive regions (*arrowheads*) as well as distributed in apparently nonsynaptic regions (*arrows*). Scale bar, 5 μM. *C*, A Western blot of rat brain subcellular fractions (homogenate, synaptosome, and PSD) and lysate from CHO.T cells was probed with an anti-insulin receptor β-subunit antibody. High levels of β-subunit are seen in CHO.T cells (a cell line engineered to overexpress insulin receptors). The β-subunit of the insulin receptor is detected in brain homogenate and is enriched in synaptosome and PSD fractions.

Insulin receptors are a component of PSD fractions

We next wished to compare the biochemical fractionation profiles of insulin receptor and IRSp58/53 from brain. In agreement with earlier findings, the molecular weight of the insulin receptor β-subunit in brain is ~5 kDa less than that expressed by peripheral tissues (Heidenreich et al., 1983). Western blotting showed that the insulin receptor β-subunit was detected in homogenate and was enriched in both synaptosome and PSD fractions (Fig. 8*C*). The degree of enrichment of insulin receptor in PSD fractions was not as great as that observed for PSD components such as NMDA receptor subunit NR1, α-CaMKII, and IRSp58/53 (Fig. 1). This observation is in agreement with the localization of the insulin receptor to both nonsynaptic and synaptic regions (Fig. 8*B*; see Discussion). Together, these findings show that both the β-subunit of the insulin receptor tyrosine kinase and its substrate IRSp58/53 are components of the PSD fraction. This co-localization suggests that these molecules are part of an insulin-dependent signaling pathway at the postsynaptic apparatus.

DISCUSSION

Insulin is likely to have diverse roles in the CNS. In addition to its probable function in glucose metabolism, there is a growing body of evidence that insulin signaling may factor in cell–cell communication and plasticity (for reviewed, see Wickelgren, 1998). The diverse outcomes of insulin signaling may be coordinated through the spatially regulated expression of insulin receptor tyrosine kinase substrates. Here, we show that the insulin receptor substrate IRSp58/53, and insulin receptors themselves, are localized at synapses in the brain and are components of the postsynaptic density. Signaling via IRSp58/53 may define a synapse-specific role for insulin in the brain.

IRSp58/53 and insulin receptor are localized to synapses

We began our investigation of synaptic insulin signaling proteins at the level of the PSD, an electron-dense conglomeration of proteins that lies just below the postsynaptic membrane at excitatory synapses. We purified a pair of previously unidentified proteins that were selectively concentrated in PSD fractions. MALDI-TOF mass spectrometry, peptide sequencing, two-dimensional electrophoresis, and Western blotting demonstrated that these PSD proteins, p58 and p53, are the insulin receptor substrate p58/53 (IRSp58/53). The IRSp58/53 that we purified from rat is very similar to that cloned from hamster (Table 1).

The striking enrichment of IRSp58/53 in PSD fractions suggested that it may be predominantly expressed at excitatory synapses. Indeed, immunocytochemistry showed that IRSp58/53

is expressed in the synapse-rich layers of the cerebellum. Furthermore, labeling of cultured hippocampal neurons demonstrated that IRSp58/53 is selectively concentrated at synapses. Neither Western blotting nor immunocytochemistry detected IRSp58/53 expression in cultured glial cells (our unpublished observations). Thus, IRSp58/563 is selectively localized at synapses in the CNS.

The synaptic distribution of IRSp58/53 raised the possibility that insulin receptors are also localized at these structures. Previous work has shown that insulin receptors have been detected in both neurons and glia throughout the brain (Wozniak et al., 1993). However, their subcellular localization was not established. Using immunocytochemistry and Western blotting of brain fractions we show that the insulin receptor is localized at synapses. Together, these findings support the proposal that insulin signaling plays a role at synapses.

Structure of IRSp58/53

We consistently observed that IRSp58/53 migrates as a pair of polypeptides. However, we could find little evidence that IRSp58 and IRSp53 differed in their primary sequences. HPLC chromatograms of tryptic fragments from p58 and p53 were virtually identical. MALDI-TOF analysis of purified p58 and p53 also revealed similar profiles; only two p58 masses and one p53 mass were unique. Although these masses could represent divergent primary sequences, they could also be attributable to post-translational modification or proteolysis. Indeed, the relative expression of IRSp58 and IRSp53 is cell- and tissue-specific. Transfection of the IRSp53 cDNA into fibroblasts results in expression of only the IRSp53 species (Yeh et al., 1996). Furthermore, we detect only IRSp58 in PSD fractions from porcine brain. Finally, using RT-PCR we detected only a single species of IRSp53 mRNA in the brain, and a survey of the EST database yielded no evidence of multiple mRNA species. However, our comparative analysis of the IRSp53 cDNA and total rat brain cDNA does not exclude the possibility that differences exist 5′ or 3′ to the IRSp53 coding region. Analysis of the IRSp53 cDNA reveals an open reading frame that encodes for a predicted protein of 57.6 kDa (Yeh et al., 1996). Interestingly, downstream of this first ATG codon are at least six subsequent potential start sites. Use of one of these in particular would yield a polypeptide with a predicted molecular weight of 53.6 kDa. Therefore, it is possible that use of alternative initiation sites is the basis for the observation of this pair of polypeptides of 58 and 53 kDa. Nevertheless, we think our data best fit a scenario whereby IRSp58 and IRSp53 derive from an identical mRNA coding region, and the difference in these polypeptides is the result of a species- and cell background-dependent, post-translational process.

Our investigation of IRSp58/53 was an outgrowth of our use of an antiserum directed against β-dystroglycan (Ab98). However, comparison of the IRSp53 and β-dystroglycan sequences revealed very limited sequence homology. The immunological cross-reactivity that Ab98 demonstrated for IRSp58/53 is presumably attributable to a proline-rich stretch of amino acids within its amino acid sequence (KPLPVPPELAPF) that is similar to the β-dystroglycan peptide used to generate Ab98 (KAPLPPPEY-PSQ). Notably, another group has reported a PSD fraction protein (not IRSp58/53) that is immunologically related to β-dystroglycan (Mummery et al., 1996). To date, however, neither the identity of this 164 kDa PSD fraction protein nor its relationship to β-dystroglycan has been shown. In sum, our data provide no evidence for the expression of β-dystroglycan or a related molecule in PSD fractions.

Interactions of IRSp58/53

There is compelling evidence in support of the functional classification of IRSp58/53 as an insulin receptor substrate in cell lines (Yeh et al., 1996). Furthermore, Yeh and colleagues (1996) demonstrated that IRSp58/53 isolated from brain can be tyrosine-phosphorylated *in vitro* by insulin receptors isolated from CHO.T cells. We have found that after *in vitro* phosphorylation of PSD fractions, IRSp58/53 displayed a gel shift consistent with phosphorylation by an endogenous kinase(s). Moreover, the insulin receptor is localized at synapses and is a component of PSD fractions. Together, these observations suggest that IRSp58/53 acts as a substrate of the insulin receptor tyrosine kinase at synapses. Studies are currently in progress to determine whether insulin stimulation leads to phosphorylation of IRSp58/53 in intact neurons.

The predicted domain structure of IRSp53 indicates many potential sites for protein–protein interactions, including an Src homology region 3 (SH3) domain, an SH3-binding domain, and a proline-rich WW-binding domain (Yeh et al., 1998). An interaction between an IRSp53 homolog and the intracellular domain of Fas ligand (FasL) has been detected using a yeast two-hybrid assay (GenBank accession U70669). However, we have been unable to demonstrate an interaction between IRSp58/53 and FasL biochemically. We also tested whether IRSp58/53 interacts with the WW domain of dystrophin, a PSD-enriched cytoskeletal protein, but we were unable to co-immunoprecipitate IRSp58/53 and *in vitro*-expressed dystrophin fragments. Finally, we did not detect co-immunoprecipitation of any native PSD fraction proteins with IRSp58/53 (our unpublished observations). Other investigators have similarly been unable to demonstrate binding partners for IRSp58/53 (Yeh et al., 1996).

IRSp58/53 may define a synapse-specific insulin signaling pathway

In the periphery, the actions of insulin are effected by distinct sets of signal transduction molecules with characteristic cellular and subcellular distributions (Anai et al., 1998). Similar compartmentalization may also occur in the CNS. Key components of the insulin signaling mechanism, such as insulin receptors and IRS-1, are widely expressed in the brain, where they are often co-localized. However, there are several areas of the brain, including regions of the cerebellum, in which insulin receptor but not IRS-1 is detected (Baskin et al., 1994; Folli et al., 1994; Yamada et al., 1997). In the current study we found that insulin receptors, although co-localized with IRSp58/53 at synapses, are also found in nonsynaptic areas of the dendrite. It seems likely that the insulin receptor will associate with other insulin receptor substrates at these sites. These observations indicate that insulin action in the brain is likely to be subserved by distinct sets of downstream signaling elements.

The data presented here suggest that IRSp58/53 may define a novel class of insulin signaling at excitatory synapses in the brain. One expects that the effect of insulin at synapses is distinct from its global, metabolic control. It seems likely that elucidating the role of insulin signaling at synapses will provide important insights into synaptic function and plasticity.

REFERENCES

Altschul SF, Gish W, Miller W, Myers EW, Lipman DJ (1990) Basic local alignment search tool. J Mol Biol 215:403–410.

Anai M, Ono H, Funaki M, Fukushima Y, Inukai K, Ogihara T, Sakoda H, Onishi Y, Yazaki Y, Kikuchi M, Oka Y, Asano T (1998) Different subcellular distribution and regulation of expression of insulin receptor

substrate (IRS)-3 from those of IRS-1 and IRS-2. J Biol Chem 273:29686–29692.
Baltensperger K, Karoor V, Paul H, Ruoho A, Czech MP, Malbon CC (1996) The beta-adrenergic receptor is a substrate for the insulin receptor tyrosine kinase. J Biol Chem 271:1061–1064.
Baskin DG, Schwartz MW, Sipols AJ, D'Alessio DA, Goldstein BJ, White MF (1994) Insulin receptor substrate-1 (IRS-1) expression in rat brain. Endocrinology 134:1952–1955.
Carlin RK, Grab DJ, Cohen RS, Siekevitz P (1980) Isolation and characterization of postsynaptic densities from various brain regions: enrichment of different types of postsynaptic densities. J Cell Biol 86:831–845.
Clarke DW, Mudd L, Boyd Jr FT, Fields M, Raizada MK (1986) Insulin is released from rat brain neuronal cells in culture. J Neurochem 47:831–836.
Craft S, Newcomer J, Kanne S, Dagogo-Jack S, Cryer P, Sheline Y, Luby J, Dagogo-Jack A, Alderson A (1996) Memory improvement following induced hyperinsulinemia in Alzheimer's disease. Neurobiol Aging 17:123–130.
Dosemeci A, Reese TS (1993) Inhibition of endogenous phosphatase in a postsynaptic density fraction allows extensive phosphorylation of the major postsynaptic density protein. J Neurochem 61:550–555.
Dosemeci A, Gollop N, Jaffe H (1994) Identification of a major autophosphorylation site on postsynaptic density-associated Ca2+/calmodulin-dependent protein kinase. J Biol Chem 269:31330–31333.
Fletcher TL, Cameron P, De Camilli P, Banker G (1991) The distribution of synapsin I and synaptophysin in hippocampal neurons developing in culture. J Neurosci 11:1617–1626.
Folli F, Bonfanti L, Renard E, Kahn CR, Merighi A (1994) Insulin receptor substrate-1 (IRS-1) distribution in the rat central nervous system. J Neurosci 14:6412–6422.
Frolich L, Blum-Degen D, Bernstein HG, Engelsberger S, Humrich J, Laufer S, Muschner D, Thalheimer A, Turk A, Hoyer S, Zochling R, Boissl KW, Jellinger K, Riederer P (1998) Brain insulin and insulin receptors in aging and sporadic Alzheimer's disease. J Neural Transm 105:423–438.
Goslin K, Banker G (1991) Rat hippocampal neurons in low-density culture. In: Culturing nerve cells, pp 251–281. Cambridge, MA: MIT.
Hall ZW, Sanes JR (1993) Synaptic structure and development: the neuromuscular junction. Neuron [Suppl] 10:99–121.
Heidenreich KA, Zahniser NR, Berhanu P, Brandenburg D, Olefsky JM (1983) Structural differences between insulin receptors in the brain and peripheral target tissues. J Biol Chem 258:8527–8530.
Hong M, Lee VM (1997) Insulin and insulin-like growth factor-1 regulate tau phosphorylation in cultured human neurons. J Biol Chem 272:19547–19553.
Hoyer S (1998) Is sporadic Alzheimer disease the brain type of non-insulin dependent diabetes mellitus? A challenging. J Neural Transm 105:415–422.
Kang H, Schuman EM (1995) Long-lasting neurotrophin-induced enhancement of synaptic transmission in the adult hippocampus. Science 267:1658–1662.
Kennedy MB (1997) The postsynaptic density at glutamatergic synapses. Trends Neurosci 20:264–268.
Lannert H, Hoyer S (1998) Intracerebroventricular administration of streptozotocin causes long-term diminutions in learning and memory abilities and in cerebral energy metabolism in adult rats. Behav Neurosci 112:1199–208.
Lohof AM, Ip NY, Poo M-M (1993) Potentiation of developing neuromuscular synapses by the neurotrophins NT-3 and BDNF. Nature 363:350–352.
Malgaroli A, DeCamilli P, Meldolesi J (1989) Distribution of alpha latrotoxin receptor in the rat brain by quantitative autoradiography: comparison with the nerve terminal protein synapsin I. Neuroscience 32:393–404.
Morrissey JH (1981) Silver stain for proteins in polyacrylamide gels: a modified procedure with enhanced uniform sensitivity. Anal Biochem 117:307–310.
Mummery R, Sessay A, Lai FA, Beesley PW (1996) beta-dystroglycan: subcellular localisation in rat brain and detection of a novel immunologically related, postsynaptic density-enriched protein. J Neurochem 66:2455–2459.
Peters A, Palay SL, Webster HD (1991) The fine structure of the nervous system: neurons and their supporting cells. New York: Oxford UP.
Qiu WQ, Walsh DM, Ye Z, Vekrellis K, Zhang J, Podlisny MB, Rosner MR, Safavi A, Hersh LB, Selkoe DJ (1998) Insulin-degrading enzyme regulates extracellular levels of amyloid beta-protein by degradation. J Biol Chem 273:32730–32738.
Salpeter MM (1987) Vetebrate neuromuscular junctions: general morphology, molecular organization, and functional consequences. In: The vertebrate neuromuscular junction, pp 1–54. New York: Liss.
Schechter R, Beju D, Gaffney T, Schaefer F, Whetsell L (1996) Preproinsulin I and II mRNAs and insulin electron microscopic immunoreaction are present within the rat fetal nervous system. Brain Res 736:16–27.
Sheng M (1997) Excitatory synapses. Glutamate receptors put in their place [news, comment]. Nature 386:221–223.
Sheng M, Wyszynski M (1997) Ion channel targeting in neurons. Bioessays 19:847–853.
Shepherd PR, Withers DJ, Siddle K (1998) Phosphoinositide 3-kinase: the key switch mechanism in insulin signalling. Biochem J 333:471–490.
Somogyi P, Tamas G, Lujan R, Buhl EH (1998) Salient features of synaptic organisation in the cerebral cortex. Brain Res Brain Res Rev 26:113–135.
Unger J, McNeill TH, Moxley RT, White M, Moss A, Livingston JN (1989) Distribution of insulin receptor-like immunoreactivity in the rat forebrain. Neuroscience 31:143–157.
Wan Q, Xiong ZG, Man HY, Ackerley CA, Braunton J, Lu WY, Becker LE, MacDonald JF, Wang YT (1997) Recruitment of functional GABA(A) receptors to postsynaptic domains by insulin. Nature 388:686–690.
Wei LT, Matsumoto H, Rhoads DE (1990) Release of immunoreactive insulin from rat brain synaptosomes under depolarizing conditions. J Neurochem 54:1661–1665.
White MF, Yenush L (1998) The IRS-signaling system: a network of docking proteins that mediate insulin and cytokine action. Curr Top Microbiol Immunol 228:179–208.
Wickelgren I (1998) Tracking insulin to the mind [news]. Science 280:517–519.
Wozniak M, Rydzewski B, Baker SP, Raizada MK (1993) The cellular and physiological actions of insulin in the central nervous system. Neurochem Int 22:1–10.
Wu L, Wells D, Tay J, Mendis D, Abbott MA, Barnitt A, Quinlan E, Heynen A, Fallon JR, Richter JD (1998) CPEB-mediated cytoplasmic polyadenylation and the regulation of experience-dependent translation of alpha-CaMKII mRNA at synapses. Neuron 21:1129–1139.
Yamada M, Ohnishi H, Sano S, Nakatani A, Ikeuchi T, Hatanaka H (1997) Insulin receptor substrate (IRS)-1 and IRS-2 are tyrosine-phosphorylated and associated with phosphatidylinositol 3-kinase in response to brain-derived neurotrophic factor in cultured cerebral cortical neurons. J Biol Chem 272:30334–30339.
Yeh TC, Ogawa W, Danielsen AG, Roth RA (1996) Characterization and cloning of a 58/53-kDa substrate of the insulin receptor tyrosine kinase. J Biol Chem 271:2921–2928.
Yeh TC, Li W, Keller GA, Roth RA (1998) Disruption of a putative SH3 domain and the proline-rich motifs in the 53-kDa substrate of the insulin receptor kinase does not alter its subcellular localization or ability to serve as a substrate. J Cell Biochem 68:139–150.
Yoshida M, Mizuno Y, Nonaka I, Ozawa E (1993) A dystrophin-associated glycoprotein, A3a (one of 43DAG doublets), is retained in Duchenne muscular dystrophy muscle. J Biochem (Tokyo) 114:634–639.
Ziff EB (1997) Enlightening the postsynaptic density. Neuron 19:1163–1174.